FINAL TECHNICAL REPORT

Covering the Period

1 January 1974 - 31 August 1976

NASA Research Grant No. NGR-22-009-766

MONITORING SPACECRAFT ATMOSPHERE CONTAMINANTS

BY LASER ABSORPTION SPECTROSCOPY

Professor J.I. Steinfeld, Principal Investigator

B.D. Green, Research Assistant

Department of Chemistry
Massachusetts Institute of Technology
Cambridge, Massachusetts   02139

The NASA Technical Officer for this grant is:

FINAL TECHNICAL REPORT

Covering the Period

1 January 1974 - 31 August 1976

NASA Research Grant No. NGR-22-009-766

MONITORING SPACECRAFT ATMOSPHERE CONTAMINANTS

BY LASER ABSORPTION SPECTROSCOPY

Professor J.I. Steinfeld, Principal Investigator

B.D. Green, Research Assistant

Department of Chemistry
Massachusetts Institute of Technology
Cambridge, Massachusetts 02139

Contents

Abstract

Laser-based spectrophotometric methods which have been proposed for the detection of trace concentrations of gaseous contaminants include Raman backscattering (LIDAR) and passive radiometry (LOPAIR). In this report, we discuss remote sensing techniques using laser spectrometry, and in particular a simple long-path laser absorption method (LOLA), which is capable of resolving complex mixtures of closely related trace contaminants at ppm levels.

A number of species were selected for study which are representative of those most likely to accumulate in closed environments, such as submarines or long-duration manned space flights. Absorption coefficients at CO_2 laser wavelengths were measured to an accuracy of $\pm$ 1% or better, for each of these species. This data base was then used to determine the presence and concentration of the contaminants in prepared mixtures of twelve to fifteen gases. Computer programs have been developed which will permit a real-time analysis of the monitored atmosphere. Minimum detectable concentrations for individual species are generally in the ppm range, and are not seriously degraded by interferences even in complex mixtures. Estimates of the dynamic range of this monitoring technique for various system configurations, and comparison with other methods of analysis, are also given.

I   CURRENT MONITORING TECHNIQUES

A. Background

Pollution is not merely the addition of substances to the air as a result of man's activities. Most of the substances considered to be pollutants are already present in the environment from many natural processes. There does exist, however, an assimilation capacity of the environment (ACE),[1] which through dilution is able to maintain a balance. The ACE is fairly substantial for most substances but not infinite. If the addition of substances to the environment is below the ACE, the effect is not noticeable, and no "pollution" results. In the last century the growth in population, along with a corresponding increase in wealth and consumption, has resulted in increased waste per capita, which is severely straining the ACE, especially in urban areas. Common property resources (air, water, public recreational facilities) are saturated. In addition, present industrial technology is moving toward use of non-biodegradable substances (ACE is very low or zero for aluminum beer cans) or substances like pesticides which are cumulative in organisms high in food chains.

The air and water are viewed as free, and consequently these resources are wastefully used. Until some value is placed on these environmental resources, the present misuse will continue.[2] The social costs of pollution include maintenance and cleaning costs, loss of recreational facilities, and the ultimate consideration, effects on health and mortality. These will be discussed further below.

Changes can only be brought about by placing a value on clean air. Suggested methods include:

1. Incentive pricing by means of graduated fines, redistribution of the burden of paying for pollution, and adjustments to receptors;

2. Federal subsidizing to help industry change generating processes, encourage recycling, and to provide tax incentives for complying corporations; and

3. Regulation through use of large fines and strict non-beneficial enforcement.

Regional management is needed for complete control of problems. A program combining all three approaches would be best. An integral part of such a program would be an accurate monitoring scheme both to force compliance to the law and to permit the study of pollution dispersion and thus the program's effectiveness.

The sources of various atmospheric pollutants have been listed often.[3-5] However, their physiological effects have not received as much publicity. In order to form a basis for understanding the toxicity of polluted atmospheres, we will consider the effect of pollution on human health next.

Effects of individual pollutants are relatively easy to assign. Carbon monoxide bonds with hemoglobin 210 times more readily than O_2, and thus requires lungs and heart to work faster.[6] At levels presently found in downtown areas, sensory response is impaired. At higher concentrations symptoms include headache and nausea. There appears to be no threshold below which symptoms are not in evidence. SO_2 affects the upper respiratory tract, constricting airways and slowing mucous flow, permitting bacteria to have longer residence time in the lung. NO_2 destroys alveoli (which permit gaseous exchange between the blood and air) and destroys lower lung cilia, which sweep bacteria and particles out of the lungs, thus lowering resistance to pneumonia. A secondary effect of NO_2 (and

-3-

chlorofluoromethanes) pollution might be the destruction of the ozone

layer,[7] permitting solar ultraviolet radiation to reach the surface of

the earth with a resultant increase in the incidence of skin cancer.

Chlorofluoromethanes are relatively non-toxic and are widely used as

refrigerants and propellants. It must be said, however, that the

actual effect of chlorofluoromethanes on the upper atmosphere is still

a matter of considerable uncertainty and controversy. Ozone disrupts

the cell membranes, causing fluid leaks into the lungs, and lowers

the diffusion of gases in the alveoli. At high concentrations, headaches

and lethargy are symptoms. Fortunately, O_3 concentrations inside buildings

are usually much lower than outdoors, due to the rapid first-order decay

of O_3 on rubber, plastic, or textile surfaces.[8]

Hydrocarbons generally are not toxic in the concentrations present

in most polluted atmospheres, but participate as reactants in photo-

chemical smog, forming peroxyacylnitrates (PAN) and other carcinogens.[9]

Some widely used commercial substances are also suspected of causing

cancer. These include CCl_4 (liver, kidney), $CHCl_3$ (heart, liver, kidney),

and vinyl chloride (liver, kidney, lung, spleen, bone marrow).[10,11]

The threshold limiting values (TLV's) set for several common pollutants

for work room air are listed in Table I. Table II shows concentrations

found in "clean" air in urban environments[12] and the level set by the

Environmental Protection Agency (EPA) in 1971.[13] Many feel that the EPA

permitted levels are too high. A consideration of the levels during

past pollution episodes will provide a perspective.

In London in 1952, a four-day fog claimed an increased fatality

count of over 4,000 people, mostly the old and the very young. Pollution

-4-

Table I

Some Maximum Permissible Contaminant Levels in Closed Environments

Compound	Work Room Air (8 hour exposure) in ppm[10]	Ambient Level Extended Period - 6 months[20] in ppm
acetaldehyde	100	10
acetone	1000	300
acetonitrite	40	1
ammonia	25	25
benzene	10	1
t-butanol	100	40
2-butenone	200	20
carbon monoxide	50	15
cyclohexane	300	60
o-dichlorobenzene	50	5
Freon 12	1000	100
Freon 113		50
1,2-dichloroethane	50	10
ethyl acetate	400	50
ethanol	1000	50
furan		0.04
isopropanol	400	40
methanol	200	40
methylchloroform	350	50
nitric oxide	25	
nitrogendioxide	5	0.5
ozone	0.1	
sulfur dioxide	5	1

Table II

Pollutant Concentrations in Atmosphere in ppm

Compound	Background[12]	Urban[12] (annual mean)	EPA Standards*[13]
SO_2	$2-4 \times 10^{-4}$	3×10^{-2}	3×10^{-2} annual mean
			1.4×10^{-1} 24 hour max.
NO_2	$1-3 \times 10^{-3}$	5×10^{-2}	5×10^{-2}
CO	1×10^{-1}	4	9 8 hour max.
			35 1 hour max.
O_3	1×10^{-2}	3×10^{-2}	8×10^{-2} 1 hour max.
CH_4	1-1.5	2	---
Hydrocarbons other than CH_4	1×10^{-3}	5×10^{-1}	2.4×10^{-1} 3 hour max.

* The maximum values are permitted only once each year.

in London is primarily SO_2 based (stationary source combustion)[3] and
yet the highest daily averages were 1.35 ppm (parts per million) SO_2
on the last two days of the fog. This level is only ten times the EPA
maximum level, and thousands of deaths occurred. In New York City in
1966, a three-day eposide resulted in 168 extra deaths and the hourly
SO_2 levels remained between 0.3 and 0.7 ppm with only two readings at
1.0 ppm. This episode had pollution in excess of EPA standards by a
factor of only 3 or 4. Although some of the people who died during
these acute episodes may have been more sensitive than the general
population, "it seems more likely that they succumbed to the combined
effects of sulfur dioxide and other pollutants that simultaneously
accumulated during the episode."[6] This is further substantiated by
the Donora, Pennsylvania incident in 1948 when 40% of the populace
was affected and 10% had severe respiratory difficulties that per-
sisted for up to a year. Some of the fatalities had no history of

chronic disease. It is fair to state that smokers and those with a chronic cough, as well as the very young, are likely to suffer most during these episodes.

Controlled studies on the effects of mixtures of air pollutants are rare, but in general show a reduced tolerance, especially among the sensitive.[14] Consider an example of cumulative effects: NO_2 irritates the lungs, reducing pulmonary efficiency, O_3 interferes with the transport of O_2 from the blood to the tissues, SO_2 increases airways' resistance, hindering breathing, CO binds with the blood preventing O_2 transfer, and Pb prevents the synthesis of new blood, all resulting in a serious oxygen deprivation problem. Thus, realistic standards for mixtures cannot be set by the current technique of partial threshold,[10] and thorough investigation of possible synergistic effects of mixtures should be carried out. However poorly defined these standards, pollution must be held to these levels. The resulting need for monitoring devices for atmospheric study, for enforcement, and as a warning device provides an impetus for much current research.

B. Monitoring Networks

Although many types of monitoring schemes have been proposed, they may all be classified as either point sampling monitors or remote monitors. To date almost all data gathered about ambient air quality has been through the use of point sampling networks. This type of monitoring network provides information only about the conditions in the immediate vicinity of the sampler. Strategies must then be devised to guess conditions at all other locations between sampling stations. Obviously, point sampling

-7-

data may provide an accurate measure of the ambient pollution in a given area, especially in submarines and future spacecraft where good central ventilation performs thorough mixing and to a lesser extent in factories and tunnels, where there is good interior mixing, but poor exchange for fresh air. Point sampling of specific sources, such as smokestacks, is another important application. The capability for remote monitoring adds an additional dimension to a network. It can provide air quality information at many specific urban areas or sources, as well as vertical pollution profiles and averaged pollution concentration over general downtown areas. This information is necessary to validate pollution dispersion models and the effects of individual sources on general air quality. The remote techniques all rely on the interaction of radiation with the pollutants.

Point sampling techniques used in situ provide information of the air quality where people are working or spending a lot of time. It is relatively inexpensive to collect remote samples (in canisters, bottles, or bags) and analyze them all at a central location, using accurate sensitive techniques capable of detecting a variety of contaminants. Such a program would be unable to provide real-time information about air quality, thus providing no warning when emergency situations exist. A remote monitoring network would not suffer this limitation because the signal may be processed as soon as it is received. Unfortunately, unlike the point sampling schemes for which widely applicable analyzers exist, most remote methods at present have been able to provide information about only a few species, and sensitivities and reliability have not yet

reached the level attained by the best point sampling techniques. However, these limitations are technological, not fundamental, in nature and the present experimental work is directed toward solution of these shortcomings.

Real-time information is vitally important in the closed environments found on long-duration manned missions, as in spacecraft or submarines, where sudden contaminant level changes due to leaks or breaks are quickly spread through the entire environment. In addition, because the concentration of substances which are ordinarily present in harmless trace amounts can slowly accumulate to toxic levels, the monitoring system must be able to simultaneously detect levels of many contaminants over a range of concentrations.

In these closed systems where the primary sources of contaminants are outgassing of non-metals, metabolic byproducts, and fluid leaks,[15] the problem of altered toxicity due to the presence of many other contaminants is serious. Present point sampling monitors for these environments involve the use of charcoal canisters with analysis following the mission. Canisters flown aboard the Apollo and Skylab missions yielded over 300 compounds upon desorption.[16-18] The quantities of some typical substances found in the canisters are given in Table III. However, there exists no simple relation between these measurements and the actual ambient level of the compound at any given time; even the relative values are misleading due to differing adsorption coefficients for the different compounds. A striking example of the need for real-time information was the contaminant leak on descent during the recent Apollo-Soyuz mission, where ignorance of the irritant hindered medical treatment.[19]

Table III

Maximum Contaminant Level Found upon Analysis in any Canister on Manned Missions, in μg/g Charcoal [17,18]

| Contaminant | | Apollo | Missions | | | | Skylab | Missions | |
	VII	VIII	IX	X	XI	XII	3 mid	3 end	4 mid
acetonitrile	0.97	---	0.15	0.33	0.78	---	0.0	0.0	0.20
benzene	0.6	3	6.19	2.29	5.59	5.06	0.0018	0.072	0.0068
tert-butanol	0.61	2.2	0.18	0.00	0.079	1.2	0.0	0.0	0.0
cyclohexane	14.3	0.5	5.35	2.27	4.82	5.67	0.11	0.075	0.03
1,2 dichloro-ethane	---	0.0	---	---	---	---	0.0	0.0	0.0
o-dichloro-benzene	0.008	0.02	0.002	0.0012	---	---	0.0	0.0	0.0
ethyl acetate	8.3	17	6.22	2.47	4.87	4.56	5.5	3.4	0.20
Freon 12	125*	83*	412*	91.3*	3.03	1.02	0.30	0.49	0.12
Freon 113	1300	328	276	353	160	214	3.6	0.97	0.28
furan	---	0.8	0.57	0.33	1.04	1.31	1.3	0.075	0.058
isopropanol	19.2	3.8	30.2	3.4	1.06	19.2	61.	17.	12.
methyl chloroform	4.55	2.0	0.66	0.31	5.89	602.	---	---	---
methylethyl-ketone	7.2	5.4	1.7	0.16	0.25	1.74	0.0	0.0	0.0
vinyl chloride	0.13	---	---	---	---	---	0.0	0.0	0.0

* Figures for Freons 12 and 22.

Freon 12 is dichlorodifluoromethane; Freon 113 is trichlorotrifluoro-ethane; Freon 22 is chlorodifluoromethane.

C. Point Monitoring Techniques

The original point sampling standard techniques involved stoichiometric reaction of preconcentrated samples of each pollutant, and although these methods are very accurate and sensitive, they require many reagents, a trained technician for analysis, and a long collection period of one hour to one day, thus destroying real-time fluctuations.[21] There has been a constant trend toward more mechanized analysis methods requiring fewer support chemicals and allowing more routine analysis.[12]

Gas chromatography offers both sensitivity and the ability to monitor a great many species after calibration. Detection limits are in the ppm to sub-ppb (parts per billion) range, depending on the detector used at the output to the column.[4,21] Although a carrier gas and preconcentration are needed, analysis is routine for expected compounds, and this technique is vastly superior to the wet chemical methods previously used. Urban real-time observations are further prevented by the necessity of collecting samples peripherally for later central analysis. It would not be economically feasible to locate a gas chromatograph at every monitoring station. Presently, non-uniformities, degradation of the column material, and clogging of the preconcentration beds, as well as the necessity of complex flow controls, diminish this system's reliability and reduce its desirability for submarines and spacecraft. The need for a carrier gas also limits operation time,[15] although progress has been made by attempts to use H_2 or air[22] as a carrier. Recent advances in column composition and calibration methods have been reviewed by Villalobos[23] and Burchfield.[24]

Mass spectrometers represent a further advance toward mechanization. This method can provide great mass resolution, high sensitivities, or

rapid responses, but not all these characteristics can be found in a single spectrometer.[15] The necessity of carefully monitoring mass peak distributions requires a stable calibration. Analysis may be performed real-time, although sensitivity is much greater if preconcentration is used. Analysis is becoming more routine as the library of catalogued mass spectra grows[25] and better search-and-compare computer programs are created to make full use of this collection.[26] Because normal air constituents are detected along with the trace components, mass fragment coincidences with components, such as CO and ethylene, prevent detection of these trace species. The efficiency of operation is low because only a small part of the information gathered concerns the trace species; this must be compared to the spectrophotometric techniques, where all the collected information is due to the contaminant species alone. Preferential diffusion through membranes or ultrafine porous fretted tubes has resulted in some sample enrichment.[24] The monitoring of less volatile pollutants has been achieved through the use of integrated ion-current mass spectrometers.[27] Here again, sample analysis would have to be performed at a central location for urban monitoring networks. Extension to operation in isolated closed environments is hindered by calibration drift problems for the more complex mass spectrometers resulting in poor stability. One mass spectrometer system for naval applications[28] had to restrict its operation to 10 ppm sensitivity for only four or five contaminants to meet the stability and dependability requirements.

The use of a gas chromatograph as the first stage with mass spectroscopic detection, simplifies the total mass peak intensity pattern and permits sensitive detection,[15,25] but real-time capabilities are lost

and the overall complexity and support requirements (weight, power) of the system are considerably increased. One experimental model was capable of detecting halocarbons at the 5 parts per trillion level with a general accuracy of $\pm$ 5%.[29]

The unique spectral patterns absorbed or emitted by each species have been utilized as a further step toward completely mechanized detection. The only requirement is the need for frequency discrimination in the signal. Over 90% of all molecules have some absorption between 2μ and 15μ in the infrared.[30] Atoms and homonuclear diatomics, the major components of air, do not absorb in this region. Electronic absorption bands in the visible or ultraviolet may also be used to identify molecules, although the spectra are more complicated and overlaps frequently occur.[31]

Techniques using grating monochomators for frequency dispersion of broadband source radiation may require non-routine analysis of the absorption patterns. In addition, throughput is small unless resolution is poor. Analysis is real-time, only seconds being required for a spectral scan. If no interferences between absorbers exist, minimum detectable concentrations (MDC's) in the 1-1000 ppm range are possible, depending on absorption intensity.[32,33] The use of masks at the output of the monochromator to check for spectral similarity between the monitored signal and the pattern for a species molecule permits analysis, but only one or two species may be simultaneously detected. Interference with other absorbers is practically eliminated.[34] These correlation spectrometers have found wide use, especially in the ultraviolet region, when only a few species are to be monitored. These instruments, requiring frequency

dispersing elements for use with remote sources or blackbody radiators, are subject to mechanical instabilities and are generally too massive for spacecraft use. In addition, because of low throughput, sensitivity is poor.[35] Good resolution and mechanical stability has been achieved by a Fourier transform spectrometer.[36] Single pass absorption yields 10 ppm sensitivity.[37] These spectrometers combine the properties of good throughput, wide spectral range, high resolution, and rapid scan times. In addition, signal to noise may be increased by averaging a number of scans. Limitations are imposed on sensitivity by the maximum size of the mirror and on resolution by the distance the mirror can move.[38] Both urban point sampling[39,40] and air-borne instruments[36] have performed well. Use of a multipass White cell permits effective path lengths of several hundred meters and a proportional increase in sensitivity.[39]

Various schemes have been attempted to try to avoid the necessity of a monchromator for frequency discrimination. Filters generally have too broad a band pass for good discrimination.[41] The use of a Fabry-Perot with high finesse[42] has resulted in very good resolution and it is tunable over 5.2-6.4μ m of the infrared. NO, NO_2, CH_4, and H_2O all have significant absorption in this region. Gas filter non-dispersive infrared techniques (NDIR) have been recently reviewed.[40,43,44] In a comparison of NDIR with two wet chemical techniques for NO_x detection, NDIR had similar sensitivity but was simpler and faster, required much less complex analytical techniques, and could give measurements every 2-4 seconds.[45] Although NDIR is widely applicable, mechanized detection is limited to 3 or 4 species because a reference cell of each gas to be monitored is required. Sensitivities are in the 0.1-100 ppm range.[46]

Broadband sources may be eliminated if emission from a reference hot gas is used as a species-specific line source. Detection may be by monitoring absorption, fluorescence, or thermal heating of the gas.[44] The reliability and sensitivity of the best of these systems make them good candidates for monitoring the few species unable to be detected by more versatile methods.[28b]

Chemiluminescent monitors also obviate light sources.[47] Their extreme sensitivity (ppb range), rapid response (10 seconds or less)[48] are largely counterbalanced by their need for reagents and frequent calibration for quantitative detection. Their non-specificity, responding to an entire class of reagents, such as NO_2, PAN, nitrates, and nitrites,[49] also hinders quantitative analysis. In addition, only a single compound or class of compounds may be detected in each reaction chamber. Although designs for multiple chamber chemiluminescent monitors exist,[50] complexity is increased greatly. It is unlikely that chemiluminescent methods will find wide application. Other techniques involving photodissociation with conductivity detection[51] or magnetic tuning[52] are generally good for only a single species and not widely applicable. Lasers suggest themselves as radiation sources because of their extremely high spectral brightness.[53] By embodying the frequency discrimination in the source, only simple broadband detection is needed. Absorption lines are collision broadened to about 0.1 cm^{-1} in an atmosphere of air. Pressure broadening and absorption lineshapes will be considered later in the thesis. The spectrophotometric techniques discussed above were able to achieve resolutions of 0.2-0.5 cm^{-1} at best, and much potentially useful spectroscopic information is lost. The spectral bandwidths of lasers can be orders of

magnitude narrower than this, and thus they are capable of resolving absorption lines of different species, which would otherwise overlap and lead to a loss of sensitivity due to interferences. The resolution may be further increased through reduction of sample pressure and hence broadening. Gas filter NDIR methods are the only other spectrophotometric technique which similarly increases in resolution at lower pressures.[40] Absorption peak intensity is not decreased, and the sharper absorption lines result in excellent discrimination. Linewidths continue to decrease until the Doppler broadened limit is reached. Typical Doppler linewidths are on the order of 10^{-3} cm^{-1}. It should be noted that if the molecular line density is such that the lines are less than 10^{-3} cm^{-1} apart, individual lines are not resolvable at any pressure and no gain in sensitivity results from pressure reduction.[44]

Laser Raman methods rely on the inelastic scattering from atmospheric components being shifted from the laser frequency by an amount characteristic of each molecule and proportional to the energy separation between the ground and excited states. All atmospheric constituents are thus detectable by this method.[54] Efficiency of operation is low due to the very small scattering cross sections resulting in most of the laser light being wasted. Also, a monochromator is needed for discrimination of the multi-frequency scattered signal. Weight, stability, and efficiency considerations preclude use of this technique in extraterrestrial applications. Sensitivities in the 10-100 ppm range have been achieved in point sampling applications.[55] The application of Raman LIDAR for remote sensing of pollutants is discussed in a later section of this chapter.

The observation of fluorescence by the gas following an absorption
of a photon at a particular resonant frequency has also been attempted.
The reemission of light is not instantaneous, but occurs after a mean
delay, τ, called the radiative lifetime of the level. The utilization
of the large absorption cross sections in the visible-ultraviolet and in
the infrared make this approach seem promising. Unfortunately, rapid
internal energy redistribution occurs among molecular energy levels,[56]
and the radiated emission occurs over a wide frequency bandwidth, typically
tens of nanometers in the visible.[57] In addition, collisions occurring
during the lifetime of the excited state may result in loss of excitation
non-radiatively. This process is called quenching of the excited
molecule. The rate of quenching collisions is given by

$$Q = \sqrt{2} \, N \, (\sigma^2 / Z) \, \bar{v} \qquad (1)$$

where N is the density of the quenching gas in molecules/cm^3, σ^2 the
kinetic collision cross section, and $\bar{v}$ the average molecular velocity.
Z is the average number of gas collisions required to quench the excited
species. In air at standard temperature and pressure (N = 2.58 x 10^{19} cm^{-3}),
the rate of gas-kinetic collisions (Z = 1) is approximately 5 x 10^9 sec^{-1}.
The quantum yield of fluorescence is given by

$$\phi = (1 + Q\tau_r)^{-1} \qquad (2)$$

where τ_r is the radiative lifetime. If the quenching rate is much
greater than the fluorescence decay rate, very little isotropic emission
will be observed. For electronic transitions in the visible part of
the spectrum, τ_r is typically in the 10^{-5} to 10^{-8} second range.[56,58]
Quenching efficiencies have been measured for a number of common pollutant
species, including NO, NH_3, and SO_2.[59] These quantities can show large

variations, but most systems of interest have Z's on the order of 1 - 10.

For the particular case of optically excited NO_2, $\tau_r \overset{\sim}{=} 4 \times 10^{-5}$ sec

and Z for N_2 quenching is approximately 8, so that $\phi \overset{\sim}{=} 4 \times 10^{-5}$. Values

of quantum yields and effective emission cross-sections for several

atmospheric contaminants are listed in Table IV.[60] These values are

for quenching by an atmosphere of ambient air. These cross-sections

are in the $10^{-22} - 10^{-27}$ cm^2 sr^{-1} range. Fluorescent pollution detection

is thus several orders of magnitude more efficient than Raman scattering,

which has a cross-section of 10^{-30} cm^2 sr^{-1} typically. One elaborate

scheme using many optical filters was able to detect 0.6 ppb NO_2 by its

fluorescence in the red.[61]

Table IV
Fluorescence Quantum Yields for Some Pollutant Molecules

Molecule	Excitation Wavelength in nm	Quantum Yield ϕ	Effective Cross-Section σ_{eff} (cm^2 sr^{-1})
SO_2	300	1.6×10^{-5}	2×10^{-24}
NO_2	400-500	1×10^{-7}	2×10^{-27}
O_3	260	1×10^{-6}	1×10^{-24}
NO	227	3×10^{-3}	3×10^{-22}
OH	308	1.6×10^{-4}	2×10^{-22}

For vibrational fluorescence in the infrared, τ_r is generally 0.01

to 1.0 second. Quenching by collisional deactivation has been measured

for a number of small polyatomic species,[62,63] for which Z varies between

10^2 and 10^4. Water vapor is notoriously efficient in quenching vibrational

excitation.[64] A reasonable estimate for Q for infrared fluorescence

would be 5×10^6 sec^{-1}, and a quantum yield not much greater than 2×10^{-5} should be expected. Values of 10^{-5} and 4×10^{-4} have been estimated for NO fluorescence around its fundamental at 5 μm.[64,65] Thus the signal for fluorescent processes may be quite small and laser light sources will be required. Power requirements are not as severe as for Raman scattering detection, and filters may be used in place of a monochromator. Unfortunately, regions must be found where only a single pollutant absorbs or fluoresces strongly. The necessary diversity of laser wavelengths may not be available with a single tunable laser, and the desirability of the technique is decreased, especially for spacecraft and submarine operation. In addition, quenching strongly depends on the concentrations of various quenchers present and quantitative concentration determination may be difficult.[66] Sample dilution with a gas having a small quenching cross-section provides a reduction of the effect of other quenchers present.[66d]

The energy not reemitted by fluorescence is degraded to thermal energy of the molecules. As we have seen, this may be nearly 100% of the absorbed energy. Detection methods measuring the increased pressure (due to temperature rise) in a sample were proposed originally using broadband sources in non-dispersive configurations. Use of these spectrophones with laser light sources has resulted in tremendously increased sensitivity and specificity. Detection of concentrations at 0.1-10 ppb level has been achieved using high power gas lasers.[67-70] Early predictions claimed that microphone Johnston noise or Brownian motion in the gas cell would be the limiting factor and sub-parts per trillion sensitivities would be possible,[69] but the presence of atmospheric absorbers, such as water, tends to limit the

ultimate sensitivity. Even if no spectral overlap exists, window and wall absorption would give rise to a larger signal than Brownian motion in the microphone.[72] The ultimate sensitivity of the method has been predicted to be 0.1 ppb for air pollutants with strong absorption in a region where water absorption is weak.[73] Use of an acoustically resonant cavity with a feedback loop slaving chopping frequency to a resonant frequency of the absorption cell has been attempted.[72,74] Dewey[72] envisions a system which would achieve the same sensitivity as Kreuzer,[67] but with the use of much weaker laser sources, thus opening the way for the implementation of tunable sources. The resonant enhancement results in an increase in system complexity and a large decrease in reliability. Non-resonant schemes must rely on chance overlaps of strong pollutant absorption with fixed-frequency high power sources.

Heterodyne detection has also been proposed[75] as a method for improving detection system sensitivity. A laser is required to act as a stable frequency local oscillator. The signal, thermal emission lines from hot pollutant gases, and the local oscillator beam are both incident on an infrared detector such as copper-doped germanium. The detector acts as a mixer and in its output there exists a frequency component at the difference frequency between the laser and molecular line centers. The amplitude of this component is linearly proportional to the signal from the gas.[76] If this intermediate frequency (IF) is limited to frequencies less than 1 GHz by the IF amplifier, a single molecular line (at most) may be observed. This IF bandwidth is on the order of the molecular linewidth at atmospheric. If the laser local oscillator is alternately operated at two different frequencies, on and off resonance

with the molecular species, background may be eliminated because the difference in the signals at the two frequencies will be proportional to the molecular concentration. Interference with water vapor emission lines and other species would tend to be the limiting factor in detection sensitivity. Detection of fluorescence using heterodyne detection suffers greatly from the narrow IF bandwidth. Only a single line in the entire fluorescence band may be observed resulting in utilization of only 2% of the fluorescence signal.[63] The noise equivalent power of this infrared heterodyne radiometer is given by the formula[77]

$$N.E.P. = 2 \ (h\nu/\eta) \ (B_{if}/\tau)^{\frac{1}{2}} \qquad (3)$$

where ν is the detection frequency, η is the quantum efficiency of the mixer (which may be as high as 0.5), B_{if} is the IF bandwidth, and τ is the postdetection integration time. At 10 μm for B_{if} = 1 MHz, τ = 0.1 seconds, and η = 0.5, N.E.P. = 2.5 x 10^{-16}W. The N.E.P. of the heterodyne detection method is actually greater than for the ideal direct detection for equal integration times because of the large value of B_{if}, but in the infrared the N.E.P. for the direct detectors is very much greater than ideal due to thermal noise in the detector or circuitry. The N.E.P. for heterodyne detection is on the same order as for photon counting systems in the ultraviolet. As a result, in the infrared a heterodyne detection system may be four to five orders of magnitude more sensitive than an optimized direct detection system.[78] Experimental investigations[76] were able to achieve detection within an order of magnitude of the theoretical limit. Fifty ppm of SO_2 at 390° K was detectable in a meter long path. This method has been adapted as a remote source monitor for smokestacks and other thermal sources when

in the passive mode. Although ambient temperature detection is possible, the method is not as sensitive as NDIR techniques. Applications using a second laser and active monitoring of remote ambient concentrations will be discussed in the next section.

Both opto-acoustic and heterodyne detection schemes are more sensitive than direct detection, but heterodyne methods do not lend themselves well to point sampling and opto-acoustic detection has neither the reliability, stability, nor rapid response of the direct detection schemes[79] and as a result, the detection scheme chosen would depend on the application. For long duration missions, where reliability is essential, a direct detection system is obviously preferred.

Many other proposed detection schemes have severe limitations. Microwave rotational spectroscopy requires low pressures to remove pressure broadening and large amounts of electrical power.[80] Detection limits are in the ppm range. Use of an absorption cell in the laser results in sensitive (sub-ppm) detection, but this process is severely non-linear in absorber concentration and analysis is difficult.[81]

Magnetic tuning of molecules[82] or of the laser[83] and Stark tuning of vinyl chloride[84] has resulted in ppm sensitivities, but these schemes, in addition to requiring electromagnets or parallel electric plates, are not widely applicable and are generally too complex to warrant their implementation as a single gas detector when NDIR techniques have comparable sensitivity.

Laser methods offer significant improvements over blackbody spectrophotometric techniques for both absorption (because of the additional spectral information available) and fluorescence. A direct detection method

to measure the differential absorption of laser emission at many frequencies appears to be very promising both from the standpoint of sensitivity and the possibility of application for monitoring of many pollution species. We will return to considerations of laser detection capabilities when we discuss remote monitoring applications below.

The final point sampling technique that will be considered is a hybrid method involving spectrophotometry and mass spectrometry. Most mass spectrometers rely on an electron beam colliding with the sample and ionizing it. The fragments are detected by their mass/charge ratio after suitable focusing by magnetic or electric fields. If, however, photoionization is used, frequencies may be selected which do not result in the ionization of the major atmospheric constituents. Such a scheme has obtained ppm sensitivities, and envisions ppb MDC levels with ionization frequency maximization.[85]

The use of two-step photoionization involving a tunable infrared photon and an ultraviolet photon not individually capable of ionization has been suggested.[86] Tuning of the infrared frequency would result in changing mass peak patterns in the mass spectrometer output. This two-dimensional variability could be used to distinguish substances with nearly identical mass peak patterns, but different infrared absorption spectra.

D. Remote Monitoring Techniques

Remote monitoring schemes must be based on spectrophotometric methods. Extension of these methods, however, is not straightforward. Broadband incoherent sources soon meet intensity limitations. Substitution

of solar or sky background radiation as a light source has had mixed success.[87-91] Unfortunately, with these light sources, operation is restricted to daylight hours, and performance is severely hampered by rapid changes in sky brightness.[87] In addition, dispersive instruments, with their low throughput, are confined to low resolution work to gain sufficient signal intensity.[88] If direct solar radiation is used, the system's spatial variability is destroyed.[89] Nonetheless, sensitivities in the parts per billion range are achieved for many substances,[89-91] and light source improvement is the obvious remedial action. Here, as in the point sampling applications, the narrow frequency bandwidth, high intensity, and easy beam collimation recommend the use of laser light sources. All the proposed monitoring systems rely on atmospheric attenuation of the beam giving rise to frequency discrimination. Atmospheric attenuation may be simply described by the Lambert relation[92]

$$I/I_0 = \exp \left\{ - \int_0^L \alpha(x) \, dx \right\} \tag{4}$$

where $\alpha(x)$ is the local attenuation coefficient per unit length and I/I_0 is the fraction of radiation remaining in the beam at distance L. Atmospheric attenuation has three major sources: Elastic scattering by atmospheric gases, elastic scattering by aerosols, and absorption by gaseous constituents in beam path. Inelastic Raman scattering by molecules gives rise to a small attenuation also.

The atmospheric elastic scattering component due to scatterers much smaller than the wavelength of the incident radiation is called Rayleigh scattering. It is primarily attributed to scattering by atmospheric gaseous constituents, and is given by the formula:[93]

$$\alpha_R(\lambda) = \frac{8 \pi^3 q^4}{3 \omega_o^4 \epsilon_o^2 m_e^2} \frac{1}{\lambda^4} \qquad (5)$$

where ω_o is the center frequency of the nearest resonance, q is the charge of the electron, m_e is its mass, and ϵ_o is the free space permittivity. Rayleigh scattering is most important in the ultraviolet due to its inverse λ^4 dependence. Values for the Rayleigh elastic scattering coefficients, $\alpha_R(\lambda)$, at different wavelengths are given in Table V.

Table V

Rayleigh and Mie Scattering Coefficients

λ (micron)	$\alpha_R(\lambda)$ (km^{-1})	$\alpha_M(\lambda)$ (km^{-1}) V=1 km	V=5 km	V=10 km
0.2	0.70	7.0	2.2	1.4
0.3	0.14	5.6	1.4	0.84
0.4	0.044	4.7	1.1	0.58
0.6	0.0083	3.7	0.72	0.35
0.8	0.0026	3.1	0.54	0.24
1.0	0.0006	2.8	0.43	0.18
5.0	0.000001	1.1	0.086	0.024
10.0	0.00000006	0.72	0.043	0.010

The elastic scattering by particles or droplets of size comparable to the wavelength of light is called Mie scattering. Because a complex size distribution exists for particles between 0.1 and 10 μm, use is made of an approximate formula relating the Mie elastic scattering coefficient, $\alpha_M(\lambda)$, to the visual range[94]

$$\alpha_M(\lambda) = \frac{3.91}{V} \left[\frac{0.55}{\lambda}\right]^{0.585\ V^{1/3}} \quad km^{-1} \qquad (6)$$

V is the visual range in kilometers and λ is the wavelength in microns. Mie scattering is much less wavelength dependent than Rayleigh scattering. In contrast, Mie scattering is much more a function of changing atmospheric conditions than Rayleigh scattering. Mie elastic scattering coefficients, $\alpha_M(\lambda)$, are also given in Table V for different λ and V values. The combined atmospheric elastic scattering coefficient, $\alpha_E(\lambda)$,

$$\alpha_E(\lambda) = \alpha_M(\lambda) + \alpha_R(\lambda) \tag{7}$$

is plotted as a function of wavelength for various visibilities in Figure 1.[95]

Atmospheric attenuation due to absorption of radiation is related to the concentration of the absorber present by Beer's Law[92]

$$\frac{I}{I_o} = \exp\left(-\int_0^L \sigma(\lambda) \, N \, dx\right) = \exp\left(-\int_0^L \varepsilon(\lambda)c \, dx\right) \tag{8}$$

where I/I_o is the fraction of light remaining at distance L, $\sigma(\lambda)$ is the absorption cross-section (cm^2), N is the number of absorbers present per cm^3, $\varepsilon(\lambda)$ is the molar absorption coefficient per unit concentration per unit length, and c is the molar concentration. The elastic scattering processes have a much more slowly varying frequency dependence than the absorption cross-sections, and thus it is possible to tune across several absorption features maintaining the same elastic background attenuation. However, overlap may exist and several species may absorb radiation of the same wavelength. Infrared monitoring is limited to spectral regions where absorption due to the natural atmospheric constituents CO_2 and H_2O is small. Below 250 nm in the ultraviolet O_2 absorption becomes severe and limits operation distances. Atmospheric constituent absorption interferences are shown in Figure 2.[44,58]

Figure 1: Atmospheric Scattering as a Function
of Wavelength and Meteorological Visibility for a
Number of Different Wavelengths (from Ref. 95)

Figure 2: Atmospheric Constituent Interferences
and Atmospheric Transmission Windows (from Ref. 58)

Figure 3: Background Sky Radiance as a Function
of Wavelength (taken from Reference 58)

FIGURE 1

ATMOSPHERIC SCATTERING AS A FUNCTION OF
WAVELENGTH AND METEOROLOGICAL VISIBILITY
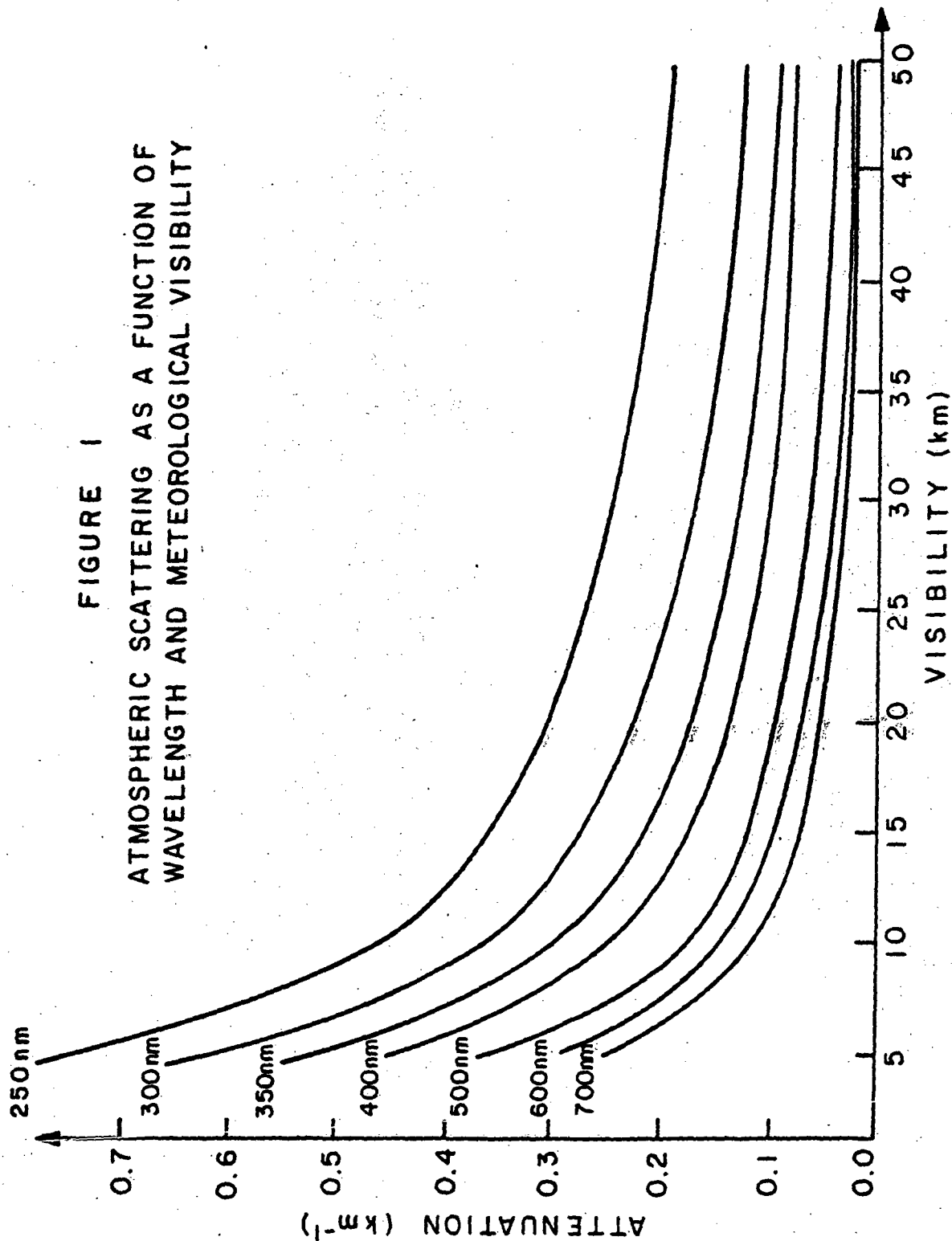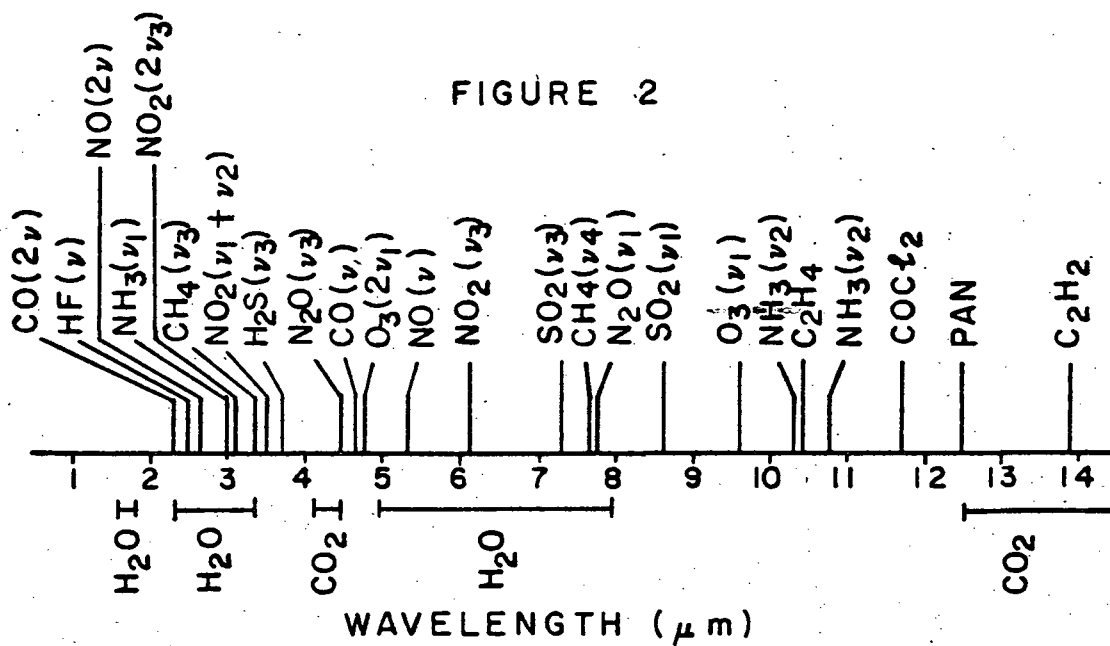
FIGURE 2

FIGURE 3
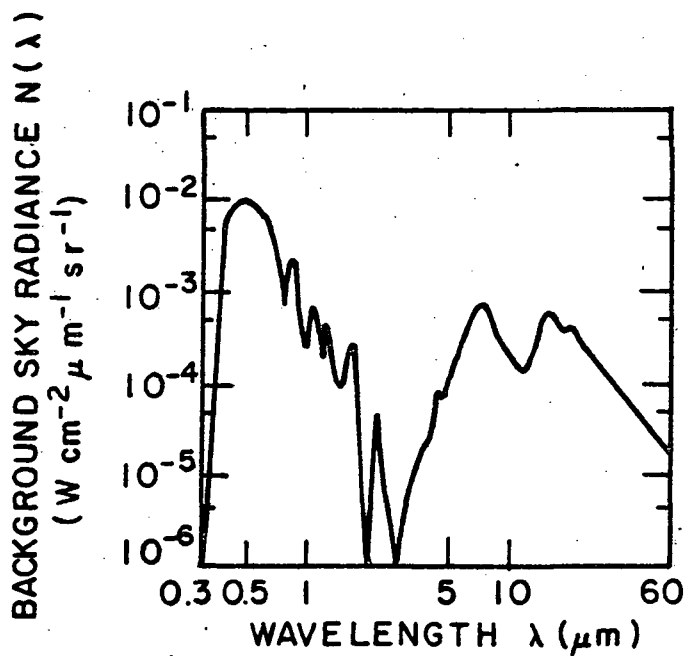
Both single and double-ended absorption monitors have been proposed.[96-110]
Single-ended operation relying on remote reflectors is preferred because
only a single detection system is required. Spatial inhomogeneities are
not detected, only the average concentration in the absorption path is
monitored. Thus we have for this monitoring system

$$I_{sig} = I_{eff} \exp\left[-2L \sum_i \sigma_i(\lambda) \bar{N}_i\right] C' = I_{eff} \exp\left[-2L \alpha_A(\lambda)\right] C' \qquad (9)$$

with

$$I_{eff} = I_o f \exp\left[-2 \alpha_E(\lambda)L\right] \qquad (10)$$

where I_{sig} is the measured intensity of the returned light, L is the
distance to the reflector, $\bar{N}_i$ is the average concentration (cm^{-3}) of
absorber i, $\sigma_i(\lambda)$ is the wavelength dependent absorption cross-section
for species i, I_{eff} accounts for the reduction of signal due to atmospheric
elastic scattering and loss at the remote reflector, f being the fraction
of incident intensity returned by the reflector, and C' is a collection
efficiency factor dependent on beam spread and detector size and efficiency.
The wavelength dependence of $\sigma(\lambda)$ will be different for each absorber,
and by tuning across a sufficiently wide wavelength region, individual species
would be identifiable. Proper choice of wavelength would minimize or remove
absorption overlap simplifying detection of that species. Placement or
choice of reflectors at radially increasing distances from the monitoring
station would permit spatial resolution. Objects such as trees[96] and
buildings [97] have been used as remote reflectors for laser beams. Reflec-
tivities of over ten percent have been achieved using these non-cooperative
reflectors.[111] Because absorption cross-sections are large, $10^{-17} - 10^{-21}$
cm^2,[112] this method should have good sensitivity even for low laser powers.

Before an evaluation of the limitations of this method, laser backscatter techniques will be considered.

Monitoring schemes which rely on atmospheric attenuation to provide intensity which is scattered back in the direction of the detector have been widely proposed. For this situation, the measured intensity of the returned light, I_{sig} is given by

$$I_{sig} = I_{eff} \exp \left[- \{\alpha_E(\lambda) + \alpha_A(\lambda)\} \ L \right]_{back} C \qquad (11)$$

where now

$$I_{eff} = \alpha_j(\lambda) \ D \ I_0 \ \exp \left[-\{\alpha_E(\lambda) + \alpha_A(\lambda)\} \ L \right]_{out} \qquad (12)$$

I_{eff} is the total intensity of the backscattered radiation, and is dependent on the amount of intensity reaching the sampled region $(I_0 \ \exp \left(\quad \right))$, on the length of the sampled region (D) and on the magnitude of the scattering process ($\alpha_j(\lambda)$). Once the radiation is scattered, further atmospheric attenuation, both elastic and absorption, occurs between the scattering region and the detector. Because the radiation is scattered isotropically, the factor C is introduced, which takes into account the solid angle subtended by the detector and the detector efficiency. Range resolution is possible by gating the detection electronics to monitor the backscattered signal at varying delays after the laser pulse. Three different LIDAR approaches to remote monitoring exist: Raman, fluorescence, and differential absorption.

The Raman inelastic scattering cross-section is extremely small, typically 10^3 less than Rayleigh cross-sections, and thus Raman processes were not considered to give rise to significant attentuation of the beam. Like Rayleigh scattering, Raman backscattering has an inverse

λ^4 dependence:[56]

$$\sigma_R(\lambda) = \left(\frac{32\pi^3}{135} \right) \frac{(\nu - \Delta\nu)^4 \, h \, g}{\{1 - \exp(-hc\,\Delta\nu/kT)\}c\Delta\nu} \quad X$$

$$\left(45(\alpha')^2 + 7(\gamma')^2 \right) P \qquad (13)$$

where ν is the wavenumber of the exciting beam, $\Delta\nu$ is the Raman wavenumber shift, g is the degeneracy, h and k are the Planck and Boltzmann constants, T is the temperature of the molecules, α' is the isotropic part of the derivative of the polarizability tensor and γ' is the anisotropic part of that derivative. P is the incident laser power.

Thus,

$$\alpha_j(\lambda) = \sigma_R(\lambda) \bar{N} \qquad (14)$$

in equation (12), where $\bar{N}$ is the average concentration (cm^{-3}) in the sampled region. The λ value used in equation (12) is the laser wavelength. The wavelength of the backscattered radiation in equation (11) is the shifted wavelength, the shift being characteristic of each atmospheric constituent present.[113-118] Some molecular absorption, $\alpha_A(\lambda)$, of the backscattered radiation may occur in addition to atmospheric elastic scattering, further complicating determination of pollutant concentrations. Use of a monochromator or filters at the central detection location would allow possible detection of all trace species.[54] Because tunability is not necessary, more powerful fixed frequency lasers can be used. The ν^4 dependence favors work in the ultraviolet. If an electronic transition of one of the gaseous pollutants happens to be nearly resonant with the laser

frequency, an enhancement of the scattering cross-section of several orders of magnitude can occur.[119,120] The Raman cross-sections of several gases at different wavelengths are given in Table VI. Resonant Raman cross-sections are also shown to demonstrate the enhancement. Unfortunately, the resonant enhancement would be in effect for only, at most, a few species for any given wavelength, and a tunable source, which has lower power levels, would be needed. Because Raman processes are instantaneous,[121] the laser pulse width alone determines the limit of depth resolution by this method. The overlapping of the Raman spectra from various molecules results in loss of some sensitivity. Use of the rotational Raman effect, which has a cross-section a factor of 100 larger than the vibrational Raman effect, has been suggested as possible through use of a Fabry-Perot filter to eliminate pump laser light and much of the background. No monochromator would be needed. The free spectral range of the etalon would be the rotational line separation. A different etalon would be required for each species to be detected.[122]

The remote monitoring of resonant fluorescence emission has also been suggested. Here H_2O and particulate quenchers cannot be removed, and in addition, the fluorescent emission bandwidth requires a wide receiver bandwidth, making background intensity more of a consideration. For fluorescence monitoring $\alpha_j(\lambda)$ in equation (12) is

$$\alpha_j(\lambda) = \sigma(\lambda) \phi \bar{N} \tag{15}$$

where $\sigma(\lambda)$ is the species absorption cross-section at the laser wavelength, ϕ is the quantum yield defined in equation (2) and $\bar{N}$ is the average density of the monitored species in molecules/cm^3. For this

Table VI

Raman and Resonance Raman Cross-sections

Molecule	Raman Cross-section $(cm^2 sr^{-1})$	Wavelength (nm)	Ref.	Res. Raman Cross-section[119] $(cm^2 sr^{-1})$	Wavelength (nm)
O_2	2.5×10^{-30}	347.1	123		
	3.0×10^{-30}	347.1	124		
	2×10^{-31}	694.3	115		
N_2	3.0×10^{-30}	347.1	123		
	2.5×10^{-30}	347.1	124		
	1.9×10^{-31}	694.3	115		
H_2O	9.5×10^{-30}	347.1	123		
	$6-8 \times 10^{-30}$	347.1	124		
NO_2				5.6×10^{-27}	454.7
NO	$0.2-1.0 \times 10^{-30}$	347.1	124	1.3×10^{-23}	226.2
	$1-5.5 \times 10^{-29}$	337.1	56		
CO				4.5×10^{-30}	206.3
SO_2	1.3×10^{-29}	347.1	124	1.0×10^{-25}	300.0
	3.0×10^{-31}	694.3	115		
	4.8×10^{-29}	337.1	56		
NH_3	1.0×10^{-29}	347.1	124		
C_2H_6	1.4×10^{-29}	347.1	124		
CO_2	5.5×10^{-29}	337.1	56		
	$3-4.5 \times 10^{-30}$	347.1	124		
	7.3×10^{-31}	694.3	115		
N_2O	7.3×10^{-30}	347.1	124		

method λ in equation (12) is the laser wavelength and λ in equation (11) is the wavelength band of the output fluorescence. Molecular absorption in equation (11) by species present, including the fluorescing one, could give rise to too low remote concentration estimates. Elastic scattering losses also reduce the returned signal. Laser wavelength constraints are the same as for absorption, a frequency must be found which has a significant absorption cross-section. Excited state lifetimes, even with the presence of quenching collisions, are several microseconds[64] in the infrared, limiting range resolution to 1 km or more. In the ultraviolet, lifetimes are shorter and resolution may be limited to laser pulse duration or electronics gating interval.

The differential absorption technique relies on atmospheric elastic scattering to provide a remote light source which is relatively constant over a range of wavelengths. The differential molecular absorption of this returned signal is then used to determine the average concentration of the absorbing species between the observed scattered region and the detector. Thus

$$\alpha_j (\lambda) = \alpha_E (\lambda) \qquad (16)$$

and the laser and backscattered intensities are at the same wavelength. Elastic scattering occurs instantaneously and the depth resolution is limited only by the laser pulse width. By varying the gating delay, different atmospheric regions are used as the remote source and a radial map of absorber concentrations can be constructed. Here again a tunable source is required and monitoring must be performed in a region where there is a structured absorption pattern. The sensitivity of the method is increased

as the difference in absorption cross-sections between two nearby wavelengths increases. Substituting in equations (11) and (12) for two wavelengths λ and λ' and ratioing the results, we see

$$\frac{I_{sig}(\lambda')}{I_{sig}(\lambda)} = \exp\left[-2\ (\sigma' - \sigma)\ \bar{N}\ L\right] \tag{17}$$

if only a single species absorbs λ and λ'. Even if several species absorb, monitoring of a sufficient number of frequencies should allow determination of all absorbers present. The value of I_{eff} may be small on clear days or at larger distances on foggy days, resulting in a low signal level returned to the detector. As in the absorption method, the returned signal is at the laser frequency and narrow bandwidth detection is possible.

We now have a sufficient basis for comparing the remote detection schemes. Many comparisons have been performed previously,[56,58,62,125,126] but none considered all of these methods together or attempted to compare them with as few variables as here. Rewriting the equations for each of the proposed monitoring schemes yields

$$I_{sig} = I_o\ \exp\{-2\ \alpha_E L\}\ \left[f\ C'\ \exp\ \{-2\ \alpha_A L\}\right] \qquad \text{Absorption with reflector}$$

$$I_{sig} = I_o\ \exp\{-2\ \alpha_E L\}\ \left[f\ C'\ (.05)\ \exp\{-2\ \alpha_A L\}\right] \qquad \text{Absorption with non-cooperative target}$$

$$I_{sig} = I_o\ \exp\{-2\ \alpha_E L\}\ \left[D\ C\ \exp\{-\alpha_{A_{out}}\ L\}\ \sigma(\lambda)\ \phi\ \bar{N}\right] \qquad \text{Fluorescence backscatter}$$

$$I_{sig} = I_o\ \exp\{-2\ \alpha_E L\}\ \left[D\ C\ \sigma_R(\lambda)\ \bar{N}\right] \qquad \text{Raman backscatter}$$

$$I_{sig} = I_o\ \exp\{-2\ \alpha_E L\}\ \left[D\ C\ \exp\{-2\ \alpha_A L\}\ \alpha_E(\lambda)\right] \qquad \text{Differential absorption backscatter}$$

Henceforth, we let $S = \left[\qquad\qquad\qquad\qquad\right].$

The assumptions that have been made are:

1. $\alpha_E(\lambda)_{out} = \alpha_E(\lambda)_{back}$ for Raman and fluorescence backscatter.

2. $\alpha_A(\lambda)_{out} = \alpha_A(\lambda)_{back} = 0$ for Raman backscatter.

3. $\alpha_A(\lambda)_{back} = 0$ for fluorescence backscatter.

4. A 5% reflectivity from the non-cooperative remote reflector.

Assumptions 2 and 3 would give rise to a larger return signal than would be the case if atmospheric absorption was not zero. The factor $I_o \exp\{-2\alpha_E(\lambda)L\}$ is common to all schemes and will be neglected temporarily. Let us now determine the relative returned signal from a pollutant present at low concentrations, 1 km distant. Range resolution will only be 300m, finer resolution will result in proportionally decreased signals. The value of $\sigma_R(\lambda)$ is chosen as 10^{-28} cm^2· molecule^{-1} steradian^{-1}, $\sigma(\lambda)$ as 3×10^{-19} cm^2/ molecule steradian,[58] and ϕ as 10^{-2} to 10^{-6}. Values of the terms compared, S, are given in Table VII for 1 ppm and 10 ppb average pollution concentrations, and for different remote distances from the detector. Use of 10cm radius collection optics and 10% photon to signal efficiency gives $C = 1 \times 10^{-9}$ at 1 km. fC' has been previously estimated as less than 10^{-4}, depending on beam collimation and reflector size, using a similar scheme to that above.[100]

As expected, the return signal for absorption is many orders of magnitude greater than the rest. For all the absorption schemes, not the total signal returned, but the change in signal as a function of wavelength is important. Thus, if a 1% change in signal is just barely detectable, and the change in absorption coefficient in

Table VII

Comparison of Remote Monitoring Techniques

Method	Concentration		Values of S for Remote Ranges, L, of .		
		10 km	1 km	100 m	10 m
Absorption	1 ppm	1.7×10^{-12}	2.1×10^{-5}	8.6×10^{-4}	9.8×10^{-3}
with Reflector	10 ppb	8.6×10^{-6}	9.8×10^{-5}	1.0×10^{-3}	1.0×10^{-2}
Absorption with Topographical Reflector	1 ppm	8.5×10^{-14}	1.1×10^{-6}	4.3×10^{-5}	4.9×10^{-4}
	10 ppb	4.3×10^{-7}	4.9×10^{-6}	5.0×10^{-5}	5.0×10^{-4}
Raman	1 ppm	7.8×10^{-22}	7.8×10^{-20}	2.6×10^{-18}	2.6×10^{-16}
Backscatter	10 ppb	7.8×10^{-24}	7.8×10^{-22}	2.6×10^{-20}	2.6×10^{-18}
Fluorescent Backscatter	1 ppm $\phi=10^{-6}$	9.7×10^{-22}	1.1×10^{-16}	2.2×10^{-14}	2.3×10^{-12}
	1 ppm $\phi=10^{-2}$	9.7×10^{-18}	1.1×10^{-12}	2.2×10^{-10}	2.3×10^{-8}
	10 ppb $\phi=10^{-6}$	2.2×10^{-20}	2.3×10^{-18}	2.4×10^{-16}	2.4×10^{-14}
	10 ppb $\phi=10^{-2}$	2.2×10^{-16}	2.3×10^{-14}	2.4×10^{-12}	2.4×10^{-10}
Differential	1 ppm	$5.0 \times 10^{-19} V$	$6.3 \times 10^{-11} V$	$8.7 \times 10^{-9} V$	$9.7 \times 10^{-7} V$
Absorption	10 ppb	$2.6 \times 10^{-12} V$	$2.9 \times 10^{-10} V$	$1.0 \times 10^{-8} V$	$1.0 \times 10^{-6} V$

of Backscatter where $V = 5.1$ for visibility of 1 km at 400 nm.

$V = 1.5$ for visibility of 5 km at 400 nm.

$V = 0.043$ for visibility of 5 km at 10 μ m.

equation (17) is 1.5×10^{-19} cm^2/molecule.steradian, we have

$$\left| \frac{I_{sig}(\lambda')}{I_{sig}(\lambda)} \right|_{min} = \exp\left\{-2(\sigma'(\lambda) - \sigma(\lambda)) \bar{N}L\right\} \qquad (17)$$

$$\ln(0.99) = -2(1.5 \times 10^{-19}) \; cm^2/molec.\cdot str \; (\bar{N}L)$$

$$(\bar{N}L)_{min} = 1.2 \times 10^3 \; ppm\text{-}cm \qquad (18)$$

and if a minimum range resolution of 300m is desired, 0.041 ppm is the

minimum detectable concentration for this resolution for any distance

where $I_{sig}(\lambda)$ is significantly above background.

As a comparison, the standard wet chemical Saltzman method would require

six hours of preconcentration in order to achieve this sensitivity. The

sensitivities of various methods for detection of NO_2 are presented in

Table VIII. The remote methods are all listed for 300m range resolution.

It is seen that the differential absorption method provides comparable

or superior sensitivity to the other remote monitoring schemes, and is

capable of detecting ambient NO_2 at a level below the EPA Maximum Exposure

Level for this resolution. Point sampling methods are currently more

sensitive, but if remote monitors are capable of sufficient sensitivity

to monitor ambient concentrations, a single remote probe will obviate an

entire network of local point samplers. Currently, equivalency standards

between path and point monitors are being set.[130] Once these relations

are established, remote monitors may be used to establish the adequacy of

a point monitor to represent the ambient conditions in its local area.

We will now consider the range capabilities of the various remote detection

schemes.

Photon limited detectors in the visible have minimum detectable powers

of 9×10^{-11} W, if background radiation power is comparable or smaller in

Table VIII

Detection Capabilities for NO_2 for Various Techniques

Method	Detection Limit in ppm	Reference
Point Sampling:		
Saltzman (colorimetric) Method with 1 hour preconcentration	0.24	45,127,129
Phenoldisulfonic Acid	10	128
Derivative Absorption Spectroscopy with multipass cell	0.01	33
Chemiluminescence	0.01	48
Fluorescence	0.001	61
Optoacoustic	0.0001	67
Remote Monitoring:		
Non-dispersive Infrared	10	90b
Fluorescence	1	60
Differential Absorption of Back-scattered Radiation (visible)	0.15	145
Differential Absorption of Back-scattered Radiation with Heterodyne Detection (infrared)	0.2	78
Absorption	0.04	Predicted, this work.

magnitude.[58] _[See Appendix I.]_ The background power received at the

detector for an extended source filling the receiver field of view is

$$I_{background} = \exp\{-(\alpha_E(\lambda) + \alpha_A(\lambda))L\} \, \Delta\lambda \, V \, A \, N(\lambda) \qquad (19)$$

where $\Delta\lambda$ is the optical bandwidth of the system, V is the field of

view of the collection optics, and $N(\lambda)$ is the spectral radiance of

the background source. The spectral radiance of the sky under clear

daytime conditions is shown in Figure 3.[58] In the visible

$N(\lambda) = 10^{-2}$ watts cm^{-2} μm^{-1} steradian^{-1}. For the absorption schemes

the optical bandpass may be very narrow (10^{-3} μm) and for 1° field of

view and for a 1 μsecond gate time (300m resolution),

$$I_{background} = 1.5 \times 10^{-11} \text{ W}$$

for 5cm radius collection optics, and these methods are not background

limited. Assuming a 100 KW, 1 μsecond tunable laser in a wavelength

region where significant absorption changes occur we have, substituting

in equations (11) and (12) using Table VII, for absorption using the

atmospheric attenuation coefficients in Table V

$$I_{sig}(\lambda) = 10^5 \text{ W} \times 4.6 \times 10^{-2} \times 2.1 \times 10^{-5} = 9.7 \times 10^{-2} \text{W for 1 ppm V=5km}$$
$$= 4.5 \times 10^{-1} \text{W for 10ppb V=5km}$$

for 1km. $I_{sig}(\lambda)$ values for absorption, and differential absorption of

backscattering are given in Table IX for various distances and visibilities.

Note that $I_{sig} \cong I_{background}$ at much smaller distances for the backscattered

signal. Note also that both methods are useful at greater distances in

the infrared. This calculation does not take into account atmospheric

absorption by atmospheric gases in the infrared where total atmospheric

attenuation is about 1% per kilometer[131-133] and poses no serious

Table IX

Comparison of Absorption and Differential Backscatter Methods

Method	Visibility (km)	Wavelength (μm)	Signal in Watts for 10ppb Pollutant Concentration over Ranges of 10 km	1 km
Absorption	10	0.4	1.8×10^{-9}	1.3
with	5	0.4	0	4.5×10^{-1}
Reflectors	1	0.4	0	3.4×10^{-4}
	10	10	7.0×10^{-1}	9.6
	5	10	3.6×10^{-1}	8.9
	1	10	4.8×10^{-7}	2.3
Differential	10	0.4	5.4×10^{-16}	3.9×10^{-6}
Absorption of	5	0.4	0	2.0×10^{-6}
Backscatter	1	0.4	0	5.1×10^{-9}
	10	10	2.1×10^{-9}	2.8×10^{-7}
	5	10	4.7×10^{-9}	1.1×10^{-6}
	1	10	1.0×10^{-13}	4.9×10^{-6}

limitation to beam transmission.

Using a similar laser to detect fluorescence backscattering yields

$$I_{sig} (\lambda) = 10^5 W \times 4.6 \times 10^{-2} \times 1.1 \times 10^{-12} = 5.1 \times 10^{-9} \text{ for 1ppm V=5km}$$

$$= 5.1 \times 10^{-11} \text{ for 10ppb V=5km}$$

However, for fluorescent reemission a broader observation bandwidth is neces-
sary, unless much of the signal is to be lost.[64] Using a 50nm bandwidth
in equation (18) yields $I_{background} = 7.5 \times 10^{-10}$ W/ μsecond. Limitation
of the gate width to 1 μsecond may also result in the loss of some signal
intensity. It is seen that although a single pulse may be able to detect
1 ppm (S/N = 1), 10^4 pulses, at least, and signal averaging are needed for
10 ppb sensitivity, and real-time aspect may be lost.

Raman backscatter may make use of a fixed frequency laser having a 10 MW, 100 μsecond pulse. Then

$$I_{sig}(\lambda) = (10^7 W) \times 4.6 \times 10^{-2} \times 7.8 \times 10^{-20} = 3.6 \times 10^{-14} W \text{ for 1 ppm } V = 5 km$$

Increasing size of the collection optics will result in an increase in background radiation also. By increasing collection optics size to 50 cm radius, while decreasing field of view to $0.01°$ (2×10^{-4} steradian) the background radiation power may be held constant while I_{sig} is increased by 10^2. Nevertheless, 10^3 pulses are required to achieve 1 ppm sensitivity, 10^7 pulses for 10 ppb sensitivity. All real-time information would be lost in the time required for this large number of pulses of these low repetition rate lasers. It has, in addition, been assumed that all background interference by elastic atmospheric scattering was removed by the monochromator or filter. Because elastic scattering cross-sections are 10^3 larger than Raman cross-sections, and the Raman signal arises from only 10^{-6} of the molecules present (1 ppm), the elastic signal may be 10^9 larger and not be completely removed by frequency filtering.[58] The resulting sensitivity increase for resonance Raman scattering is at least partially canceled by 10^2 lower assumed power for a tunable laser. Raman schemes have had some success at detecting remote sources of pollution up to a kilometer distant with sensitivities in the 0.1 - 100 ppm range depending on the complexity of optical detection system.[134-139]

A few fluorescence backscattering schemes have been proposed,[56,60,64] but none as yet has been implemented. Differential absorption techniques have been optimistically touted as a method providing range resolution

with large return signal levels.[97,98,140-143] Several experimental investigations using tunable visible lasers have resulted in 0.1 - 1 ppm detection limits for 300m resolution for SO_2 and O_3[144] and NO_2.[145-147] Alternate operation at two wavelengths was used for differential absorption. Simultaneous operation on two different wavelengths 1.3 nm apart has been achieved through use of an intra-cavity Glan-Thompson prism and two different gratings.[97] In this configuration, atmospheric turbulence effects, as well as attenuation effects, are minimized. Nevertheless, because of the relatively small backscattered signal, workers using this method required 11 hours to map the concentration of NO_2 in a 300m x 400m area, 750m distant, with a 100m resolution.[147] Over 4×10^4 laser pulses were required. Obviously, mapping time could be decreased by technological improvements giving rise to a faster pulse repetition rate, but this method currently seems far removed from a city-wide monitoring network using a visible laser. With the application of heterodyne detection techniques, detection quantum efficiencies in the infrared approach those of visible detectors. Here again minimum detectable concentrations of pollutants are expected to be in the 0.1 ppm range.[148,78] In the infrared interference from water vapor lines tends to limit the sensitivity of the method since atmospheric scintillation is much less than in the visible.[149] In view of this, several authors have claimed ultimate sensitivities in the 10 ppb range for regions free of interference.[150,151]

Use of heterodyne detection for passive remote monitoring has been proposed[152,153] and results in a sensitivity of 0.1 - 10 ppm. A similar increase in range and sensitivity would result if heterodyne detection were

used in a differential absorption monitor. The additional expense and increase in complexity is probably not warranted for this technique, which already has excellent capabilities in both these areas.

E. Conclusions

It has been demonstrated that absorption methods are capable of sensitivities comparable or greater than other remote monitoring schemes, while having a much larger signal returned to the detector. Sensitivity is increased with distance sampled. The use of multipass cells[39,44] should permit similar sensitivities for point sampling applications. In this situation where background may be neglected, low power cw lasers may be used. The low power requirements of the absorption techniques make it especially desirable. Eye safety maximum permissible exposure (MPE) set by the American National Standards Institute are 5×10^{-7} J cm^{-2} in the visible, and $0.56t^{1/4}$ J cm^{-2} in the infrared.[62] The MPE value in the visible will severely restrict use of high energy pulse lasers in urban applications. The IR standard may be easily met for both pulsed and cw operation.

Because the absorption technique appears promising both for point and remote monitoring, and because the minimum absorption requirements are not stringent, there exists the possibility of being able to use a single laser source to simultaneously detect many atmospheric contaminants. Experimental work has been undertaken in order to further evaluate the desirability of this method.

II MONITORING COMPLEX MIXTURES OF TRACE CONTAMINANTS

A. Introduction

It was seen in the previous chapter that a laser monitoring scheme which is capable of detecting a single substance with no interference from other pollutants present may be desirable as a species-specific detector, but such a scheme would require a complex monitoring network of many different lasers to adequately monitor ambient air quality. A necessary consequence of the versatility to be gained by operation in the infrared is the possibility of spectral overlap between different absorbing species. Due to spectral complexity, a reference frequency marker is needed to insure reproducibility and accuracy if a continuously tunable laser source is used. All other frequency measurements could then be made with reference to this frequency. On the other hand, if a line-tunable CO_2 laser is used, the laser lines may be carefully stabilized to the zero velocity molecular transition frequency, and reproducibility ensured. Knowledge of the absorption coefficients of each gas at selected laser frequencies will permit the absorption of a mixture of these gases to be assigned to the relative abundance of each absorber, provided a _sufficient_ number of frequencies are used.

This project was to determine the feasibility of using a frequency stabilized CO_2 laser for the detection of each trace component in a mixture of absorbers and to find the number of frequencies required for sensitive reproducible detection. The experimental work consisted of three parts:

     1. Frequency stabilization of the CO_2 flowing gas laser;

2. Setting up a detection system capable of detecting a wide range of attenuations to permit accurate absorption coefficient determination for a number of likely contaminants;

3. Analysis of mixtures of these gases to test the detection capabilities of this absorption method.

A CO_2 laser was chosen because the laser frequencies, which span the 929 cm^{-1} to 1082 cm^{-1} region of the infrared, are in an atmospheric transmission window. Water vapor absorption is insignificant for short path lengths.[131] Molecular oxygen and nitrogen do not absorb anywhere in the infrared. Thus, absorption will be due solely to atmospheric contaminants, providing high information content in the detected signal. Because over 100 laser transitions have been observed for the CO_2 laser,[217] there is a large degree of freedom in number and choice of wavelengths to be used for mixture monitoring.

B. Laser and Detection System

The CO_2 laser gain medium was a water-cooled low pressure flowing gas electrical discharge sustained by a current regulated 10 kV power supply. The laser cavity is composed of a curved mirror (f = 5m) with a centered output hole and a grating blazed for 10μm (Bausch and Lomb). An intracavity iris diaphragm near the front mirror confines lasing to the TEM_{00} mode on a single transition and controls output power levels. Instabilities in the laser frequency and intensity arise from linear expansion of the aluminum support girder due to thermal fluctuations. As a result, the frequency of the cavity modes are shifted. The resultant laser frequency is pulled off the peak of the gain curve

to a frequency intermediate to the frequencies of peak gain in the laser medium and cavity gain. To insure that the CO_2 laser frequency is stable, the maximum of a cavity mode is kept centered on the gain distribution of the medium. This is done by mounting the cavity mirror on a piezoelectric transducer. A reference sine wave is generated by a lock-in amplifier (PAR Model 120), is then amplified by a KEPCO OPS 2000 Op-Amp and applied to the transducer. The resultant mechanical oscillations of the mirror produce synchronous fluctuations in the laser intensity as the cavity mode (and hence the laser frequency) is swept across a small part of the medium's gain curve. The laser intensity fluctuations are monitored by an InSb detector (Opto-electronics Mullard type ORP-10) looking at the laser output off the normal to the grating. The AC part of the detector signal is proportional to the slope of the gain curve and is smallest when the oscillation of the mirror is centered on the maximum of the gain curve, which corresponds to the zero velocity molecular transition frequency. The magnitude of this AC signal is the output of the lock-in amplifier when the detector signal is the input. The output of the lock-in is introduced in the high voltage KEPCO Op-Amp to produce a bias voltage on the transducer sufficient to center the mirror on the maximum of the gain curve.

This circuit was originally implemented by Nowak,[218] but it was discovered that the Spectra-Physics 510 Transducer used in his set-up was designed for positive voltage. The KEPCO supply is capable of producing negative high voltage only. It is doubtful that the crystal ever responded correctly to voltage of the wrong polarity. A new transducer (Burleigh Model PZ-90) which was compatible with the supply

was ordered. It was then discovered that the supply was capable of outputting up to a 3 KV transient when turned off or to 2 KV if driven by sufficient input. The transducer was designed for 1250 V maximum, either polarity. Thus it was necessary to set up a network which would limit the maximum output voltage and allow the contribution from each of the inputs to the Op-Amp to be of the correct magnitude. The circuit is shown in Figure 11. The voltage divider at the output prohibits the voltage seen by the transducer from exceeding 1130 V for a 2000 V maximum output. These resistors permitted, at most, 2 ma to flow out of Op-Amp and do not seriously load the Kepco amplifier or hamper its frequency response. The gain of the Op-Amp for each of the inputs could be calculated using the relation[219]

$$G = R_f / R_i \qquad\qquad (22)$$

where R_f is the total resistance at the output of the Op-Amp, and R_i is the effective input series resistance. The response of the transducer was 8 μm/1000 V. A 5 μm mirror translation would result in an integral change in the number of wavelengths in the cavity.[218] Allowing the lock-in output to cause, at most, a shift of half this amount would permit maximum compensation capabilities while ensuring the two cavity modes would not be simultaneously competing. A series resistance of 16.56 KΩ was introduced into this input to the Op-Amp and correspondingly the maximum high voltage output that could arise from the lock-in signal was 310 V (2.5 μm translation). The sine-wave reference signal was amplified to give rise to a 0.5μm peak to peak oscillation of the mirror at the reference frequency. The magnitude of the amplified signal from the manual voltage

Figure 11: Frequency Stabilization Network

Figure 12: Lock-In Amplifier Sensitivity Scale
Gain Calibration Network

FIGURE II

DETECTOR

X·100 PRE - AMP

LOCK IN AMPLIFIER

SIGNAL   REFERENCE   OUTPUT

$R_i = 37 K\Omega$

$R_i = 1K\Omega$

$R_f = 10M\Omega$

$R_i = 17K\Omega$

MANUAL VOLTAGE BIAS

KEPCO OP-AMP OPS 2000

$612 K\Omega$

$474 K\Omega$

MOV

To PZT

FIGURE 12

SIGNAL

PRE-AMP

LOCK IN AMPLIFIER

$10K\Omega$ GAIN TRIM RESISTOR

EXTERNAL SWITCHING NETWORK
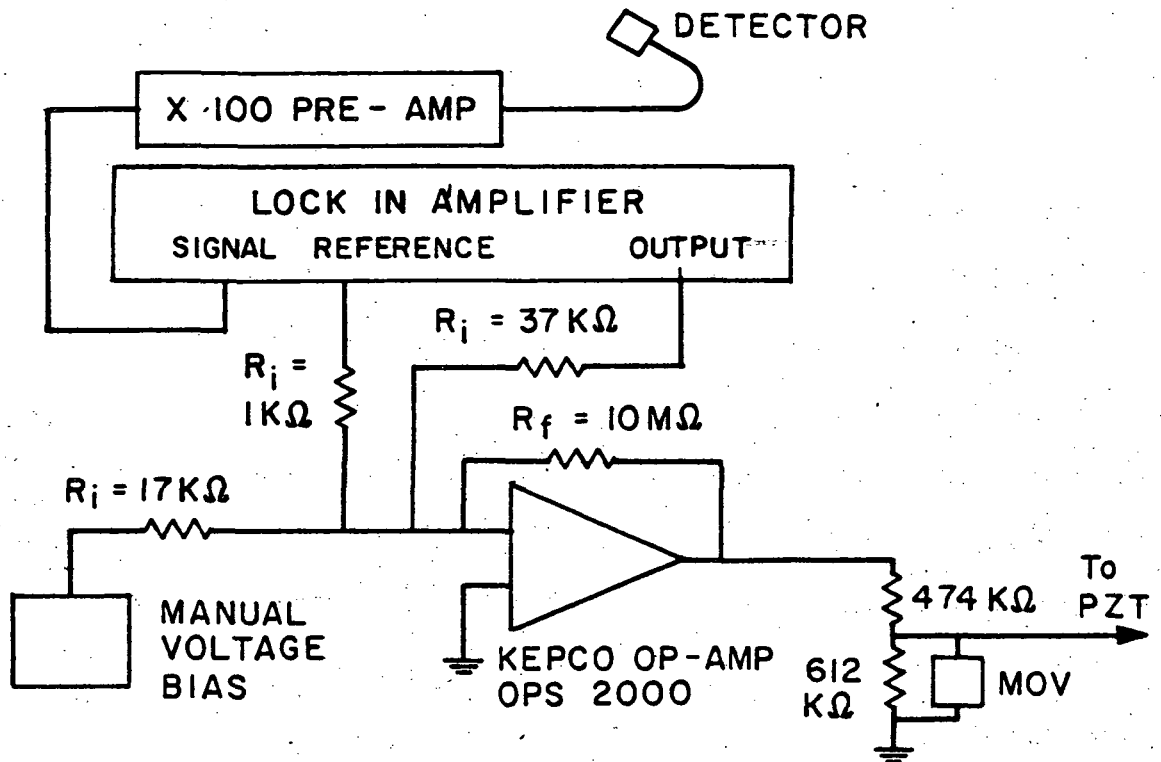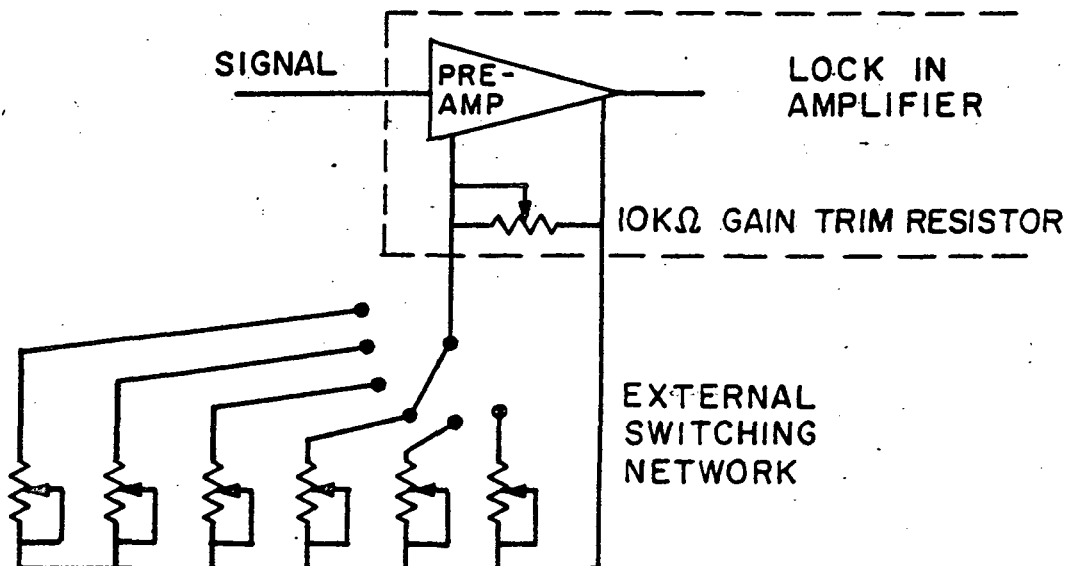
offset was adjusted to permit maximum flexibility while maintaining a safe operating environment for the crystal. A manual offset of 6.8μm was possible, insuring that a cavity mode would always be within the biasing range. A pair of General Electric Metal Oxide Varistors (V420PA406 Power MOV) were connected across the output in parallel to the transducer. These devices have essentially infinite resistance below a 1000 V input and a rapidly decreasing resistance above this value. With these MOV in the circuit, voltage spikes were prevented from harming the transducer. With these adjustments, the transducer was capable of following cavity length fluctuations for periods of 1/4 - 2 hours without manual adjustment. This period is exclusively a function of the room temperature fluctuations. The only remaining frequency instability is due to the oscillation introduced by the reference sine wave. This results in a $\pm$ 4 MHz oscillation about the center of the gain curve.

Cavity alignment procedure was as follows:

1. A helium-neon laser was positioned so that it passed through the mirror hole and was incident on the grating. The laser plasma tube was centered around this optic axis.

2. The zeroth order reflection off the grating was found by manually rotating the grating around the optic axis and locating a spot which did not rotate.

3. With the reflected orders off the grating all lying in a horizontal plane, the 17th order spot was sent back down the optic axis and through the hole in the front mirror. Due to mode impurities, not all the laser light passes out of cavity.

4. The ring of reflected light off the front mirror was then positioned along the optic axis by adjusting the front mirror.

5. The Brewster angle window holders were secured to the end of the glass tube, and slight readjustments of optical mounts were made to align cavity exactly. The laser light was introduced into a monochomator using a $f = 4$ cm Ge focusing lens. Resolution of the monochromator was sufficient; observed slitwidths were five or six times less than the line separations. Lasing on a single line was observed for each laser grating setting. If more than one line is lasing, the intensity of the adjacent lines is less than 1.5% of the major laser line.

Because a low maintenance system is desired, pyroelectric detectors which operate at ambient temperatures were chosen. These Barnes T-301 Detectors were 1 mm^2 in area and capable of handling up to 1 W cw. Responsivity was 1.5 $\mu a/W$ for chopping frequencies below 500 Hz. These detectors were found to be susceptible to electrical noise and thermal fluctuations in the room. Accordingly, they were shielded and enclosed as completely as possible. To insure that all of the laser beam was incident on the small detector elements, a pair of 1" f/1 Irtran lenses were used to focus the light onto the detectors. These lenses also helped insulate the detectors from air currents. The signals from these detectors are put into a pair of PAR lock-in amplifiers. With this configuration the measured laser intensity was stable to 0.2% over a few minutes and 0.7% stable over the period between manual adjustment of the voltage bias offset. Thus the stabilization of the frequency, as expected, results in a stabilization of the laser intensity as well. The dual channel detection scheme was implemented to eliminate errors due to short term intensity fluctuations.

The lock-in amplifier's gain may be calibrated for the least sensitive scale, but the error in the accuracy of the gain for the more sensitive scales may be $\pm$ 5%.[220] To permit accurate readings of the detector's signal for high attenuations (small signals), a set of multi-turn poten- tiometers were inserted in parallel with the gain trim resistor of each lock-in. With proper switching, these resistors permitted accurate cali- bration of each sensitivity scale ranging over a factor of 50. This circuit is shown schematically in Figure 12. Calibration was performed using a voltage divider network and the internal reference frequency sine wave of each lock-in. One sensitivity scale was calibrated against the next, and interscale gain errors were reduced to a negligible magnitude in this manner. Any nonlinearities in response should be due to detector limitations and not detection circuit errors.

A current-buffered analog divider network was constructed to permit ratioing of the two signal channels. An Intronics M 506 Multiplier and 904 Analog Devices Power Supply were used [see Figure13]. Because the integrated cirucit was designed for multiplication, the division becomes unstable for small denominators. Since interscale switching errors had been eliminated, the input signals into the divider need never be less than 4V. The output of the divider network is given by

$$Y = 10 \ Z/X \hspace{3cm} (23)$$

where Y is the ratio in volts, Z the signal from the sample channel lock-in, and X is the signal from the reference channel lock-in. X must be negative in sign. The terminals are labeled in the circuit diagram. Calibration of the divider network was performed using stable voltage sources

Figure 13: Dual-Beam Divider Network

The 741C chips act as current buffers for

analog divider network. X_0 and Out Trim

permit zeroing and calibration. Z is the numer-

ator, X is the denominator and Y is the output

ratio. 15 Voltages (+ and -) must be

supplied.

FIGURE 13

-56-
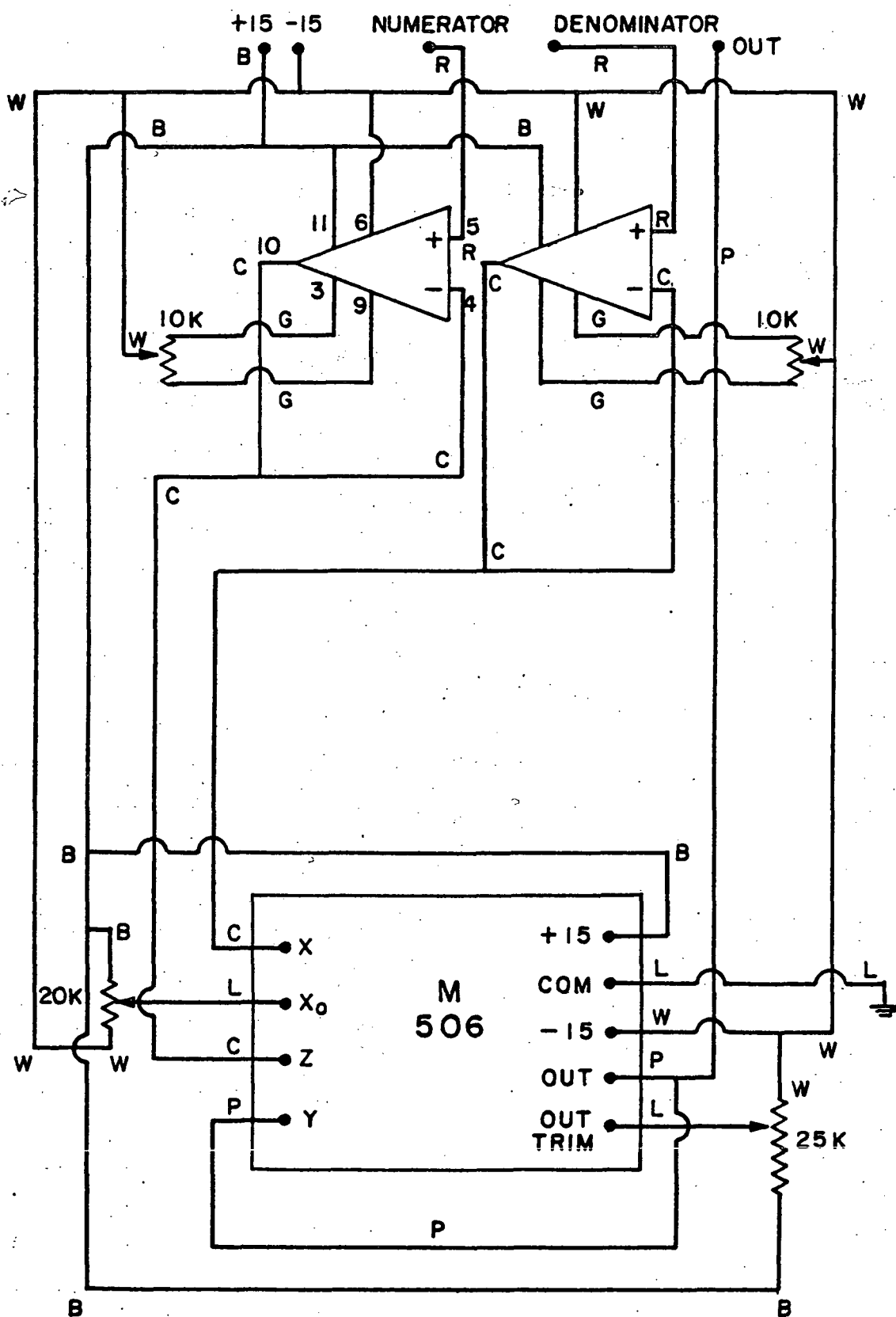
(Heathkit IP 18) and a 4½ digit digital multimeter (Data Precision Model 245). After the output trim potentiometer was zeroed for zero input numerator, the trim pots for the numerator and denominator were adjusted to minimize the error for all inputs between four and ten volts, $| Z | < | X |$. In this manner the error in the divider network could be kept to less than 0.7% for all input signals, and less than 0.2% for denominators larger than 8.5 V. The ratio of the laser signal in the two beams displayed on the digital multimeter was found to be stable to ± 0.8% and reproducible from day to day to greater than 2%. Because of the day to day variation, all measurements were made cell in - cell out. Variable density beam attenuators (polyethylene film) were used to adjust for intensity variation in the different laser lines. These permitted the reference channel lock-in to observe a nearly full scale signal at each frequency, and as a result, divider circuit errors were minimized.

The cell used for the absorption measurements was 50 cm long, 5 cm in diameter, and was fitted with NaCl windows. In this detection scheme, all laser output frequencies are collinear and no variation of the ratio of the two channels with frequency was expected or observed. The absorption of the empty cell was measured at each wavelength. The measurements were found to have a standard deviation of 1.5% (108 values). Some attenuation variation with frequency was observed, and remains unexplained. Great care was taken to reposition the absorption cell consistently. It has since been learned that the pyroelectric detectors exhibit a non-linear response acorss the face of the detector, and that slight variations in angle and position of the beam incident on the

focusing lens might result in signal variations. This change could
result from thermal expansion of the steel beam supporting the detector or
slight changes in the spatial position of the laser beam.

C. Absorption Coefficient Determinations

Absorption coefficients were determined from equation (21):

$$\sigma NL = \varepsilon CL = A = -\left[\ln(I/I_o)_{cell \ \& \ sample} - \ln(I/I_o)_{cell}\right]$$

The reproducibility in A values is listed in Table XIII for various amounts
of attenuation by the sample. It is seen that large attenuations give rise

---

Table XIII
Data Precision for Various Sample Attenuations

I/I_o *	No. of Points	σ**	Typical A with 95% Confidence Limits for Normal Distribution (2σ)
0.5-0.3	27	.013	2.00 ± .026 (1.3%)
0.15-0.11	33	.013	4.00 ± .026 (0.7%)
0.07-0.04	72	.03	6.00 ± .06 (1.0%)
0.025-0.007	13	.03	9.00 ± .06 (0.7%)

---

* $I/I_o = (I/I_o)_{sample \ \& \ cell} \Big/ (I/I_o)_{cell}$

** $\sigma = \left(\frac{1}{N-1} \sum_i \delta_i^2\right)^{\frac{1}{2}}$

---

to A values which are more reproducible than small attenuations. For small
attenuations the two terms in parentheses are of comparable magnitude and
the uncertainties in each contribute to the uncertainties in A, while for
larger attenuations the first term will be dominant and the errors in A
will be due exclusively to that term alone. For very small attenuations
the uncertainties in the two ratios are on the order of their difference

and A is completely uncertain. Because the gain of each sensitivity scale of the lock-in was calibrated, little loss of accuracy occurred for small signals. Thus an effort was made to obtain large attenuations for as many laser wavelengths as possible for each gas, in order to achieve maximum accuracy and precision. The uncertainty in A was estimated to be 3% for I/I_o between 0.5 and 0.9.

Reagent grade chemicals were used whenever possible for these determinations. All samples were further purified by a freeze-pump-thaw cycle repeated several times before use. All pressures were measured on a dibutyl phthalate vacuum manometer. Readings were taken with a cathetometer and are accurate to $\pm$ 1.5% or 0.04 Torr, whichever is greater. The manometer response was found to linear and accurate when compared with a Hg McLeod gauge. Absorption in the manometer was found to be negligible during pressure measurements, and the manometer was pumped on thoroughly after each use. Pressures up to 35 Torr could be measured using the manometer (ρ = 1.046 g/cc, 25°c). The absorption coefficients of the fifteen gases listed in Table XIV were measured at the 52 strongest lines of the CO_2 laser. These are the P(6) - P(36) and R(6) - R(32) lines of the $00^{\circ}1 - 10^{\circ}0$ transition and the P(8) - P(34) and R(10) - R(24) lines of the $00^{\circ}1 - 02^{\circ}0$ transition. Measurements were made both on the low pressure gas sample alone, and on the atmospheric pressure mixture with air. A few minutes were allowed for mixing of the gas with the air. /A rough calculation shows this to be sufficient; see Appendix II./ These coefficients are presented graphically in Figures 14-19. Table XV lists the absorption

Figure 14: Laser line absorption coefficients for
low pressure trace contaminants; acetonitrile
(34.8 Torr); benzene (16.4 Torr); cyclohexane
(34.7 Torr); 1,2-dichloroethane (28.9 Torr);
and ortho-dichlorobenzene (0.4 Torr). Values
in meters/Newton (1 m/N= 1.33322 $Torr^{-1}cm^{-1}$).

Figure 15: Laser line absorption coefficients
as in Figure 14 for ethyl acetate (5 Torr);
Freon-12 (0.8 Torr); Freon-113 (3 Torr); furan
(4 Torr); and isopropanol (10.6 Torr).

Figure 16: Laser line absorption coefficients
as in Figure 14 for methyl chloroform (3.36 Torr);
methyl ethyl ketone (29.4 Torr); t-butanol
(4 Torr); vinyl chloride ((·) 4.1 Torr; (+) 4.1
Torr& 756 Torr air); and iodopropane (12.3 Torr).

ABSORPTION COEFFICIENT (m/n)

ACETONITRILE

0.0006
0.0003

BENZENE

0.002
0.001

CYCLOHEXANE

0.0003
0.0001

1,2-DICHLOROETHANE

0.0002
0.0001

O-DICHLOROBENZENE

0.005

CO_2
LASER LINES

R (00°1−02°0) P   R (00°1−10°0) P

9.2   9.5   10.2   10.6

$\lambda, \mu m$
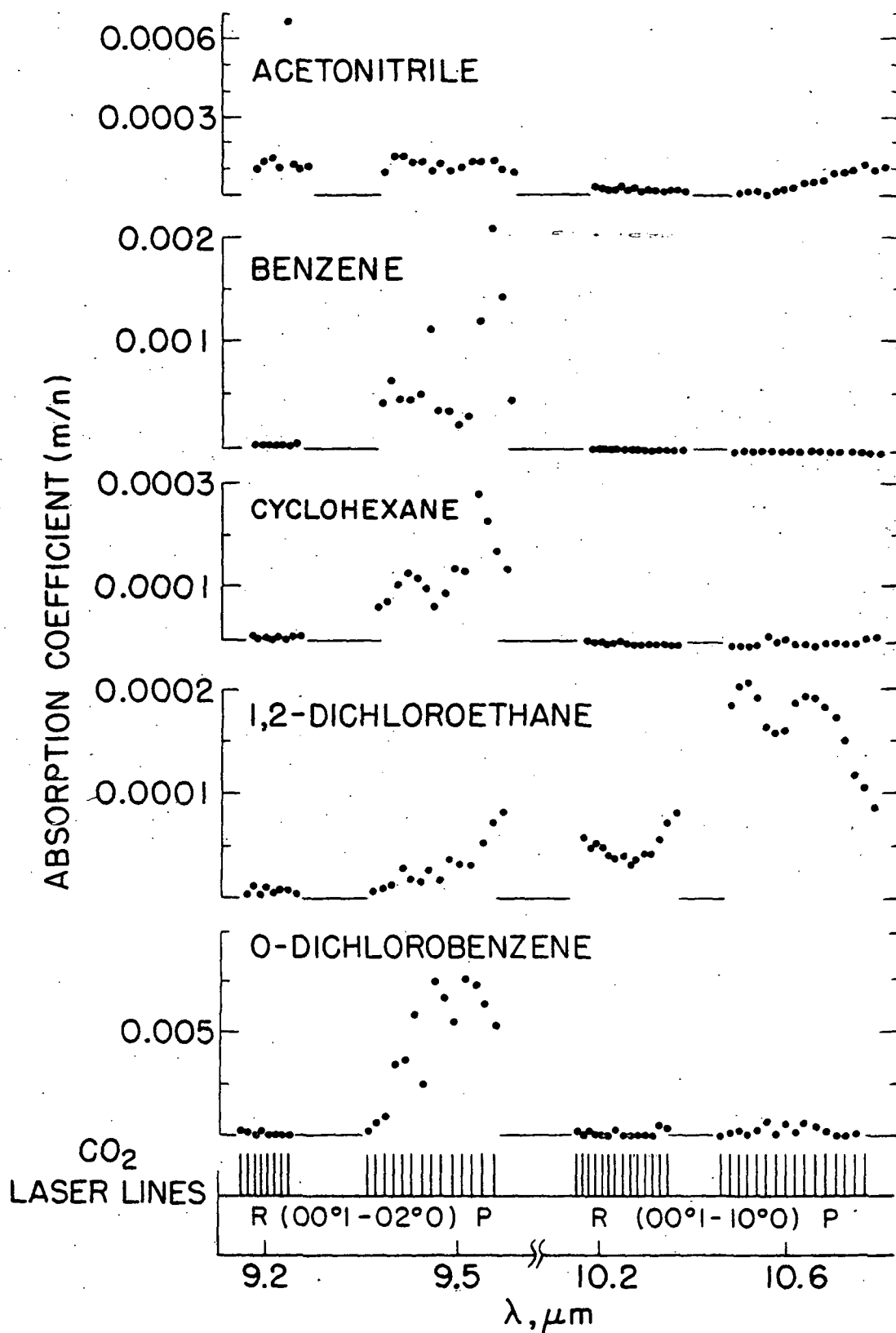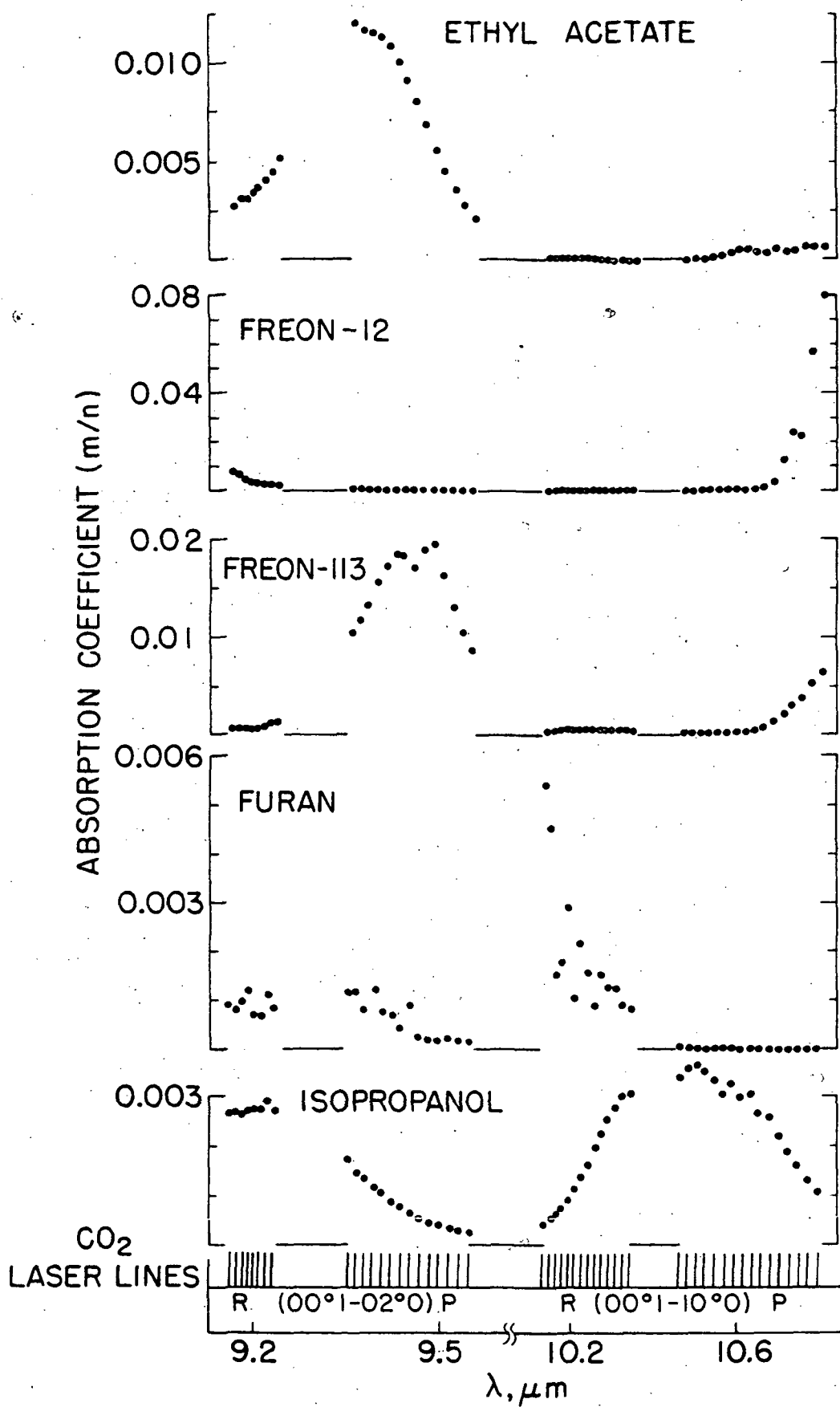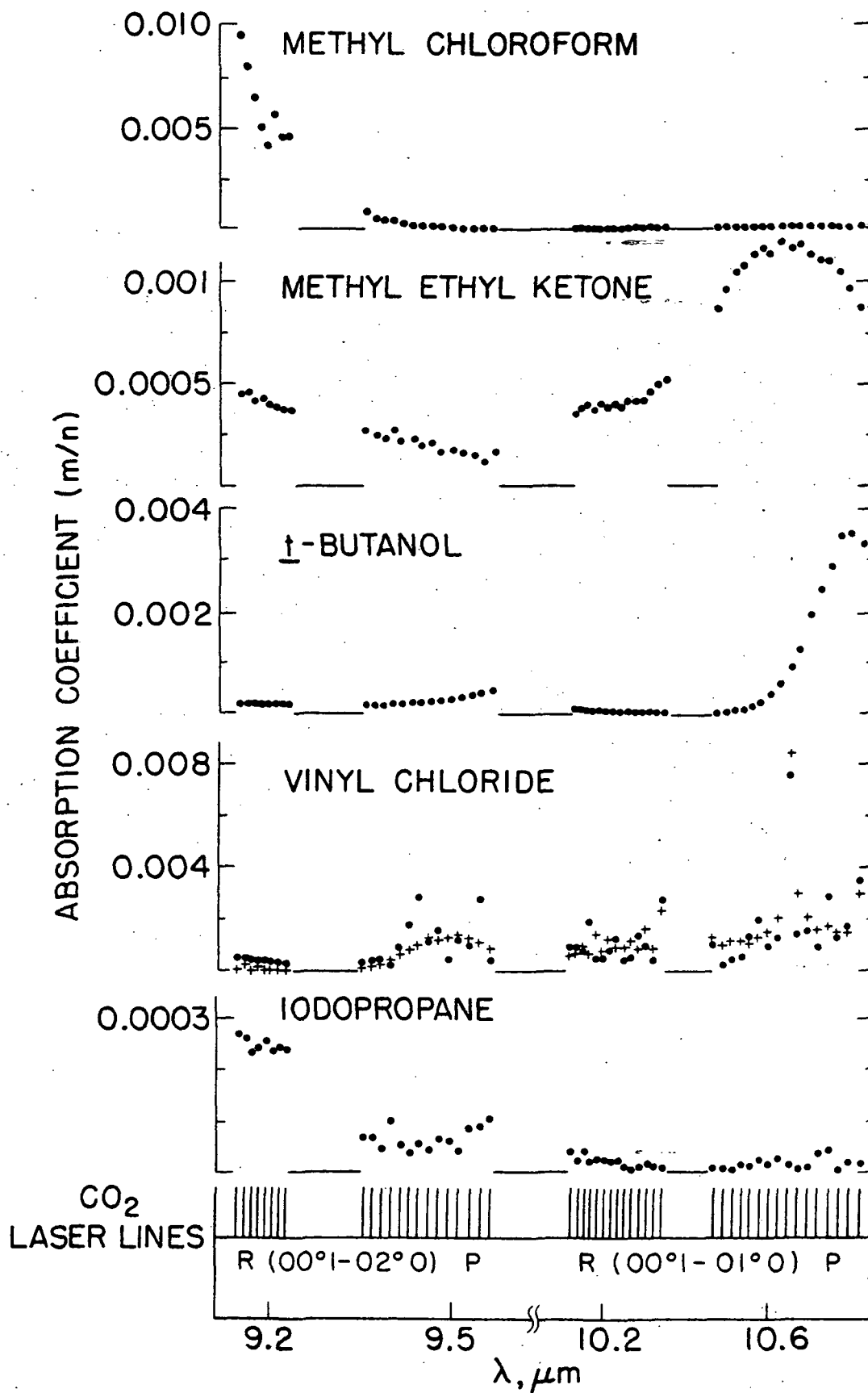
Figure 17: Laser line absorption coefficients
for trace contaminants in a mixture with air.
The partial pressures of contaminant gases
are the same as in Figures 14-16; the total
pressure is 1 atm. Acetonitrile; benzene;
cyclohexane; 1,2-dichloroethane; and ethyl
acetate.

Figure 18: Laser line absorption coefficients
as in Figure 17 for Freon-12; Freon-113; furan;
and isopropanol.

Figure 19: Laser line absorption coefficients
as in Figure 17 for methyl chloroform; methyl
ethyl ketone; t-butanol; vinyl chloride ((·) 4.1
Torr alone and (+) 4.1 Torr + 756 Torr air);
and iodopropane.

absorption coefficient (m/n)

acetonitrile

0.0004
0.0002

benzene

0.002
0.001

cyclohexane

0.0004
0.0002

1,2-dichloroethane

0.0002
0.0001

ethyl acetate

0.010
0.005

CO₂ Laser lines

R (00°1 −02°0) P   R (00°1 − 10°0) P

9.3   9.5   9.7   10.2   10.4   10.6

λ, μm

Freon-12

Freon-113

furan

isopropanol

CO_2 Laser
lines

R (00°I-02°0)   P   R (00°I-I0°0)   P

0.04

0.02

0.02

0.01

0.004

0.002

0.003

absorption coefficient (m/n)

9.3   9.5   9.7   10.2   10.4   10.6

$\lambda,\ \mu m$
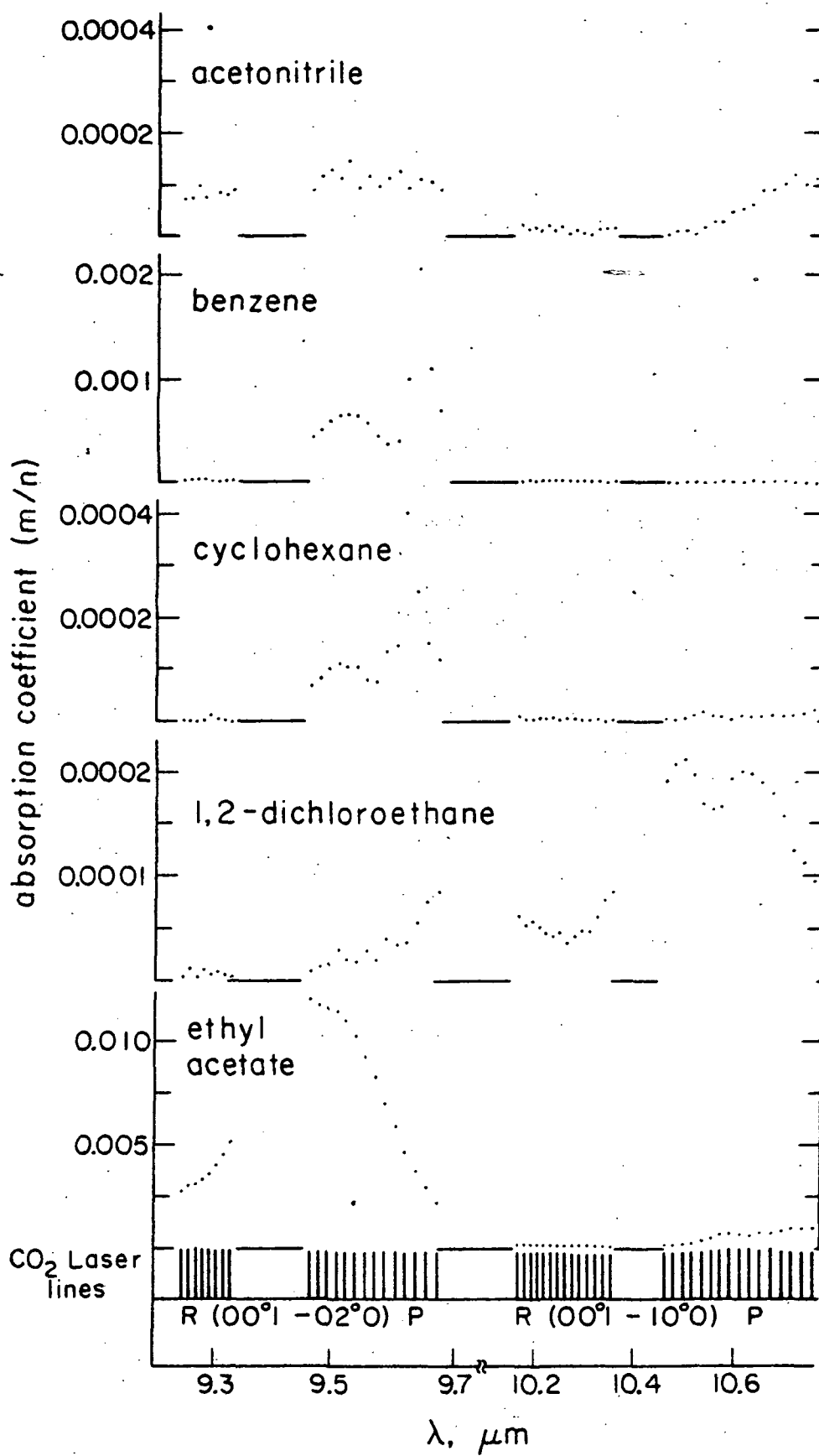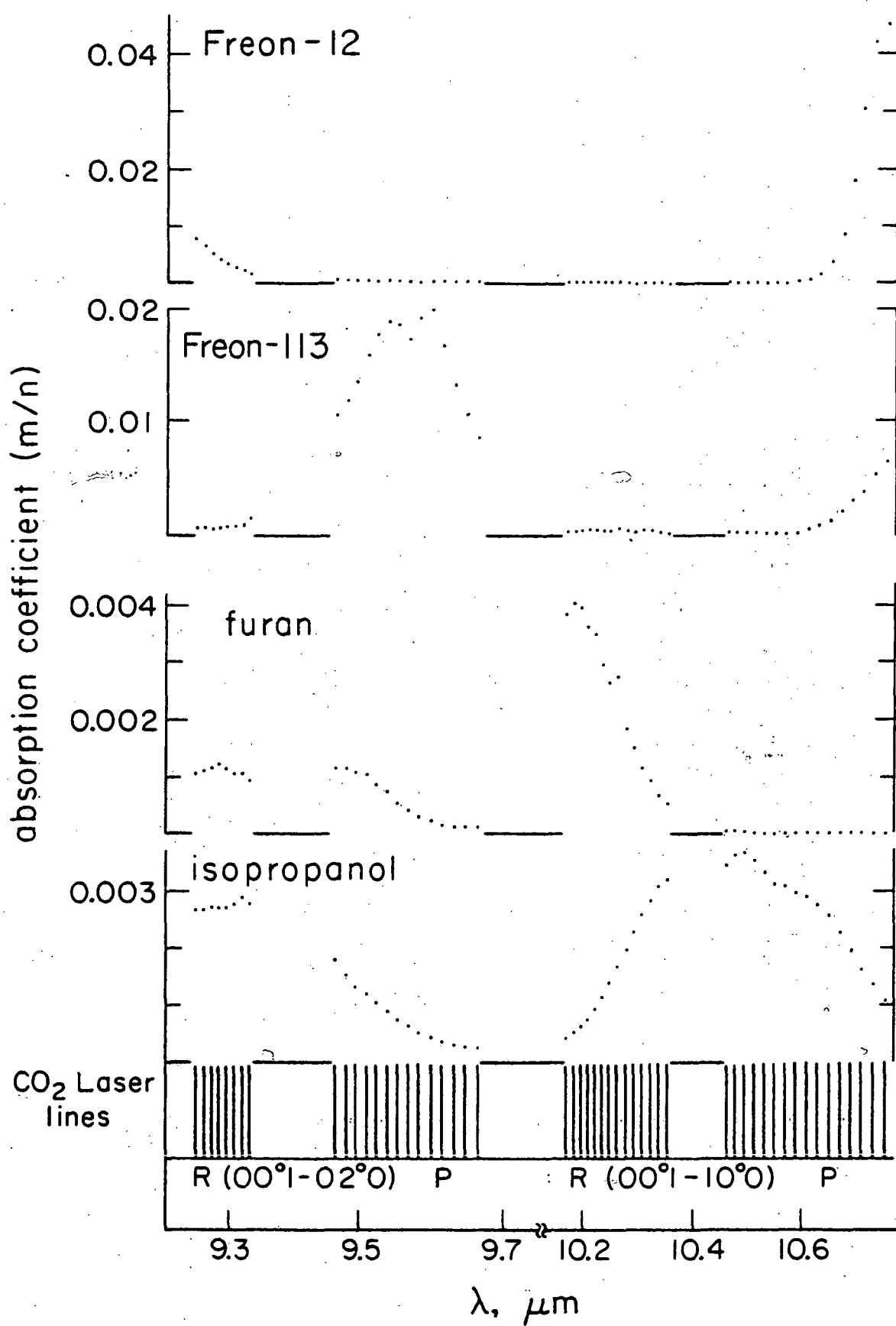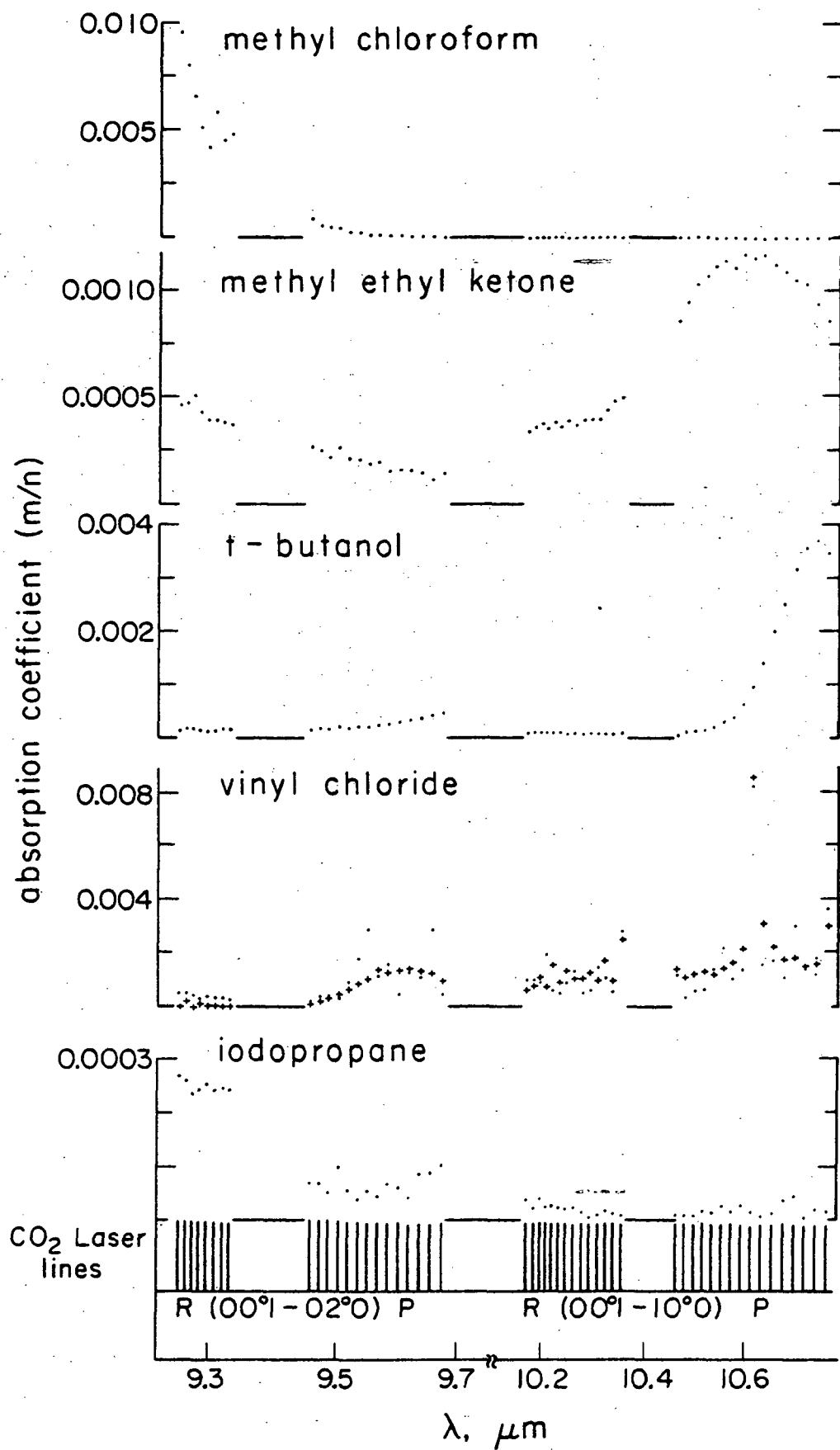
Table XIV   Minimum Detectable Concentrations of Atmospheric Contaminants
For a 10 m Absorption Path

Contaminant	MDC of gas alone in ppm 20% error	MDC of gas in mixture in ppm ±error as shown()		Comm. on Tox. Stds. Short-term (1 hour)	Long-term (6 mos.)
acetonitrile	125	400	(33%)	40	4
benzene	25	200	(6%)	100	1
		47	(86%)		
cyclohexane	126	167	(50%)	300	60
1,2-dichloroethane	236	1000	(30%)	200	10
ethyl acetate	4.2	9	(23%)	300	50
dichlorodifluoromethane*	1	5.3	(38%)	5000	100
trichlorotrifluoroethane**	2.5	9.2	(7%)	500	50
furan	13	33	(20%)	4	0.04
		6	(66%)		
isopropanol	14	40	(10%)	200	40
methyl chloroform	5.3	9.2	(14%)	300	50
methylethylketone	43	200	(20%)	100	20
tert-butanol	14	73	(25%)	200	40
vinyl chloride	6.4	17	(50%)	1	1
o-dichlorobenzene	7	50	(100%)	50	5
iodopropane	199	465	(20%)	not set	

*Freon 12   **Freon 113

coefficients of the gas alone. Table XVI gives the atmospheric mixture absorption coefficient values. An uncertainty of $\pm$ 3% (95% confidence limits) exists for all values of absorption coefficients greater than 4×10^{-4} m/N. This is due to the combined errors in A and the concentration measurements. It was experimentally determined that fluctuations in the value of the ratio give rise to an uncertainty in $\overline{\varepsilon}$ of 1×10^{-5} m/N, when A is small even for large concentrations over 30 Torr. (See equation (21).)

It must be noted that the self-broadening of these gases will present a problem, possibly even in the atmospheric mixture. Thus, even though the absorption coefficients were determined over a range of pressures for each gas in order to obtain good accuracy for both strong and weak extinction coefficients, the low pressure measurements were used whenever possible. High pressure of the sample gas was needed only for frequencies at which there was weak attenuation. Self-broadening values have been determined for some molecules[221] and are larger than air broadening values. Care must be exercised because self broadening could result in overestimation of the absorption coefficients and, consequently, underestimation of trace contaminant concentrations. This problem could have been circumvented if a longer cell or multiple-pass cell were used for these measurements. A more systematic study of the pressure broadening in these gases would be desirable, and these concerns form the basis for the next chapter. For such studies, a broadly tunable laser source is preferable to a line-tunable CO_2 laser.[222]

It was hoped that use of absorption coefficients taken with low sample

Table XV

Absorption Coefficients of Trace Gases at Low Pressure (m/N)*

Laser Line	aceto-nitrile	benzene	cyclo-hexane	ethyl acetate	Freon 12	Freon 113
R(24)	.000074	.000018	.000008	.00276	.00730	.00068
R(22)	.000099	.000016	.000000	.00309	.00690	.00066
R(20)	.000117	.000019	.000001	.00314	.00470	.00064
R(18)	.000077	.000017	.000002	.00341	.00353	.00063
R(16)	.000662	.000009	.000005	.00368	.00347	.00064
R(14)	.000090	.000010	.000000	.00408	.00261	.00077
R(12)	.000076	.000006	.000004	.00454	.00222	.00099
R(10)	.000087	.000021	.000008	.00530	.00161	.00106
P(8)	.000066	.000431	.000069	.0123	.00023	.0107
P(10)	.000125	.000670	.000078	.0120	.00018	.0119
P(12)	.000126	.000470	.000109	.0119	.00021	.0141
P(14)	.000103	.000458	.000135	.0116	.00022	.0159
P(16)	.000112	.000520	.000125	.0112	.00019	.0177
P(18)	.000075	.00118	.000104	.0104	.00019	.0189
P(20)	.000109	.000359	.000071	.00940	.00018	.0187
P(22)	.000080	.000355	.000095	.00830	.00015	.0174
P(24)	.000088	.000241	.000146	.00720	.00013	.0192
P(26)	.000114	.000308	.000140	.00580	.00009	.0200
P(28)	.000110	.00126	.000293	.00475	.00020	.0167
P(30)	.000113	.00217	.000239	.00380	.00011	.0133
P(32)	.000082	.00150	.000181	.00296	.00010	.0108
P(34)	.000070	.000474	.000147	.00227	.00008	.0089
R(32)		.000006	.000006	.000278	.00011	.000468
R(30)		.000007	.000003	.000257	.00004	.000505
R(28)		.000006	.000005	.000240	.00005	.000535
R(26)		.000008	.000000	.000215	.00009	.000530

Left margin label: $(00^{\circ}1 - 02^{\circ}0)$ Transition

* 1 m/N = 1.33322 torr^{-1}cm^{-1} = 4.1 x 10^{-17} cm^{2}sr^{-1} at 25°C.

Table XV

Absorption Coefficients of Trace Gases at Low Pressures (m/N)

Laser Line	benzene	cyclo-hexane	ethyl acetate	Freon 12	Freon 113
R(24)	.000010	.000002	.000208	.00005	.000570
R(22)	.000005	.000005	.000187	.00004	.000560
R(20)	.000007	.000000	.000181	.00004	.000570
R(18)	.000010	.000001	.000166	.00005	.000550
R(16)	.000009	.000000	.000158	.00010	.000540
R(14)	.000006	.000000	.000142	.00005	.000540
R(12)	.000009	.000000	.000140	.00013	.000510
R(10)	.000005	.000001	.000133	.00007	.000483
R(8)	.000002	.000001	.000128	.00010	.000457
R(6)	.000002	.000003	.000120	.00000	.000357
P(6)	.000000	.000003	.000142	.00000	.000259
P(8)	.000002	.000003	.000169	.00010	.000257
P(10)	.000003	.000002	.000223	.00006	.000257
P(12)	.000006	.000005	.000304	.00009	.000277
P(14)	.000005	.000020	.000430	.00013	.000298
P(16)	.000007	.000011	.000590	.00016	.000326
P(18)	.000002	.000014	.000700	.00020	.000356
P(20)	.000011	.000005	.000730	.00033	.000440
P(22)	.000003	.000006	.000650	.00055	.000580
P(24)	.000010	.000003	.000660	.00138	.000870
P(26)	.000006	.000008	.000800	.00365	.00144
P(28)	.000006	.000009	.000740	.0125	.00224
P(30)	.000009	.000008	.000840	.0250	.00311
P(32)	.000007	.000011	.000950	.0220	.00402
P(34)	.000003	.000017	.000980	.0580	.00560
P(36)	.000000	.000024	.000960	.0810	.00660

Transition ($00°1 - 10°0$)

Table XV

Absorption Coefficients of Trace Gases at Low Pressure in (m/N)

Laser Line	furan	isopropanol	iodopropane	methyl chloroform	methyl ethyl ketone	tert-butanol	vinyl chloride
R(24)	.000900	.00275	.000274	.00980	.000463	.000178	.00048
R(22)	.000800	.00275	.000264	.00820	.000472	.000188	.00043
R(20)	.000970	.00270	.000239	.00668	.000424	.000177	.00036
R(18)	.000520	.00279	.000250	.00521	.000431	.000188	.00027
R(16)	.000725	.00282	.000259	.00422	.000400	.000176	.00034
R(14)	.000680	.00282	.000242	.00580	.000390	.000181	.00030
R(12)	.00114	.00298	.000250	.00467	.000377	.000184	.00025
R(10)	.000840	.00278	.000245	.00476	.000375	.000169	.00023
P(8)	.00119	.00175	.000071	.000870	.000270	.000188	.00022
P(10)	.00118	.00150	.000068	.000712	.000248	.000185	.00031
P(12)	.000796	.00137	.000050	.000546	.000231	.000183	.00028
P(14)	.00122	.00121	.000102	.000449	.000271	.000221	.00031
P(16)	.000774	.00105	.000054	.000296	.000223	.000195	.00090
P(18)	.000699	.000890	.000040	.000222	.000219	.000216	.00181
P(20)	.000422	.000770	.000055	.000180	.000193	.000222	.00293
P(22)	.000920	.000645	.000046	.000170	.000205	.000252	.00128
P(24)	.000255	.000530	.000069	.000133	.000167	.000266	.00166
P(26)	.000200	.000442	.000062	.000102	.000171	.000304	.00041
P(28)	.000182	.000376	.000044	.000099	.000157	.000345	.00145
P(30)	.000200	.000311	.000088	.000093	.000149	.000388	.00105
P(32)	.000152	.000272	.000092	.000084	.000121	.000427	.00288
P(34)	.000157	.000235	.000107	.000070	.000163	.000482	.00041
R(32)	.0055	.000440	.000040	.000050	.000354	.000125	.00020
R(30)	.0046	.000515	.000024	.000034	.000379	.000133	.00029
R(28)	.00157	.000620	.000042	.000026	.000388	.000132	.00119
R(26)	.00185	.000750	.000025	.000039	.000370	.000105	.00203

Transition ($02°0 - 00°1$)

Table XV

Absorption Coefficients of Trace Gases at Low Pressure (m/N)

Laser Line	furan	isopropanol	iodopropane	methyl chloroform	methyl ethyl ketone	tert-butanol	vinyl chloride
R(24)	.00298	.000930	.000028	.000031	.000396	.000125	.00055
R(22)	.00108	.00116	.000026	.000039	.000379	.000113	.00051
R(20)	.00225	.00140	.000022	.000035	.000402	.000110	.00085
R(18)	.00160	.00165	.000026	.000052	.000385	.000098	.00139
R(16)	.00090	.00203	.000014	.000050	.000417	.000109	.00051
R(14)	.00156	.00234	.000007	.000060	.000414	.000094	.00062
R(12)	.00131	.00263	.000014	.000061	.000418	.000083	.00148
R(10)	.00126	.00286	.000015	.000056	.000455	.000103	.00110
R(8)	.000920	.00310	.000012	.000051	.000490	.000110	.00053
R(6)	.000836	.00316	.000007	.000072	.000515	.000101	.00284
P(6)	.000074	.00348	.000008	.000080	.000890	.000104	.00116
P(8)	.000054	.00372	.000009	.000068	.000970	.000128	.00033
P(10)	.000034	.00374	.000005	.000056	.00106	.000153	.00053
P(12)	.000009	.00361	.000016	.000057	.00109	.000169	.00065
P(14)	.000020	.00343	.000011	.000054	.00114	.000225	.00136
P(16)	.000017	.00316	.000026	.000039	.00118	.000317	.00220
P(18)	.000012	.00337	.000015	.000047	.00115	.000450	.00107
P(20)	.000010	.00308	.000023	.000033	.00121	.000668	.00143
P(22)	.000006	.00314	.000012	.000038	.00118	.001000	.00814
P(24)	.000005	.00274	.000006	.000022	.00119	.00137	.00160
P(26)	.000004	.00267	.000011	.000023	.00114	.00208	.00175
P(28)	.000010	.00227	.000036	.000030	.00111	.00255	.00102
P(30)	.000009	.00196	.000045	.000025	.00111	.00305	.00310
P(32)	.000000	.00167	.000004	,000019	.00105	.00363	.00166
P(34)	.000003	.00136	.000019	.000028	.000970	.00370	.00499
P(36)	.000000	.00113	.000017	.000034	.000885	.00347	.00880

(00°1 - 10°0) Transition

Table XVI

Absorption Coefficients of Trace Gases in an Atm. Mixture with Air (m/N)

	Laser Line	aceto-nitrile	benzene	cyclo-hexane	1,2-di-chloro-ethane	ortho-dichloro-benzene	ethyl acetate
	R(24)	.000073	.000024	.000005	.000004	.0002	.00273
	R(22)	.000075	.000018	.000000	.000011	.0002	.00306
	R(20)	.000100	.000024	.000000	.000003	.0000	.00313
	R(18)	.000075	.000022	.000002	.000012	.0002	.00338
	R(16)	.000412	.000006	.000009	.000005	.0000	.00365
	R(14)	.000084	.000001	.000000	.000009	.0000	.00402
	R(12)	.000081	.000011	.000003	.000008	.0000	.00450
	R(10)	.000092	.000014	.000000	.000004	.0000	.00530
	P(8)	.000091	.000438	.000071	.000009	.0004	.0122
	P(10)	.000122	.000510	.000086	.000013	.0006	.0120
	P(12)	.000128	.000600	.000102	.000015	.0009	.0118
$(00^\circ 1 - 02^\circ 0)$ Transition	P(14)	.000116	.000660	.000113	.000030	.0035	.0117
	P(16)	.000148	.000680	.000110	.000022	.0037	.0111
	P(18)	.000097	.000660	.000106	.000019	.0059	.0104
	P(20)	.000119	.000580	.000082	.000031	.0026	.00940
	P(22)	.000097	.000460	.000079	.000018	.0076	.00830
	P(24)	.000114	.000372	.000139	.000041	.0067	.00700
	P(26)	.000127	.000400	.000150	.000035	.0056	.00590
	P(28)	.000096	.00102	.000411	.000034	.0076	.00470
	P(30)	.000114	.00210	.000253	.000057	.0074	.00375
	P(32)	.000104	.00111	.000153	.000077	.0064	.00296
	P(34)	.000095	.00069	.000123	.000088	.0054	.00227
$(00^\circ 1 - 10^\circ 0)$	R(32)	.000022	.000017	.000008	.000065	.0002	.000277
	R(30)	.000014	.000009	.000006	.000056	.0000	.000254
	R(28)	.000015	.000008	.000004	.000058	.0002	.000237
	R(26)	.000012	.000010	.000008	.000054	.0000	.000216

Table XVI

Absorption Coefficients of Trace Gases in Atm. Mixture with Air (m/N)

Laser Line	acetonitrile	benzene	cyclohexane	1,2-dichloroethane	orthodichlorobenzene	ethyl acetate
R(24)	.000019	.000012	.000006	.000047	.0000	.000205
R(22)	.000009	.000009	.000007	.000044	.0000	.000194
R(20)	.000016	.000010	.000003	.000048	.0003	.000175
R(18)	.000002	.000010	.00005	.000039	.0000	.000161
R(16)	.000009	.000013	.000004	.000045	.0000	.000160
R(14)	.000004	.000008	.000002	.000050	.0000	.000142
R(12)	.000000	.000015	.000004	.000050	.0000	.000140
R(10)	.000008	.000008	.000006	.000064	.0000	.000131
R(8)	.000012	.000007	.000001	.000081	.0005	.000126
R(6)	.000012	.000000	.000003	.000089	.0004	.000120
P(6)	.000001	.000000	.000004	.000197	.0000	.000162
P(8)	.000009	.000003	.000004	.000215	.0001	.000174
P(10)	.000011	.000007	.000008	.000218	.0003	.000217
P(12)	.000002	.000006	.000013	.000203	.0000	.000302
P(14)	.000013	.000008	.000019	.000175	.0003	.000428
P(16)	.000023	.000001	.000013	.000171	.0006	.000580
P(18)	.000025	.000008	.000010	.000173	.0000	.000700
P(20)	.000045	.000006	.000004	.000200	.0006	.000730
P(22)	.000048	.000012	.000009	.000208	.0000	.000650
P(24)	.000058	.000005	.000008	.000204	.0006	.000660
P(26)	.000085	.000007	.000009	.000197	.0002	.000790
P(28)	.000090	.000015	.000011	.000187	.0006	.000740
P(30)	.000098	.000006	.000011	.000163	.0004	.000840
P(32)	.000116	.000006	.000012	.000129	.0002	.000950
P(34)	.000099	.000000	.000016	.000118	.0000	.000970
P(36)	.000106	.000005	.000020	.000100	.0002	.000950

($00^{\circ}1 - 10^{\circ}0$) Transition

Table XVI

Absorption Coefficients of Trace Gases in an Atm. Mixture with Air (m/N)

Laser Line	Freon 12	Freon 113	furan	isopro-panol	methyl chloro-form	methyl ethyl ketone
R(24)	.00820	.000680	.00111	.00273	.00980	.000469
R(22)	.00670	.000680	.00116	.00274	.00830	.000478
R(20)	.00510	.000640	.00121	.00277	.00680	.000519
R(18)	.00401	.000640	.00124	.00278	.00531	.000436
R(16)	.00352	.000640	.00117	.00277	.00434	.000397
R(14)	.00289	.000780	.00108	.00284	.00593	.000401
R(12)	.00209	.001000	.00109	.00297	.00472	.000384
R(10)	.00165	.00106	.000950	.00284	.00494	.000377
P(8)	.00033	.0108	.00121	.00176	.000915	.000277
P(10)	.00023	.0120	.00118	.00155	.000630	.000254
P(12)	.00029	.0137	.00111	.00137	.000528	.000226
P(14)	.00029	.0162	.00107	.00123	.000441	.000268
P(16)	.00036	.0178	.000880	.00107	.000299	.000223
P(18)	.00020	.0190	.000760	.00092	.000224	.000220
P(20)	.00019	.0189	.000562	.00077	.000182	.000199
P(22)	.00024	.0175	.000452	.00065	.000168	.000204
P(24)	.00016	.0195	.000336	.00054	.000138	.000165
P(26)	.00019	.0202	.000241	.000458	.000104	.000172
P(28)	.00016	.0169	.000182	.000388	.000116	.000161
P(30)	.00010	.0134	.000153	.000329	.000097	.000148
P(32)	.00013	.0109	.000134	.000282	.000090	.000120
P(34)	.00008	.0088	.000129	.000250	.000073	.000155
R(32)	.00009	.000468	.00393	.000440	.000050	.000353
R(30)	.00009	.000497	.00413	.000520	.000035	.000381
R(28)	.00002	.000535	.00407	.000630	.000024	.000389
R(26)	.00006	.000556	.00369	.000770	.000036	.000368

(00°1 - 02°0) Transition

(00°1-10°0)

Table XVI

Absorption Coefficients of Trace Gases in Atm. Mixture with Air (m/N)

Laser Line	Freon 12	Freon 113	furan	iospro-panol	methyl chloro-form	methyl ethyl ketone
R(24)	.00014	.000563	.00356	.000940	.000031	.000396
R(22)	.00005	.000573	.00304	.00116	.000039	.000376
R(20)	.00011	.000569	.00271	.00140	.000040	.000405
R(18)	.00001	.000556	.00279	.00170	.000053	.000384
R(16)	.00014	.000531	.00227	.00200	.000057	.000412
R(14)	.00004	.000531	.00157	.00232	.000059	.000416
R(12)	.00004	.000517	.00120	.00265	.000062	.000416
R(10)	.00013	.000482	.000970	.00292	.000058	.000460
R(8)	.00009	.000451	.000709	.00314	.000053	.000497
R(6)	.00004	.000412	.000538	.00324	.000073	.000515
P(6)	.00006	.000259	.000063	.00352	.000070	.000880
P(8)	.00003	.000256	.000048	.00370	.000067	.000970
P(10)	.00013	.000258	.000037	.00376	.000055	.00106
P(12)	.00009	.000275	.000025	.00362	.000060	.00110
P(14)	.00017	.000302	.000020	.00342	.000051	.00115
P(16)	.00014	.000327	.000020	.00319	.000045	.00117
P(18)	.00016	.000364	.000012	.00316	.000043	.00115
P(20)	.00035	.000450	.000014	.00303	.000038	.00120
P(22)	.00059	.000597	.000010	.00298	.000034	.00119
P(24)	.00151	.000910	.000009	.00280	.000024	.00120
P(26)	.00367	.00146	.000008	.00261	.000027	.00115
P(28)	.00870	.00232	.000011	.00232	.000029	.00112
P(30)	.0180	.00321	.000007	.00198	.000023	.00111
P(32)	.0308	.00407	.000005	.00167	.000028	.00106
P(34)	.0429	.00560	.000005	.00138	.000031	.000970
P(36)	.0463	.00660	.000004	.00114	.000030	.000890

Transition ($00^0 1 - 10^0 0$)

Table XVI

Absorption Coefficients of Trace Gases in Atm. Mixture with Air (m/N)

Laser Line	tertiary butanol	vinyl chloride	Laser Line	tertiary butanol	vinyl chloride
R(24)	.000170	.00000	R(24)	.000130	.00154
R(22)	.000202	.00022	R(22)	.000120	.00093
R(20)	.000170	.00000	R(20)	.000117	.00139
R(18)	.000195	.00015	R(18)	.000100	.00104
R(16)	.000171	.00004	R(16)	.000106	.00105
R(14)	.000187	.00000	R(14)	.000100	.00126
R(12)	.000186	.00000	R(12)	.000086	.00096
R(10)	.000163	.00002	R(10)	.000100	.00175
P(8)	.000189	.00017	R(8)	.000108	.00099
P(10)	.000189	.00023	R(6)	.000094	.00247
P(12)	.000189	.00031	P(6)	.000101	.00147
P(14)	.000227	.00046	P(8)	.000130	.00114
P(16)	.000200	.00069	P(10)	.000162	.00130
P(18)	.000220	.00085	P(12)	.000163	.00136
P(20)	.000229	.00105	P(14)	.000223	.00128
P(22)	.000257	.00140	P(16)	.000322	.00149
P(24)	.000263	.00128	P(18)	.000438	.00172
P(26)	.000306	.00140	P(20)	.000666	.00224
P(28)	.000351	.00145	P(22)	.000990	.00884
P(30)	.000384	.00133	P(24)	.00144	.00321
P(32)	.000432	.00123	P(26)	.00207	.00233
P(34)	.000480	.00098	P(28)	.00255	.00180
R(32)	.000110	.00068	P(30)	.00322	.00193
R(30)	.000137	.00077	P(32)	.00364	.00169
R(28)	.000135	.00107	P(34)	.00380	.00169
R(26)	.000113	.00073	P(36)	.00353	.00317

Left column transitions: rows R(24)–P(34) are ($00^{\circ}1 - 02^{\circ}0$) Transition; rows R(32)–R(26) are ($00^{\circ}1 - 10^{\circ}0$) Transition.

Right column transition: ($00^{\circ}1 - 10^{\circ}0$) Transition.

pressures would exhibit self-broadening which was negligible compared with atmospheric broadening, and accurate detection of each gas in a mixture would be possible. This is discussed further later in the chapter.

From these absorption coefficients, the sensitivity of a laser absorption method for detecting each trace gas contaminant in the atmosphere could be estimated. The minimum detectable concentration (MDC) of each gas was set at the level for which there is a 20% uncertainty in A at the gases' most strongly attenuating frequency. These MDC values are listed in Table XIV. It may be seen from the Table that single gases may be detected at the 1-200 ppm level for a 10m path.

The gases to be used in preparing a mixture were purified as above. After an amount of each gas reached equilibrium in the gas manifold and its pressure was measured, the cell was closed off from the manifold and the gas in the cell was cryopumped into the sidearm bulb of the cell, using liquid nitrogen. This bulb was of known volume relative to the volume of the absorption cell. Care was taken to insure all the contaminant was condensed into the bulb. After all the gases were stored in the bulb in this manner, the bulb was warmed to room temperature and the gases were allowed to expand into the absorption cell and mix for several hours. Air was then added to the cell to bring the mixtures to atmospheric pressure. Calculations of the times necessary for diffusion are given in Appendix II.

Mixtures were prepared in such a way as to find the effect of the following conditions on the accuracy of the concentration determination procedure:

1. The variation of the absorption for similar mixtures;i.e., mixtures with the same relative concentrations of the gases, but different total pressures of the contaminant mixture;

2. The variation of the relative concentrations of two gases with very similar absorption spectra;

3. The presence of a relatively high concentration of a broadly absorbing gas.

D. Mixture Analysis

Several different approaches to the solution process are possible.[223] A best fitting of the calculated concentration by a linear vector space analysis for a single species has been performed.[132] Here four wavelengths of a CO_2 laser were chosen to permit maximum discrimination for O_3 detection. A least-squares fitting of a high resolution continuous spectrum has been done for up to 25 contaminant species.[91] This method relies on determining the concentration of each species from a distinguishing feature or set of features in the absorption spectrum. The method chosen here to determine the concentration of each gas present in the prepared mixtures involved a least-squares fitting of the absorption data prior to solution. As a result, the magnitude of the errors due to experimental fluctuations was minimized, and greater stability during matrix manipulation was achieved.

Because only as many simultaneous equations were required as unknowns, fifty-two absorption measurements on a twelve component mixture form an overdetermined system. Early attempts at choosing appropriate

wavelengths for discrimination as in[132] for even a three component system resulted in low accuracy and a large dependence of the solution on the choice of wavelengths. It would seem that the linear vector space analysis used by Craig[132] worked sufficiently well for the simple one-component system, but that poor stability would result for a multi-component mixture using their iterative approach. As a result, a method utilizing all the experimental information was implemented. The expected absorption at each wavelength, if the absorption due to each species present is additive, would be given by

$$\left(\frac{1}{\ell}\right) y_i = \sum_{j=1}^{N} \epsilon_{ij} c_j \qquad j = 1, 2, \ldots, \lambda \qquad (24)$$

where y_i is the expected absorption at the ith wavelength, ϵ_{ij} is the experimentally determined absorption coefficient of gas j at wavelength i, and c_j is the "unknown" concentration of gas j. The experimentally measured absorption values of the mixture, A_i, are subject to the uncertainties and fluctuation errors discussed above, and as a result will generally be different from y_i values. The best set of solutions for the concentrations of the contaminants occurs when the differences between A_i and y_i values are smallest (but not necessarily zero). This solution is achieved when the sum of the squares of the residuals between A_i and y_i are minimized with respect to variation of the solutions c_j, giving

$$\frac{\partial \eta}{\partial c_j} = 0 \quad (j = 1, \ldots, N) \; ; \; \eta = \sum_{i=1}^{\lambda} (y_i - A_i)^2 \qquad (25)$$

For this system $N = 12$, $\lambda = 52$. Substituting equation (24) into equations (25) and performing the partial differentiation results in a set of N

simultaneous equations after rearrangement.

$$f_{j1} c_1 + f_{j2} c_2 + f_{j3} c_3 + \cdots + f_{jn} c_n = d_j \qquad (26)$$

$$j = 1, 2, \ldots, N.$$

where

$$f_{jk} = \sum_{i=1}^{\lambda} \varepsilon_{ij} \varepsilon_{ik} \qquad \text{and} \qquad d_j = \sum_{i=1}^{\lambda} \varepsilon_{ij} A_i / \ell \qquad (27)$$

It is seen that each f_{jk} and d_j matrix element is the sum of fifty-two

products. In this manner all the information is collapsed into an

N-dimensional matrix. In matrix notation equation (26) may be written

$FC = D$ where $F = \varepsilon^T \varepsilon$ and $D = \varepsilon^T A / \ell$. Because the F matrix is

symmetric positive definite, elimination methods requiring non-vanishing

positive pivots may be employed. In particular, the triangular decomposi-

tion method of Cholesky[224] which breaks F into two triangular matrices

which are transpositions of one another, introduces very little mathe-

matical instability into the solution process through minimization of

the rounding errors in the matrix elements calculated during the

decomposition. The solutions are then found by back-substitution. A

fuller explanation and an example are given in Appendix III. Methods

requiring matrix inversion for solution are far more unstable. They

are particularly unstable for near-vanishing pivot elements. This would

be the case if the sum of the absorption coefficients for two gases were

similar $\left(\sum_{i=1}^{\lambda} (\varepsilon_{ij})^2 \approx \sum_{i=1}^{\lambda} (\varepsilon_{ik})^2 \right)$. We noticed that, in fact,

matrix inversion methods were unable to reach stable solutions for the

twelve component mixtures in these experiments. The computer solution

program, DPELZC, is given in Appendix IV. An IBM System/360 Model 67

computer was used in this analysis on a time-sharing basis. The memory
storage of the PDP 8/L mini-computer in the laboratory was insufficient
for these large matrices, and the word length did not allow sufficient
precision during computation.

Occasionally gases were omitted from the mixture and if the cal-
culated concentration of the gas was negative or zero, that species was
removed from the calculation process, reducing the number of simultaneous
equations by one. If the calculated concentration of an omitted gas
was non-zero, or if the concentration of a trace gas present in the mix-
ture was calculated to be zero, the error in the solution was taken as a
total uncertainty in the presence of the contaminant at that level. Gen-
erally, as the concentration of any gas decreased, the percent error
between the calculated and known input values increased even for similar
mixtures. This increase is expected because the relative contribution of
that gas to the absorption by the mixture is decreased and closer to the
noise level of the detection system. However, these errors were a function
of the interference effects in each particular mixture and not just the
contaminant's concentration. For example, benzene and cyclohexane have
very similar absorption coefficient distributions, as listed in Table XVII.
Benzene absorbs more strongly in this region and its maximum absorption
is shifted by one CO_2 laser line toward lower frequency. The MDC of
cyclohexane is increased when benzene is present in an amount sufficient
to dominate the relative absorption. Under these conditions, the benzene
MDC is decreased below the value expected from concentration considerations
alone. The concentration effect is predominant over most of the relative

Table XVII

The Absorption Coefficients in m/N of Benzene and
Cyclohexane in the P Branch of the $(00^{\circ}1 - 02^{\circ}0)$
Transition *

Transition	Frequency (cm^{-1})	(Benzene)	(Cyclohexane)
P (8)	1057.3002	.00043 (1)	.000070 (2)
P (10)	1055.6251	.00050 (1)	.000084 (2)
P (12)	1053.9235	.00059 (1)	.000100 (3)
P (14)	1052.1956	.00065 (1)	.000111 (3)
P (16)	1050.4413	.00066 (1)	.000108 (3)
P (18)	1048.6608	.00065 (1)	.000104 (3)
P (20)	1046.8542	.00057 (1)	.000080 (3)
P (22)	1045.0217	.00045 (1)	.000077 (3)
P (24)	1043.1633	.00036 (1)	.000136 (4)
P (26)	1041.2791	.00039 (1)	.000147 (4)
P (28)	1039.3693	.00100 (1)	.000403 (8)
P (30)	1037.4341	.00206 (2)	.000248 (5)
P (32)	1035.4736	.00108 (1)	.000150 (4)
P (34)	1033.4881	.00068 (1)	.000121 (4)

* The absorption coefficients at all other laser frequencies are
near zero for both gases.

concentration range investigated, and thus this method of solution is suffi-
ciently sensitive to easily distinguish the two gases.

The concentrations of the gases at which the difference between cal-
culated and known values becomes sizable for the twelve component mixtures
are given in Table XV. It is seen that the presence of other absorbers
tends to increase the MDC value of each contaminant, general to about
five times that of the isolated gas. Mixtures containing only a few com-
ponents should have MDC values intermediate to those of the twelve com-
ponent mixture and single gas MDC levels. The errors listed in Table XIV
are the observed differences for the gas at that concentration in a mix-
ture. Interference effect do not permit the MDC levels to be set as
uniformly as for the isolated gases.

Another interference effect in the mixture may be used to increase
the sensitivity of detection. When all the gases are present in low con-
centrations, the absorption of the laser light by the mixture is small,
and the A_i values are largely uncertain due to baseline fluctuations.
The addition of a broadly absorbing gas decreases the effect of the
fluctuations and actually increases the sensitivity of detection of the
other trace species. For example, isopropanol exhibits two broad absorp-
tions in the region of the spectrum covered by the laser $/$See Figure 20$/$.
Two mixtures of twelve gases were prepared containing concentrations of
the gases at or below their MDC values determined above. One contained
an amount of isopropanol near its MDC value, and the other contained
an amount roughly nine times MDC, resulting in 80-95% absorption of the
light at many frequencies. The calculated concentrations are compared in

Figure 20: The absorption coefficients of
isopropanol at the CO_2 laser frequencies.
The frequencies at which the following gases
have strong absorption coefficients are
indicated: acetonitrile (A), 1, 2-dichloro-
ethane (D), ethyl acetate (E), Freon 12 (12)
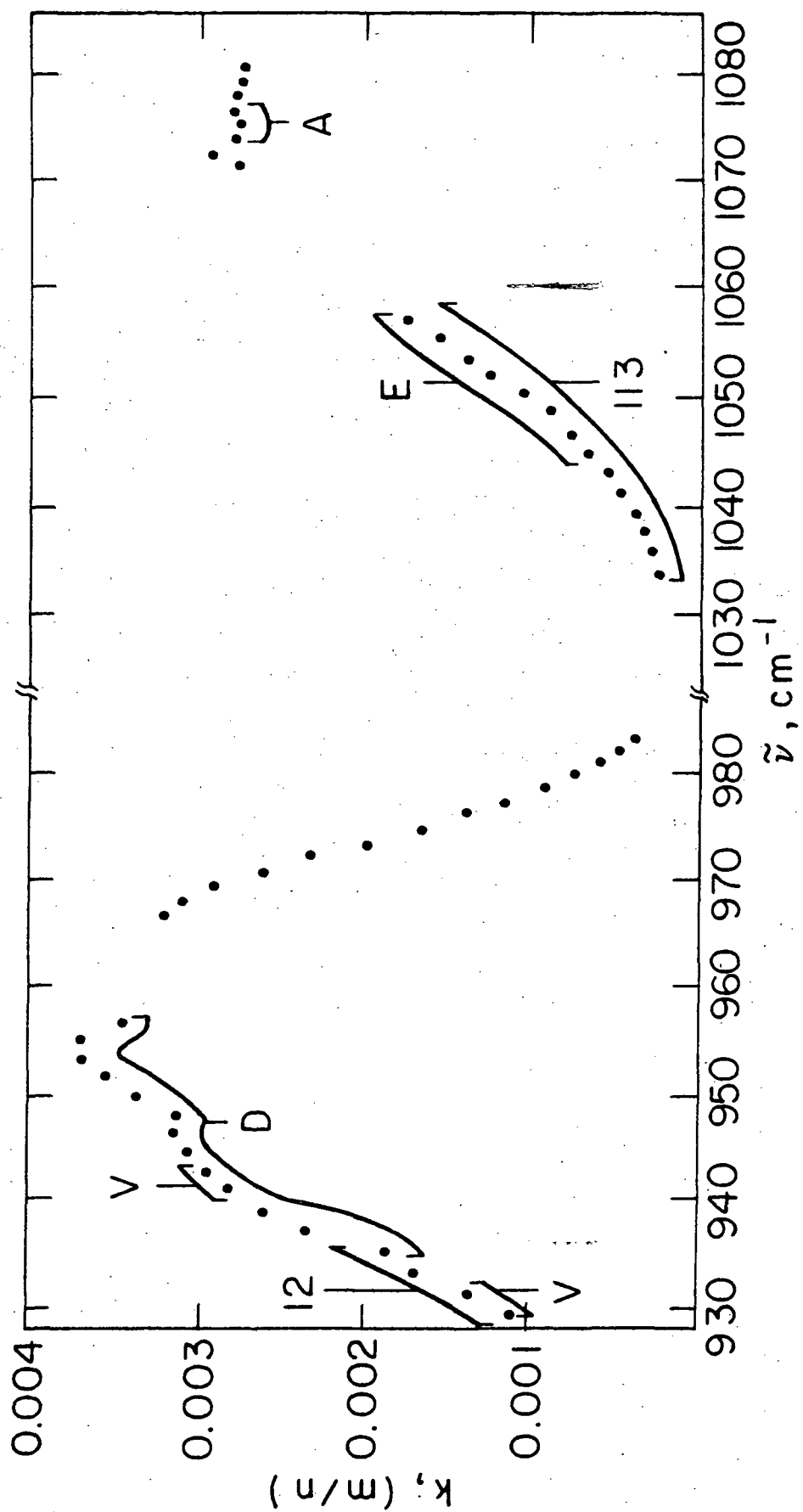Freon 113 (113), and vinyl chloride (V).

Table XVIII. A large increase in sensitivity resulted for those contaminants which have their strongest absorptions in a region where the addition of isopropanol greatly increases the total absorption. Acetonitrile, 1,2 dichloroethane, and vinyl chloride are in this category /See Figure 20/. The frequencies at which ethyl acetate, Freon 12, and Freon 113 have their strongest absorption coefficients are also indicated in the Figure. It is seen that the total absorption at those wavelengths would not be greatly increased by the addition of isopropanol, and little improvement is observed in Table XVIII.

Normal atmospheric attenuation over a 10 m path due to water vapor and carbon dioxide is less than 0.2% for all frequencies.[131,133] In closed environments, both these gases may accumulate to high levels.[225] If their absorption is significant, they may be treated as additional atmospheric contaminants and an attempt could be made to quantitatively detect them. Water vapor would give rise to, at most, 0.3% absorption for a 10 m path,[132] and hence is undetectable since experimental measurement fluctuations are on the order of 1%. Carbon dioxide, on the other hand, might be present in sufficient quantities to result in 10% absorption at some laser frequencies, and thus could be quantitatively detected. In these closed environments, ambient CO_2 may serve as a broad absorber and enhance sensitivity. The additional errors introduced into the solution process would be small and the accuracy of the detection method would then be independent of cabin atmosphere composition. The presence of unexpected trace absorbers will greatly perturb the calculated solutions.[226] As a result, all species which might occur in the closed environment must be enumerated and the appropriate absorption coefficients stored in memory.

Table XVIII

The Effect of a Broadly Absorbing Gas on the MDC

Values in ppm *

| Gas | Ratio of the calculated concentration to the known value for the mixture with: | | MDC of gas from Table XV | MDC of gas due to presence of isopropanol |
	All Gases near MDC	Addition of isopropanol	$1 = 10$ m	$1 = 10$ m
acetonitrile	2.62	1.34	400 (33%)	140 (33%)
benzene	1.82	1.10	200 (6%)	50 (10%)
cyclohexane	1.54	0.64	167 (50%)	130 (30%)
1,2-dichloroethane	1.02	0.52	1000 (30%)	125 (50%)
ethyl acetate	2.45	1.18	9 (23%)	9 (15%)
Freon 12	0.66	0.85	5 (38%)	9 (15%)
Freon 113	0.89	1.16	9.2 (7%)	9 (22%)
furan	1.12	0.93	33 (20%)	40 (7%)
isopropanol	2.64	1.04	40 (10%)	-
methyl chloroform	0.82	0.95	9 (14%)	20 (5%)
t-butanol	2.98	1.65	73 (25%)	47 (58%)
vinyl chloride	0.49	0.81	17 (50%)	17 (18%)

* 1 N/m^2 = 9.878 ppm

Elimination of species not actually present will permit eventual matrix simplification.

The enhanced sensitivity brought about by the addition of a broadly absorbing gas verifies the fact that more strongly attenuated laser frequencies give absorptions which are more reproducible. Thus one might consider weighting the absorptions differentially to try to improve the accuracy of the solution method. In this case equation (26) becomes

$$\underset{\sim}{\varepsilon}^T \underset{\sim}{\omega} \underset{\sim}{\varepsilon} \underset{\sim}{C} = \underset{\sim}{\varepsilon}^T \underset{\sim}{\omega} \underset{\sim}{A} / \ell \tag{28}$$

where $\underset{\sim}{\omega}$ is a $\lambda \times \lambda$ diagonal weighting matrix. Heavier weighting of strong absorptions was tried initially, but a decrease in accuracy resulted. The least-squares fitting part of the solution process tends to treat large absorptions preferentially, and no improvement is gained by weighting. More heavily weighting the small or medium absorptions was also used in an attempt to determine whether or not the least-squares fitting process stressed the large absorptions too strongly. These solutions were not significantly improved over the unweighted scheme. Apparently the unbiased least-squares fit of the data produces the best set of solutions and further attempts at weighting offer no significant improvement. A weighted computer solution program, W2DPAZC, is given in Appendix IV.

Because the MDC depends on interferences in the mixtures, a computational technique was developed which assigns a relative uncertainty to the calculated concentration values for each specific mixture. No additional experimental data was needed and the extra computer time required

is insignificant. Such a self-evaluating procedure is desirable when interference with other absorbers may cause a trace species to become partially obscured or much too prominent.

The first approach to this self-evaluation involved calculation of the residuals between the calculated and exact solutions of the matrix.[227] The c_j solutions were used to calculate y_i value using equation (24). The difference between y_i and A_i is taken and this value is used as the A_i value in equation (26) and (27). The D matrix calculated is the residual due to computer rounding and experimental fluctuation errors. If the experimental A_i values were exact, then the residual would reflect the mathematical stability. The c_j values calculated using the residual D matrix are the errors in the concentration values previously calculated. The relative importance of the two sources of error can be estimated as follows. If the number of certain digits in the experimental values is q and the word length of the computer is p, it follows that if the uncertainty in the $(p + 1)^{st}$ digit gives rise to a residual M_R, then the uncertainty in the $(q + 1)^{st}$ digit gives rise to a minimum error in the concentration solutions of the order of magnitude $10^{(p-q)} M_R$. Thus the error due to physical uncertainties $P_R \geq 10^{(p-q)} M_R$ and the residuals calculated by this process, R, are $R \leq M_R (1 + 10^{(p-q)})$. For the IBM System/360 Model 67 computer used in this analysis, p = 7. The standard deviation in the experimental absorptions is less than 0.5% for all reasonable absorptions $\underline{/}$See Table XII$\underline{I}/$. The D vector is composed of the product of these values and the standard deviation in the mean of each d_j value is related to that of the A_i values which compose it,[228]

$$\sigma_D = \frac{1}{\sqrt{\lambda}} \sigma_A = 0.139 \quad \sigma_A = 0.07\% \tag{29}$$

The computer rounding errors may be considered to be completely random. Hence $q = 3$ and $P_R = 10^4 M_R \geq R$. The mathematical errors introduced by the solution process are negligible compared to the errors introduced by the experimental uncertainties. The residuals calculated using this technique give rise to an estimate of the uncertainties in the concentrations of 0.03% or greater, due exclusively to the experimental measurement fluctuations.

However, the observed errors are much larger than this and so a finer estimate of the effect of the physical errors on the stability and accuracy of the solutions is needed. A method allowing modification of the experimentally determined absorption values was implemented. After the concentrations are found, these values are used to calculate y_1, the expected absorption at the first wavelength. This value is compared to A_1 and A_1 is allowed to vary by up to 2% in the direction of y_1. This new value (A_1'), along with the other 51 unchanged A_i values, is used to recalculate the concentrations, which are, in turn, used to adjust A_2. This is repeated for all the wavelengths, and the entire process may be repeated until the differences between y_i and the modified A_i are arbitrarily small. Typically, fewer than five iterations were needed to make $y_i - A_i' < 0.001$. The mathematical round errors accumulate, however, and are as much as 260 times greater than for the simple solution. This is still less than the minimum physical uncertainty expressed above. The final set of concentrations represent the exact solutions of the equations using modified absorptions. This minimization of absorption method produced solutions whose values were different from the original calculated solutions by only a

small amount for gases far above their MDC; i.e., for gases responsible

for significant absorption of the light. For gases at concentrations near

their MDC, the differences were larger by up to a factor of 10 than the

error in the original calculated solutions. These new solutions are not

necessarily in the direction of decreased error compared to the known

input concentrations and are not meant to improve the accuracy of the cal-

culated solutions, but are intended to provide a better estimate of the

magnitude of the errors due to the experimental uncertainties for each

gas in each particular mixture. This method provides a better estimate

of the uncertainties in the solutions than those calculated from the

residuals which form a lower bound for these errors. Observation of the

minimized absorptions reveals that the strong absorptions are seldom

changed by as much as 2% after 5 iterations (max. 10% change possible),

whereas the weak absorptions ($I/I_o > 0.4$) are greatly altered, with the

weakest changed by nearly 10%. Thus compounds whose strongest absorption

coefficients are in regions of low absorption of the mixture may have their

concentrations drastically altered by this minimization process. This

effect is noticeable in the solutions for concentrations of compounds that

are weak absorbers, which are made very unstable by this iteration method.

The preferential treatment received by strong absorbers in the simple

solution process, is amplified by this method, which highlights the

instabilities.

Finally, it must be noted that no systematic deviation of the calcu-

lated concentrations from the known values occurred at very low con-

taminant levels. If self-broadening were significant in the measured

absorption coefficients a consistently low concentration value would have been calculated. The least-squares fitting procedure emphasizes the role of the stronger absorption coefficients which were determined by low trace gas concentrations. Thus, it is believed that there is some self-broadening contribution to the observed absorption coefficients, but the solution procedure used results in a minimization of these effects to the point where no experimental perturbations are observable. Nonetheless, a more systematic study of pressure-broadening effects in many of these systems would be desirable. For such studies, a broadly tunable laser source is preferable to a line-tunable system such as CO_2. The use of such a source permits one to map out a complete profile, rather than just sample a single point on that profile.

E. Conclusions

It has been shown that the CO_2 laser absorption technique is capable of sensitive, real-time detection of trace contaminants. The method permits simultaneous detection of fifteen or more species at ppm levels. This sensitivity is largely due to the stability and reproducibility of data gathered using the frequency stabilized CO_2 laser and dual beam detection system. Absorption interferences have been found not to seriously degrade performance from the single gas levels. In addition, the presence of absorbers, like CO_2, in the ambient atmosphere may actually increase the sensitivity of detection. The development of a self-evaluation procedure permits assessment of the method's performance under varying ambient conditions.

The standards set by the Committee on Toxicology of the NAS Panel on Air Quality[20] for both short- and long-term exposures are listed in Table XV. The MDC's we are able to obtain for five of the gases listed in the Table are below the long-term exposure level, and an additional four are below the short-term level. In the case of vinyl chloride, the exposure levels have been set particularly low because of the carcinogenic properties of this gas. Extending the sampling path from 10 to 100 m would permit detection at or below this level. Such a configuration would be appropriate for an industrial monitoring situation, in which vinyl chloride contamination is most likely to be a problem. We have also seen that addition of a broadly absorbing gas can enhance sensitivity to low concentrations. This might be practicable for samples withdrawn from the atmosphere into an enclosed multiple-pass monitoring cell.

Currently precision is limited by the experimental variations in the absorption measurements. Either reduction in the magnitude of these fluctuations or utilization of a greater number of experimental wavelengths would improve calculated concentration precision through the least-squares fitting procedure of the absorption data. It is seen from equation (29) that the expected deviation in the D matrix is proportional to the inverse root of the number of different wavelengths used. For 52 wavelengths and 15 gases, the mathematical contribution to the error in the calculated concentration is negligible. Increasing the number of wavelengths should permit a corresponding increase in the number of simultaneously detectable gases at a reasonable level of precision and sensitivity. One way to accomplish this would be to use several isotopically pure CO_2 lasers. In this

manner several hundred lines spanning the 8.9 μm - 11.4 μm wavelength region could be employed. Such a system would be bulky and have large power requirements; separate laser cavities and support electronics would be needed for each laser. Use of a mixture of all the CO_2 isotopes is not possible due to quenching.[101]

Another way in which this could be achieved would be to use continuously tunable, rather than fixed-frequency (line-tunable) monitoring sources. If a given pollutant has sharp spectral features, then the laser can be tuned to one of these sharp features, free from interference, and good analyses can be obtained. This has been accomplished, for example, for NO using a spin-flip Raman laser[68] and for CO,[104] ethylene,[153] and SO_2[221] using a tunable diode laser. In spectral regions where all the contaminants absorb, the data reduction methods we have employed may be used to reduce these absorption measurements to derive concentrations without running into computer limitations. If semiconductor diodes were used as the tunable sources, an array of these tiny lasers could be powered by the same support equipment, and they could be chosen to insure that all contaminants of interest would have significant absorption at some laser wavelength.

APPENDIX   : Concentration Determination Procedure

A. Least-Squares Data Fitting

Substituting in for y_i in equation (25) using equation (24):

$$\eta = \sum_{i=1}^{\lambda} (y_i - A_i)^2 = \sum_{i=1}^{\lambda} \left(\{ \sum_{j=1}^{N} \varepsilon_{ij} \, c_j \, \ell \} - A_i \right)^2 \qquad (A1)$$

As an example, let $\lambda = 4$ and $N = 3$, then

$$\eta = \sum_{i=1}^{\lambda} \left((\varepsilon_{11} \, c_1 \, \ell + \varepsilon_{12} \, c_2 \, \ell + \varepsilon_{13} \, c_3 \, \ell) - A_i \right)^2 \qquad (A2)$$

$$= \sum_{i=1}^{\lambda} \{ (\varepsilon_{11}c_1\ell + \varepsilon_{12}c_2\ell + \varepsilon_{13}c_3\ell)^2 + A_i^2 - 2A_i(\varepsilon_{11}c_1\ell + \varepsilon_{12}c_2\ell + \varepsilon_{13}c_3\ell) \}$$

Performing one of the partial differentiations,

$$\frac{\partial \eta}{\partial c_1} = 0 = \sum_{i=1}^{\lambda} (2\varepsilon_{11}^2 \, c_1 \, \ell^2 + 2\varepsilon_{11} \, \varepsilon_{12} \, c_2\ell^2 + 2\varepsilon_{13}\varepsilon_{11}c_3\ell^2 - 2A_i\varepsilon_{11}\ell)$$

or

$$\sum_{i=1}^{\lambda} (\varepsilon_{11}\varepsilon_{11}c_1 + \varepsilon_{11}\varepsilon_{12}c_2 + \varepsilon_{11}\varepsilon_{13}c_3) = \sum_{i=1}^{\lambda} \varepsilon_{11}A_i/\ell \qquad (A3)$$

and using equation (27)

$$(f_{11} \, c_1 + f_{12} \, c_2 + f_{13} \, c_3) = d_1 \qquad (A4)$$

Repeating the differentiation for each c_j gives rise to an (N x N) F
matrix of the form given in equation (26).

B. Matrix Decomposition

Normal matrix decomposition products are of the form $F = L \, U$
where L and U are triangular matrices below and above the diagonal.
Both L and U matrices need to be stored. Either L or U will not be
a unit triangle. If the matrix F is symmetric and positive definite,

as must be the case for matrices obtained from a least-squares fitting, the decomposition may take the form $F = L\ L'$ where the triangles are the transpose of each other. L is now not a unit triangle. This is seen to be equivalent to the decomposition $F = L_u\ T\ L_u'$, where L_u is a unit triangle and T is diagonal non-unitary, if we take $L = L_u\ T^{\frac{1}{2}}$, where $T^{\frac{1}{2}}$ is the square root of T $\left[(t_{ii})^{\frac{1}{2}} = \sqrt{t_{ii}} \right]$. Only L or L' need be recorded. For this system

$$
\begin{pmatrix}
f_{11} & f_{12} & \cdots & f_{1N} \\
f_{21} & f_{22} & \cdots & f_{2N} \\
\vdots & \vdots & \vdots & \vdots \\
f_{N1} & f_{N2} & \cdots & f_{NN}
\end{pmatrix}
\begin{pmatrix}
c_1 \\ c_2 \\ \vdots \\ c_N
\end{pmatrix}
=
\begin{pmatrix}
d_1 \\ d_2 \\ \vdots \\ d_N
\end{pmatrix}
\tag{A5}
$$

The L' triangle is found by the following procedure:

1) $\ell_{11} = (f_{11})^{\frac{1}{2}}$, $\ell_{1s} = f_{1s}/\ \ell_{11}$, $P_1 = d_1/\ \ell_{11}$ for the first row for all $s > 1$.

2) let $q_{j1} = -\ f_{j1}/\ \ell_{11}$, then set $f_{js} = q_{j1}\ \ell_{1s} + f_{js}$ and $d_j = q_{j1}\ P_1 + d_j$ for $j = 2, \ldots ,N$ and $s = 1, \ldots ,N$.

3) $\ell_{22} = (f_{22})^{\frac{1}{2}}$, $\ell_{2s} = f_{2s}/\ \ell_{22}$, $P_2 = d_2/\ \ell_{22}$ for second row for all $s > 2$.

4) let $q_{j2} = -\ f_{j2}/\ \ell_{22}$, then set $f_{js} = q_{j2}\ \ell_{2s} + f_{js}$ and $d_j = q_{j2}\ P_2 + d_j$ for $j = 3, \ldots ,N$ and $s = 2, \ldots ,N$.

5) continue until triangularized.

Now concentration values may be found by backsubstitution in equation

$$L'\ c = P$$

As an example consider the system of equations:

$$\begin{pmatrix} 2 & 1 & 1 \\ 1 & 2 & 1 \\ 1 & 1 & 1 \end{pmatrix} \begin{pmatrix} c_1 \\ c_2 \\ c_3 \end{pmatrix} = \begin{pmatrix} 5 \\ 6 \\ 4 \end{pmatrix}$$

Solving, using the steps indicated above,

1) $\left[\begin{array}{ccc|c} \sqrt{2} & 1/\sqrt{2} & 1/\sqrt{2} & 5/\sqrt{2} \\ 1 & 2 & 1 & 6 \\ 1 & 1 & 1 & 4 \end{array}\right]$

2) $\left[\begin{array}{ccc|c} \sqrt{2} & 1/\sqrt{2} & 1/\sqrt{2} & 5/\sqrt{2} \\ 0 & 3/2 & 1/2 & 7/2 \\ 0 & 1/2 & 1/2 & 3/2 \end{array}\right]$

3) $\left[\begin{array}{ccc|c} \sqrt{2} & 1/\sqrt{2} & 1/\sqrt{2} & 5/\sqrt{2} \\ 0 & \sqrt{3/2} & \tfrac{1}{2}\sqrt{2/3} & 7/2\sqrt{2/3} \\ 0 & 1/2 & 1/2 & 3/2 \end{array}\right]$

4) $\left[\begin{array}{ccc|c} \sqrt{2} & 1/\sqrt{2} & 1/\sqrt{2} & 5/\sqrt{2} \\ 0 & \sqrt{3/2} & \tfrac{1}{2}\sqrt{2/3} & 7/2\sqrt{2/3} \\ 0 & 0 & 1/3 & 1/3 \end{array}\right]$

5) $\begin{bmatrix} \sqrt{2} & 1/\sqrt{2} & 1/\sqrt{2} \\ 0 & \sqrt{3/2} & \tfrac{1}{2}\sqrt{2/3} \\ 0 & 0 & \sqrt{1/3} \end{bmatrix} = L'$ $\begin{pmatrix} 5/\sqrt{2} \\ 7/2\sqrt{2/3} \\ \sqrt{1/3} \end{pmatrix} = P$

By back-substitution $c_3 = 1$, $c_2 = 2$, $c_1 = 1$. The computer solution programs are given in Appendix IV.

C. Calculation of Residuals

Once the solutions have been found, the magnitude of the mathematical errors in the solution process may be estimated by the following procedure:

1) Compute $R_o = D - F c$ using double precision.

2) Solve $F \delta c = R_o$ using the L' matrix already calculated.

3) Set $c' = c + \delta c$, rounding to single length.

4) Repeat using c' instead of c in step 1).

-99-

APPENDIX : COMPUTER CONCENTRATION DETERMINATION PROGRAMS

Elimination Method with Zeroing of Concentrations

```
C Source for Double Precision ELimination with Zeroing of
C negative Concentrations.
C
C      SOURCE.DPELZC
C
C This program solves a system of LAMBDA eqns. in NGASES
C unknowns, where LAMBDA>NGASES. LAMBDA may not exceed
C  55; NGASES may not exceed 15. Both are read as input.
C Only non-zero inputs need be entered, one element at a
C time preceeded by its row and column numbers. A row
C number of 99 signals end of data. The program requires
C the following parameters prior to the entering of data;
C LAMBDA: number of wavelengths for which there is data
C NGASES: number of gases in the mixture for this run
C BIGSTA: the maximum absorption to be permitted
C BIGSTE: the largest absorption coefficient to be permitted
C All input is checked for validity.
C
      DIMENSION ABSORP(55),ABSCOF(55,15),CONC(15),ACRED(15,15),-
     *            D(15),INDEX(15)
      DOUBLE PRECISION ACRED,D,SUM,TEMP,Q
      LOGICAL OK
C
C First clear arrays of data to be read in. Create index.
C
      DO 20 I=1,55
         ABSORP(I)=0.0
         DO 10 J=1,15
            ABSCOF(I,J)=0.0
 10         CONTINUE
 20      CONTINUE
      DO 25 J=1,15
         CONC(J)=0.0
         INDEX(J)=J
 25      CONTINUE
C
```

```
C Read control parameters now.
      READ(5,500) LAMBDA,NGASES,BIGSTA,BIGSTE
      NGASP1=NGASES+1
      IF(.NOT.((LAMBDA.GT.55).OR.(LAMBDA.LT.1))) GO TO 30
      IF(.NOT.((NGASES.GT.15).OR.(NGASES.LT.1))) GO TO 30
      IF(.NOT.((BIGSTE.LT.0.0).OR.(BIGSTA.LT.0.0)))GO TO 30
      WRITE(6,510)
      STOP
C
C If input parameters were bad, job was aborted.  Read in
C arrays ABSORP first.  Set counter of bad data to 0.
C Check data validity before storing.
C
   30 NERROR=0
      LIMIT=LAMBDA+1
      DO 35 KARDNO=1,LIMIT
         READ(4,515) I,J,TEMP
         IF (I.EQ.99) GO TO 36
         OK=.TRUE.
         IF((I.LT.1).OR.(I.GT.LAMBDA).OR.(J.NE.1))OK=.FALSE.
         IF(DABS(TEMP).GT.BIGSTA)OK=.FALSE.
         IF(OK) ABSORP(I)=TEMP
         IF(.NOT.OK) WRITE (6,530) I,J,TEMP
         IF(.NOT.OK) NERROR=NERROR+1
   35    CONTINUE
C
C If DO is satisfied, there were too many absorptions read.
C
      WRITE (6,540) KARDNO
      STOP
C
C Read in absorption coefficients. NERROR is cumulative.
C
   36 LIMIT=NGASES*(LAMBDA)+1
      DO 39 KARDON=1,LIMIT
         READ(7,520) I,J,TEMP
```

```
          IF (I.EQ.99) GO TO 4C
          OK=.TRUE.
          IF((I.LT.1).OR.(I.GT.LAMBDA))OK=.FALSE.
          IF((J.LT.1).OR.(J.GT.NGASES))OK=.FALSE.
          IF(DABS(TEMP).GT.BIGSTE)OK=.FALSE.
          IF(OK) ABSCOF(I,J)=TEMP
          IF(.NOT.OK) WRITE (6,530) I,J,TEMP
          IF(.NOT.OK) NERROR=NERROR+1
   39     CONTINUE
C
C If DO is satisfied, there were too many coeff. read.
C
      WRITE (6,540) KARDON
      STOP
C
C All data cards have been read, check error count, WRITE
C amount of data read.
C
   40 IF(NERROR.NE.0)WRITE(6,550) NERROR
      IF(NERROR.NE.0)STOP
      KARDS=KARDNO+KARDON-2
      WRITE(6,555) KARDS
C
C Form condensed abs. coeff. matrix.  Allows all of data
C to be used.  Each ACRED entry is the product of two
C absorption coefficients.
C
   48 DO 70 J=1,NGASES
          DO 60 K=J,NGASES
            SUM=0.0
            DO 50 I=1,LAMBDA
              SUM=SUM+(ABSCOF(I,J)*ABSCOF(I,K))
   50       CONTINUE
            ACRED(J,K)=SUM
            ACRED(K,J)=SUM
   60     CONTINUE
```

```
      70     CONTINUE
C
C Now find D(J) array.
C
      DO 90 J=1,NGASES
         SUM=0.0
         DO 80 I=1,LAMBDA
            SUM=SUM+ ABSCOF(I,J)*ABSORP(I)
   80       CONTINUE
         D(J)=SUM
   90    CONTINUE
C
C Now triangularize matrix to LL' form.
C
      K=0
      DO 130 J=1,NGASES
         K=K+1
         TEMP=1/(DSQRT(ACRED(J,K)))
         KM1=K-1
         KDIVLM=NGASES-KM1
         DO 100 KDIV=1,KDIVLM
   KMDIV=KM1+KDIV
   ACRED(J,KMDIV)=ACRED(J,KMDIV)*TEMP
  100       CONTINUE
         D(J)=D(J)*TEMP
         LINDEX=J+1
         MINDEX=K+1
         DO 120 L=LINDEX,NGASES
   Q=-(ACRED(L,K))/ACRED(J,K)
            DO 110 M=MINDEX,NGASES
               ACRED(L,M)=ACRED(L,M)+Q*(ACRED(J,M))
  110          CONTINUE
            D(L)=D(L)+Q*D(J)
  120       CONTINUE
  130    CONTINUE
C
```

```
C Zero entries in lower triangle, all information is in upper.
C
      DO 150 J=2,NGASES
         JM1=J-1
         DO 140 K=1,JM1
            ACRED(J,K)=0.0
140         CONTINUE
150      CONTINUE
C
C Now find solutions by back substitution.
C Any negative solutions are zeroed, and a record kept of
C their existence.  After all concentrations are found a
C jump is made to a subroutone to remove all the absorp-
C tion coefficients of these negative concentrations from
C the elimination calculations.  The exit is to a stage
C  where the ACRED array will be recalculated for a smaller
C  number of gases.
C
  155 SUM=0.0
      IMCONC=0
      DO 170 J=1,NGASES
         JELIM=NGASES-J+1
         CONC(JELIM)=(D(JELIM)-SUM)/ACRED(JELIM,JELIM)
         IF(CONC(JELIM).LE.0.0) IMCONC=IMCONC+1
         IF(CONC(JELIM).LT.0.0) CONC(JELIM)=0.0
         SUM=0.0
         JELIM1=JELIM-1
         IF(JELIM1.LT.1)GO TO 171
         DO 160 N=JELIM,NGASES
            SUM=SUM+ACRED(JELIM1,N)*CONC(N)
160         CONTINUE
170      CONTINUE
  171 IF(IMCONC) 172,172,200
C
C Now answers are in CONC array.  WRITE CONC in N/M*M and
C torr, and give the ratios compared to the exp. estimates.
```

```
      172 WRITE(6,560) NGASES
          DO 175 J=1,NGASES
             WRITE(6,580)INDEX(J),CONC(J)
      175 CONTINUE
          DO 180 J=1,NGASES
             CONC(J)=CONC(J)/133.322
      180 CONTINUE
          WRITE(6,570) NGASES
          DO 185 J=1,NGASES
             WRITE(6,580)INDEX(J),CONC(J)
      185    CONTINUE
          WRITE(6,590)
          I=1
          DO 190 J=1,NGASES
             READ(3,600)TEMP
             IF(INDEX(I).NE.J) GO TO 190
             IF(TEMP.EQ.0.0) GO TO 189
             TEMP=CONC(J)/TEMP
             WRITE(6,610)INDEX(I),TEMP
      189    I=I+1
      190    CONTINUE
          STOP
C
C This subroutine removes ABSCOF of zeroed concentrations
C from the calculations.  Index is the marker showing
C which of the gases have been removed.
C
      200 NCONC=NGASES
      201 DO 204 I=1,NCONC
             IF(CONC(I)) 205,205,204
      204    CONTINUE
          GO TO 48
      205 DO 210 J=I,NGASES
             JP1=J+1
             DO 208 K=1,LAMBDA
```

```
              ABSCOF(K,J)=ABSCOF(K,JP1)
  208         CONTINUE
        INDEX(J)=INDEX(JP1)
  210      CONTINUE
      NGASES=NGASES-1
      GO TO 204
  500 FORMAT(2I2,2G6.3)
  510 FORMAT('0','ERROR IN CONTROL PARAMETERS')
  515 FORMAT(2I2,G8.3)
  520 FORMAT(2I2,G10.7)
  530 FORMAT(1X,'ERROR IN CARD WITH I= ',I2,' ,J= ',I2, -
     *'  VALUE=  ',1PE14.6)
  540 FORMAT('0', 'TOO MUCH DATA INPUT')
  550 FORMAT('0', 'ERRORS FOUND IN ',I2,' DATA CARDS')
  555 FORMAT(1X,I3,' DATA POINTS READ IN.')
  560 FORMAT('0',' THE CONCENTRATIONS OF THE ',I2,' GASES -
     *ARE(IN N/M*M)'/)
  570 FORMAT('0',' THE CONCENTRATIONS OF THE ',I2,' GASES -
     *ARE(IN TORR )'/)
  580 FORMAT(1X,I2,5X,G14.7)
  590 FORMAT(1X,'THE RATIOS OF THE CALC. CONC. TO THE EXP-
     *ERIMENTAL CONC. ARE:'/)
  600 FORMAT(1X,G7.4)
  610 FORMAT(1X,I2,5X,G14.8)
      END
```

REFERENCES

1. J. Rothenberg, private communication.

2. M.I. Goldman, in Controlling Pollution (Prentice-Hall:Englewood Cliffs,1967), pp.3-39.

3. R.S. Berry, in A Study of Air Pollution, Union of Concerned Scientists (1969). (unpublished).

4. G.B. Morgan, G. Ozolins, and E.C. Tabor, Science 170,289 (1970).

5. "The Sources of Air Pollution and Their Control," Public Health Service Publication No. 1548, Dept. of H.E.W.(1968).

6. D.M. Snodderly, Jr., in Advances in Environmental Science and Technology,3, Eds. J.N. Pitts and R.L. Metcalf (Wiley:New York, 1974), pp.157-281.

7. a. J.P. Cheswick, Nature 254,275 (1975).

    b. P.J. Cicerone, R.S. Stolarski, S. Walters, Science 185,1165 (1974).

    c. M.J. Molina and F.S. Rowland, Science 188,378 (1975).

    d. N.E. Hester, E.R. Stevens, and O.C. Taylor, Atmos. Env. 9(6-7),603 (1975).

    e. P.H. Howard and A. Hanchett, Science 189,217 (1975).

    f. H.S. Johnston, in Adv. in Environmental Science and Technology,4 Eds. J.N. Pitts and R.L. Metcalf (Wiley:New York,1974), pp.263-380.

    g. H.S. Johnston, Science 173,517 (1971).

    h. Science Update, Fluorocarbon/Ozone, Ed. R.B. Ward (Du Pont:Wilmington,1976), Nos. 1 and 2.

8. a. R.H. Sabersky, D.A. Sinema, and F.H. Shair, Env. Sci. and Tech. 7(4),347 (1973).
    b. F.H. Shair and K.L. Heitner, Env. Sci. and Tech. 8(5),444 (1974).

    c. G.A. Petersen and R.H. Sabersky, J. Air Poll. Cont. Assoc. 25(10), 1028 (1975).

9. W.A. Glasson and C.S. Tuesday, Env. Sci. and Tech. 4(11),916 (1970).

10. N.I. Sax, Dangerous Properties of Industrial Materials, 4th ed. (Van Nostrand-Reinhold:New York,1975).

11. Toxicity of Vinyl Chloride and Polyvinyl Chloride,Eds. I.J. Selikoff and E.C. Hammond, Annals of the New York Academy of Science 246 (1975).

12. C.D. Hollowell, R.D. McLaughlin, and J.A. Stokes, I.E.E.E. Trans. Nuc. Sci. NS-22(2),835 (1975).

13.   Env. Sci. and Tech. 5(6),503 (1971).

14.a. J.D. Hackney, Arch. Env. Health 30(8),379 (1975).

  b. W.H. Durham, Arch. Env. Health 28(5),241 (1974).

15.   H.L. Galiana, N.A.S.A. Report NASA CR-1826 (July 1971), pp.19-38.

16.   W. Bertsch, et. al., J. Chromatography 99,673 (1974).

17.   T. Wydeven, private communication.

18.   "Chemical Analysis of Adsorbates from Three Skylab Samples," Contract
      RC4-37042 to Martin Marietta Aerospace Corp. by Analytical Research
      Laboratories, Inc. (Apr. 1974).

19.   New York Times (July 25,1975), p.8.

20.   "Atmospheric Contaminants in Spacecraft," Report of the Panel on Air
      Quality in Manned Spacecraft of the Committee on Toxicology, National
      Academy of Sciences-National Research Council (June 1972).

21.a. D.H. Ahlstrom, R.J. Kilgour, S.A. Liebman, Anal. Chem. 47(8),1411 (1975).

  b. C.H. Hartmann, Proc. of the Joint Conference on Sensing of Environ-
     mental Pollutants, Palo Alto, Ca., 8-10 Nov. 1971, AIAA Paper No.71-1046.

  c. D.A. Levaggi and M. Feldstein,ibid., AIAA Paper No. 71-1115.

  d. W. Dencker, M. Robinson, and R. Villalobos, Jr., E.P.A. Contract
     Report EPA-650/2-74-056 (July 1974).

22.   R. Villalobos and R.L. Chapman, Chimia 28(8),411 (1974).

23.   R. Villalobos, in Analytical Methods Applied to Air Pollution Measure-
      ments, Eds. R.K. Stevens and W.F. Herget (Ann Arbor Science:Ann Arbor,
      1974), Chapter 1.

24.   H.P. Burchfield, Proc. of the International Symposium on the Identi-
      fication and Measurement of Environmental Pollutants, Montreal, June
      1971 (Campbell:Ottawa,1971), p.244.

25.   S.R. Heller, J.M. McGuire, and W.L. Budde, Env. Sci. Tech. 9(3),210
      (1975).

26.   H.S. Hertz, A. Hites, and K. Biemann, Anal. Chem. 43(6),681 (1971).

27.a. R.Perry, Proc. Int. Symp. Ident. and Meas. Env. Poll., op. cit., p.130.

  b. R.C. Lao, et. al., ibid., p.144.

28.a. M. Rotheram and M.R. Ruecker, Amer. Soc. Mech. Eng. Paper No.72-ENAv-15,
      presented at the Environmental Control and Life Support Systems Con-
      ference, San Francisco, Ca., 14-16 Aug. 1972.

28.b. M.R. Ruecker, Amer. Soc. Mech. Eng. Paper No. 73-ENAs-9,presented at the Intersociety Conference on Environmental Systems, San Diego, Ca., 16-19 July 1973.

29. E.P. Grimsrud and R.A. Raumussen, Atm. Env. 9(11),1014 (1975).

30. A. Mooradian, private communication.

31. G. Herzberg, Molecular Spectra and Molecular Structure, III (Van Nostrand:Princeton,1966), Chapter 5.

32. H.C. Lord, et.al., J. Air Poll. Cont. Assoc. 24(2),136 (1974).

33. R.N. Hager, Jr., Proc. Joint Conf. Sens. Env. Poll., op. cit., AIAA Paper No. 71-1045.

34. D.E.Burch and D.A. Gryvnak, Anal. Meth. Appl. Air Poll. Meas.,op. cit., Chapter 10.

35.a. H.M. Barnes, Jr., W.F. Herget, and R. Rollins, ibid., Chapter 12.

   b. L. Langan, Proc. Joint Conf. Sens. Env. Poll., op. cit., AIAA Paper No. 71-1060.

   c. C.R. McCreight and C.L. Tien, ibid., AIAA Paper No. 71-1061.

   d. W.H. Herget, Proc. of Second Joint Conference on Sensing of Environmental Pollutants, Washington D.C., 10-12 Dec. 1973 (ISA:Pittsburgh, 1973), p.155.

36.a. R.A. Schindler, Appl. Opt. 9(2),301 (1970).

   b. R.A. Toth and C.B. Farmer, Proc. Joint Conf. Sens. Env. Poll., op. cit., AIAA Paper No. 71-1109.

37. S.H. Chan and D. Nelson, J. Quant. Spectros. and Rad. Transfer 14(4), 287 (1974).

38. T.H. Maugh, Science 177,1091 (1972).

39. P.L. Hanst, et. al., E.P.A. Contract Report No.EPA-650/4-75-006(1975).

40. P.L. Hanst, A.S. Lefohn, and B.W. Gay, Jr., Appl. Spect. 27(3),188(1973).

41. D.E. Dalsis, Ph.D. Thesis, Clemson University, 1974.

42. A.E. Roche and A.M. Title, Proc. Second Joint Conf. Sens. Env. Poll., op. cit., p.21.

43. P.L. Hanst, Proc. of the First European Electro-Optics Markets and Technology Conference, Geneva, 13-15 Sept. 1972 (IPC Sci. and Tech.: London,1973), p.7.

44. P.L. Hanst, in _Advances in Environmental Science and Technology_,2,
     Eds. J.N. Pitts and R.L. Metcalf (Wiley:New York,1971), pp.91-213.

45. G.E. Fisher and T.A. Huls, J. Air Poll. Cont. Assoc. 20(10),666 (1970).

46.a. T.V. Ward and H.H. Zwick, Appl. Opt. 14(2),2896 (1975).

  b. E.R. Bartle, S. Kaye, and E.A. Meckstroth, _Proc. Joint Conf. Sens.
     Env. Poll._, _op. cit._, AIAA Paper No. 71-1049.

47. J.A. Hodgeson, W.A. McClenny, and R.K. Stevens, _Anal. Meth. Appl.
     Air Poll. Meas._, _op. cit._, Chapter 2.

48.a. A. Fontijn and R.J. Ronco, _Proc. Joint Conf. Sens. Env. Poll._, _op.
     cit._, AIAA Paper No. 71-1066.

  b. B. Krieger, M. Malki, and R. Kummler, Env. Sci. and Tech.6(8),742(1972).

  c. J.N. Pitts, et. al., Env. Sci. and Tech. 7(6),550 (1973).

  d. F.M. Black and J.E. Sigsby, Env. Sci. and Tech. 8(2),149 (1974).

  e. D.H. Stedman, et. al., J. Air Poll. Cont. Assoc. 22(4),260 (1972).

  f. R. Byerly, I.E.E. Trans. Nuc. Sci. NS-22(2),856 (1975).

  g. S. van Heusden, Philips Tech. Rev. 34(2-3),73 (1974).

49.a. J.N. Pitts, et.al., _Proc.Int. Symp. Ident. and Meas. Env. Poll._, _op.
     cit._, p.32.

  b. A.M. Winer, et. al., Env. Sci. and Tech. 8(13),1118 (1974).

  c. J.E. Sigsby, et. al., Env. Sci. and Tech. 7(1),51 (1973).

50. W.J. Zolner, U.S. Patent 3882028 (1975).

51. R.G. Confer, Amer. Ind. Hyg. Assoc. Jour. 36(7),491 (1975).

52.a. T.T. Kikuchi, Appl. Opt. 13(2),239 (1974).

  b. T. Hadeishi, et. al., Science 187,348 (1975).

  c. E. Bretthauer, W. Beckert, and S. Snyder, _Proc. of Second Conference
     on Environmental Quality Sensors_, Las Vegas, Nv., Oct. 1973 (Gov't
     Printing Office:Washington,1974), p.I-44.

53. J.I. Steinfeld, Opt. Engineering 13(6),476 (1974).

54. H. Inaba and T. Kobayasi, Opto-Electronics 4,101 (1972).

55.a. D.A. Leonard, Opt. Quant. Electron. 7,197 (1975).

  b. R. Goulard, J. Quant. Spectros. and Rad. Transfer 14,969 (1974).

56. R.M. Measures, UTIAS Report No. 174, Ottawa, Ontario (Dec. 1971).

57.a. S.Z. Levine, Ph.D. Thesis, University of Pittsburgh, 1973.

   b. C.G. Stevens, et.al., Chem. Phys. Lett. **18**(4),465 (1973).

58.   H. Kildal and R. Byer, Proc. of I.E.E.E. **59**,1644 (1971).

59.   R.G. Gordon, W. Klemperer, and J.I. Steinfeld, <u>Ann. Rev. Phys. Chem.</u> **19**,215 (1968).

60.   S.M. Klainer, Opt. Engineering **14**(4),S110 (1975).

61.   A.W. Tucker, M. Birnbaum, and C.L. Fincher, Appl. Opt. **14**(6),1418(1975).

62.   R.L. Byer, Opt. Quant. Electron. **7**,147 (1975).

63.a. J.W. Robinson and J. Guagliardo, Spectros. Lett. **6**(5),271 (1973).

   b. N. Katayama and J.W. Robinson, Spectros. Lett. **8**(1),61 (1975).

   c. J.D. Dake, Ph.D. Thesis, Louisianna State University, 1973.

64.   R.T. Menzies, Appl. Opt. **10**(7),1532 (1971).

65.   I.M. Pikus, H.W. Goldstein, and T.R. Riethof, J. Spacecraft **10**(3), 190 (1973).

66.a. D.A. Helm and W.J. Zolner, U.S. Patent 3845309 (1974).

   b. R.T. Menzies, U.S. Patent 3891848 (1975).

   c. M. Birnbaum, U.S. Patent 3829696 (1974).

   d. H. Okabe and F.P. Schwarz, U.S. Patent 3906226 (1975).

   e. H.Okabe, U.S. Patent 3795812 (1974).

   f. C.C. Wang, et.al., Science **189**,797 (1975).

   g. F.P. Schwarz, H. Okabe, and J.K. Whittaker, Anal. Chem. **46**(8),1024 (1974).

   h. A.W. Tucker, A.B. Petersen, and M. Birnbaum, Appl. Opt. **12**(9),2037 (1973).

   i. J. Gelbwachs and M. Birnbaum, Appl. Opt. **12**(10),2442 (1973).

67.   L.B. Kreuzer, N.D. Kenyon, and C.K.N. Patel, Science **177**,347 (1972).

68.   L.B. Kreuzer, C.K.N. Patel, Science **173**,45 (1971).

69.a. E.L. Kerr and J.G. Atwood, Appl. Opt. **7**(5),915 (1968).

   b. L.B. Kreuzer, J. Appl. Phys. **42**(7),2934 (1971).

70.   W. Schnell and G. Fischer, Appl. Opt. **14**(9),2058 (1975).

71.   W. Schnell and G. Fischer, Z. Angew. Math. Phys. **26**,133 (1975).

72. C.F. Dewey, Jr., Opt. Engineering 13(6),483 (1974).

73. J. Gelbwachs, Appl. Opt. 13(5),1005 (1974).

74.a. P.D. Goldan and K. Goto, J. Appl. Phys. 45(10),4350 (1974).

b. C.F. Dewey, Jr., R.D. Kamm, and C.E. Hackett, Appl. Phys. Lett. 23(11),633 (1973).

75. M.C. Teich, Proc. of I.E.E.E. 56,37 (1968).

76. R.T. Menzies, Appl. Phys. Lett. 22(11),592 (1973).

77. R.T. Menzies, Opto-Electronics 4,179 (1972).

78. T. Kobayasi and H. Inaba, Opt. Quant. Electron. 7,319 (1975).

79. J. Jackson, Proc. First Europ. Electro-Optics Markets and Tech. Conf., op. cit., p.17.

80. L.W. Hrubesh, Joint Conf. Sens. Env. Poll., op. cit., AIAA Paper No. 71-1048.

81.a. C. Chakerian and M.F. Weisbach, J. Opt. Soc. Amer. 63(3),3425 (1973).

b. W.C. Peterson, et. al., J. Opt. Soc. Amer. 61(6),746 (1971).

82.a. P.A. Bonczyk, Rev. Sci. Instrum. 46(4),456 (1975).

b. A. Kaldor, W.B. Olsen, and A.G. Maki, Science 176,510 (1972).

c. A. Kaldor and B.W. Woodward, Air: II, Control of NO_x and SO_2 Emissions, AIChE Symposium Series 148, Vol. 71, Eds. C. Rai and R.D. Siegel (AIChE:New York,1975), p.183.

83. G.L. Linford, Appl. Opt. 12(6),1130 (1973).

84. S.M. Freund and D.M. Sweger, Anal. Chem. 47,930 (1975).

85. J.N. Driscoll and P. Warneck, J. Air Poll. Cont. Assoc. 23(10),858 (1973).

86. V.S. Letokov, private communication.

87. A.R. Barringer, et. al., Second Joint Conf. Sens. Env. Poll., op. cit., p.25.

88. H. Walter, Jr. and D. Flanigan, Appl. Opt. 14(6),1423 (1975).

89. H.W. Goldstein, et. al., Second Joint Conf. Sens. Env. Poll., op. cit., p.17.

90.a. L.L. Acton, et. al., A.I.A.A. Jour. <u>11</u>(7),899 (1973).

  b. P.L. Hanst and J.A. Morreal, J. Air Poll. Cont. Assoc. <u>18</u>(11),754 (1968).

91. V.E. Derr, et. al., E.P.A. Report EPA-650/2-74-113 (Feb. 1974).

92. G.W. King, <u>Spectroscopy</u> and <u>Molecular</u> <u>Structure</u> (Holt, Reinhart, and Winston:New York,1964), p.11.

93. P.W. Kruse, L.D. McGlauchlin, and R.B. McQuistan, <u>Elements of Infrared Technology</u> (Wiley:New York,1962), p.109.

94. <u>Ibid.</u>, pp.181-191.

95. T. Hirschfeld, S. Klainer, and R. Burton, "New Fields for Laser Raman Spectroscopy," in <u>Raman</u> <u>Reprints</u> (Block Engineering, 1975).

96. T. Henningsen, M. Garbuny, and R.L. Byer, Appl. Phys. Lett. <u>24</u>(5), 242 (1974).

97. H. Inomata and T. Igarashi, Japan. J. Appl. Phys. <u>14</u>(11),1751 (1975).

98. R.L. Byer and M. Garbuny, Appl. Opt. <u>12</u>(7),1496 (1973).

99. R.R. Patty, et. al., Appl. Opt. <u>13</u>(12),2850 (1974).

100. B.D. Green and J.I.Steinfeld, in <u>New</u> <u>Concepts</u> <u>in</u> <u>Air</u> <u>Pollution</u> <u>Research</u>, Ed. J.-O. Willums (Birkhaeuser:Basel,1974), p.125.

101. G.B. Jacobs and L.R. Snowman, I.E.E.E. J. Quant. Elect. <u>QE3</u>(11), 603 (1967).

102. L.R. Snowman and R.J. Gillmeister, <u>Joint</u> <u>Conf.</u> <u>Sens.</u> <u>Env.</u> <u>Poll.</u>, <u>op.</u> <u>cit.</u>, AIAA Paper No. 71-1059.

103. G.A. Antcliffe and J.S. Wrobel, Appl. Opt. <u>11</u>(7),1548 (1972).

104. R.T. Ku, E.D. Hinkley, and J.O. Sample, Appl. Opt. <u>14</u>(4),854 (1975).

105. K. McCormack and T. Richardson, U.S. Patent 3805074 (1974).

106. E.D. Hinkley and A.R. Calawa, in <u>Anal.</u> <u>Meth.</u> <u>Appl.</u> <u>Air</u> <u>Poll.</u> <u>Meas.</u>, <u>op.</u> <u>cit.</u>, Chapter 3.

107. A. Mooradian, A.S. Pine, and R.W. Ralston, N.S.F. Report NSF/RA-E-74-036 (Jan. 1974).

108. K. Asai and T. Igarashi, Opt. Quant. Electron. <u>7</u>,211 (1975).

109. D.C. O'Shea and L.G. Dodge, Appl. Opt. <u>13</u>(6),1481 (1974).

110. W. McClenny, et. al., E.P.A. Report EPA-650/2-74-046b (July 1974).

111. H. Tannenbaum, private communication.

112. This statement is valid for both infrared and ultraviolet spectral regions.

113. H. Inaba and T. Kobayasi, Nature 224,170 (1969).

114. H. Inaba and T. Kobayasi, Proc. of I.E.E.E. 58(10),1568 (1970).

115. T. Kobayasi and H. Inaba, Appl. Phys. Lett. 17(4),139 (1970).

116. M.P. McCormick and W.H. Fuller, Jr., Joint Conf. Sens. Env. Poll., op. cit., AIAA Paper No. 71-1056.

117. R. Goulard, J. Quant. Spectros. and Rad. Transfer 14,969 (1974).

118.a. S.H. Melfi, in Laser Raman Gas Diagnostics, Eds. M. Lapp and M.C. Penney (Plenum:New York,1974), p.231.

    b. V.E. Derr and C.G. Little, Appl.Opt. 9(9),1976 (1970).

119. H. Rosen, P. Robish, and O. Chamberlain, Appl. Opt. 14(11),2703 (1975).

120. R.L. Schiesow, Joint Conf. Sens. Env. Poll., op. cit., AIAA Paper No. 71-1086.

121. P.F. Williams, D.L. Rousseau, and S.H. Dworetsky, Phys. Rev. Lett. 32(5),196 (1974).

122.a. W.H. Smith and J.J. Barrett, Joint Conf. Sens. Env. Poll., op. cit., AIAA Paper No. 71-1078.

    b. J.J. Barrett, Laser Raman Gas Diagnostics, op. cit., p.63.

123. S.H. Melfi, Appl. Opt. 11(7),1605 (1972).

124. H.P. DeLong, Opt. Engineering 13(1),5 (1974).

125. R.M. Measures and G. Pilon, Opto-Electronics 4,101 (1972).

126.a. I. Melngailis, I.E.E.E. Trans. on Geo. Electron. GE-10(1),7 (1972).

    b. W.A. McClenny, W.F. Herget, and R.K. Stevens, Anal. Meth. Appl. Air Poll. Meas., op. cit., Chapter 6.

    c. J.A. Hodgeson, W.A. McClenny, and P.L. Hanst, Science 182,248 (1973).

127. D.H. Fine, Env. Sci. and Tech. 6(4),348 (1972).

128. B.A. Coulehan and H.W. Lang, Env. Sci. and Tech. 5(2),163 (1971).

129.   F.P. Scaringelli, E. Rosenberg, and K.A.Rehme, Env. Sci. and Tech.
       $\underline{4}$(11),924 (1971).

130.   W.A. McClenny, et. al., J. Air Poll. Cont. Assoc. $\underline{24}$(11),1044 (1974).

131.   R.A. McClatchey and J.E.A. Selby, AFCRL Report No. AFCRL-TR-74-003
       (Jan. 1974).

132.   S.E. Craig, et.al., E.P.A. Report EPA-650/2-74-046a (June 1974).

133.   R.L. Leonard, Appl. Opt. $\underline{13}$,1920 (1974).

134.   L.R. Lidholt, Opto-Electronics $\underline{4}$,133 (1972).

135.   M. Lapp, L.M. Goldman, and C.M. Penney, Joint Conf. Sens. Env. Poll.,
       op. cit., AIAA Paper No. 71-1084.

136.   S. Lederman, Appl. Opt. $\underline{11}$(9),2088 (1972).

137.   S. Kojima, Toshiba Review $\underline{90}$(3-4),21 (1974).

138.   S. Nakahara, et. al., Opto-Electronics $\underline{4}$,169 (1972).

139.   T. Hirschfield, et. al., Appl. Phys. Lett. $\underline{22}$(1),38 (1973).

140.   K.W. Rothe, U. Brinkmann, and H. Walther, Proc. VIII ICPEAC, Belgrad
       (July 1973).

141.   J. Gelbwachs, Appl. Opt. $\underline{12}$(12),2812 (1973).

142.a. S.H. Melfi, Appl. Opt. $\underline{12}$(4),901 (1973).
    b. V.L. Grantstein, M. Rhinewine, and A.H. Fitch, Appl. Opt. $\underline{12}$(7),
       1511 (1972).

143.   R.K. Seals, Jr. and C.H. Bair, Second Joint Conf. Sens. Env. Poll.,
       op. cit.,p.131.

144.   W.B. Grant and R.D. Hake, Jr., J. Appl. Phys. $\underline{46}$(7),3019 (1975).

145.   W.B. Grant, et. al., Appl. Phys. Lett. $\underline{24}$(11),550 (1974).

146.   K.W. Rothe, U. Brinkmann, and H. Walther, Appl.Phys. $\underline{3}$,115 (1974).

147.   K.W. Rothe, U. Brinkmann, and H. Walther, Appl. Phys. $\underline{4}$(2),181 (1974).

148.   H. Inaba and T. Kobayasi, Opt. Comm. $\underline{14}$(1),119 (1975).

149.   R.A. Brandwie and W.C. Davis, Appl. Opt. $\underline{11}$(7),1526 (1972).

150.   R.T. Menzies and M.S. Shumate, Joint Conf. Sens. Env. Poll., op. cit.,
       AIAA Paper No. 71-1083.

151. J. Dimeff, et. al., _ibid._, AIAA Paper No. 71-1064.

152.a. E.D. Hinkley, Opto-Electronics 4,69 (1972).

   b. E.D. Hinkley, _Proc. First Europ. Electro-Optics Mkts. Tech. Conf._, _op. cit._, p.24.

   c. E.D. Hinkley and R.H. Kingston, _Joint Conf. Sens. Env. Poll._, _op.cit._, AIAA Paper No. 71-1079.

153. E.D. Hinkley and P.L. Kelley, Science 171,635 (1971).

154. J.L. Hardwick and J.C.D. Brand, Chem. Phys. Lett. 21,458 (1973).

155. A.E. Douglas and K.P. Huber, Can. J. Phys. 43,74 (1965).

156. T. Chiba, Appl. Opt. 10(11),2456 (1971).

157. J.I. Davis, Appl. Opt. 5(1),139 (1966).

158. M.R. Wohlers, Appl. Opt. 11(6),1389 (1972).

159. J.P. Hansen and S. Madhu, Appl. Opt. 11(2),233 (1972).

160. P.P. Sorokin and J.R. Lankard, IBM J. Res. and Devel. 10,162 (1966).

161. B.B. Snavely, Proc. of I.E.E.E. 57(8),1374 (1969).

162.a. B.H. Soffer and B.B. McFarland, Appl. Phys. Lett. 10(10),266 (1967).

   b. F.C. Strome, Jr. and J.P. Webb, Appl. Opt. 10(6),1348 (1971).

163.a. A. Dienes, E.P. Ippen, and C.V. Shank, I.E.E.E. J. Quan. Elect. QE8(3),388 (1972).

   b. H.W. Kogelnik, et.al., I.E.E.E. J. Quan. Elect. QE8(3),373 (1972).

164. G. Capelle and D. Phillips, Appl. Opt. 9(12),2742 (1970).

165. S.A. Tuccio and F.C. Strome, Jr., Appl.Opt. 11(1),64 (1972).

166. H.P. Broida and S.C. Haydon, Appl. Phys. Lett. 16(3),142 (1970).

167. J.B. Marling, et. al., Appl. Opt. 13(10),2317 (1974).

168. C. Loth and Y.H. Meyer, Appl. Opt. 12(1),123 (1973).

169. M.E. Mack, Appl. Phys. Lett. 19(4),108 (1971).

170. W.W. Rigrod, J. Appl. Phys. 34(9),2602 (1963).

171. M.J. Weber and M. Bass, I.E.E.E. J. Quan. Elect. QE5,175 (1969).

172. P.P. Sorokin, et. al., J. Chem. Phys. 48,4726 (1968).

173. B.B. Snavely and O.G. Peterson, I.E.E.E. J. Quan. Elect. QE4,540 (1968).

174. B. Lengyl, Lasers, 2nd ed. (Wiley-Interscience:New York,1974), Chapter 3.

175. M. Bass, T.F. Deutsch, and M.J. Weber, Raytheon Tech. Rep. R-69, Technical Division (Nov. 1969).

176. H.W. Furumoto and H.L. Ceccon, Appl. Opt. 8(8),1613 (1969).

177. H.W. Furumoto and H.L. Ceccon, I.E.E.E. J. Quan. Elect. QE6(5), 262 (1970).

178. M. Maeda and Y. Miyazoe, Japan. J. Appl. Phys. 13(2),369 (1974).

179. M.H. Ornstein and V.E. Derr, Appl. Opt. 13(9),2100 (1974).

180. Synergetics Research Inc., coaxial Flashlamp.

181. H.V. Malmstadt, C.G. Enke, and E.C. Toren, Jr., Electronics for Scientists (Benjamin:New York,1963), P.568.

182. Synergetics Research Inc., Model 1070 flashlamp-pumped dye laser.

183. G. Holleman and J.I. Steinfeld, unpublished results.

184. M.K. Gilles, R.S. Hughes, and J.L. Thompson, Appl. Opt. 12(2),421 (1973).

185. M. Born and E. Wolf, Priciples of Optics (Pitman:Bath,1970), p.412.

186.a. D.J. Bradley, W.G.I. Caughey, and J.I. Vukusic, Opt. Comm. 4(2), 150 (1971).
  b. D.J. Bradley, J.V. Nicholas, and J.R.D. Shaw, Appl. Phys. Lett. 19(6),172 (1971).

187.a. L.D. Hutcheson and R.S. Hughes, Appl. Opt. 13(6),1395 (1974).
  b. D.J. Taylor, et. al., Appl. Phys. Lett. 19(8),269 (1971).

188.a. M. Okada, S. Shimizu, and S. Ieiri, Appl. Opt. 14(4),917 (1975).
  b. A.L. Bloom, J. Opt. Soc. Amer. 64,447 (1974).

189. J. Shah, Appl. Phys. Lett. 20(12),479 (1972).

190. S. Chandra, N. Takeuchi, and S.R. Hartmann, Appl. Phys. Lett. 21(4),144 (1972).

191. T.W. Hansch, Appl. Opt. 11(4),895 (1972).

192. M.H. Gassmann, Z. Angew. Math. Phys. $\underline{22}$(4),742 (1971).

193. B.G. Huth, G.I. Farmer, and M.R. Kagan, J. Appl. Phys. $\underline{40}$(13), 5145 (1969).

194. G.T. Schappert, K.W. Billman, and D.C. Burnham, Appl. Phys. Lett. $\underline{13}$(4),124 (1968).

195. T.C. Hall, Jr. and F.E. Blacet, J. Chem. Phys. $\underline{20}$,1745 (1952).

196. J.H. Clements, Phys. Rev. $\underline{47}$,224 (1935).

197. R.K. Asundi and R. Samuel, Proc. Ind. Acad. Sci.,A,$\underline{2}$,30 (1935).

198. A.J. Merer, Disc. Faraday Soc. $\underline{35}$,127 (1963).

199. R.W.B. Pearse and A.G. Gaydon, The Identification of Molecular Spectra (Chapman & Hall:London,1963).

200. A. Elliott, Proc. Royal Soc. London A, $\underline{123}$,629 (1929).

201.a. F.A. Jenkins, H.A. Barton,and R.S. Mulliken, Phys. Rev. $\underline{30}$(8), 150 (1927).

   b. A.G. Gaydon, Proc. Physical Soc. $\underline{56}$,95 (1944).

202. S.P. Davis and J.G. Phillips, The Red System $(A^2\pi - X^2\Sigma)$ of the CN Molecule (Univ. California:Berkeley,1963).

203.a. G. Herzberg and D.A. Ramsay, J. Chem. Phys. $\underline{20}$,347 (1952).

   b. K. Dressler and D.A. Ramsay, Phil. Trans. Royal Soc.,A $\underline{251}$,553 (1959).

204. C. Reid, J. Chem. Phys. $\underline{18}$,1299 (1950).

205. G.W. King and E.H. Pinnington, J. Molec. Spectrosc. $\underline{15}$,394 (1965).

206. Atomic Energy Levels, Vols. I-III, NBS Circular 467 (Aug. 1952).

207. E.J. Jones and O.R. Wulf, J. Chem. Phys. $\underline{5}$,873 (1937).

208.a. J.A. Myer, I. Itzkan, and E. Kierstead, Nature $\underline{225}$,544 (1970).

   b. F.B. Dunning and R.F. Stebbings, Opt. Comm. $\underline{11}$(2),112 (1974).

   c. K. Koto, Japan. J. Appl. Phys. $\underline{11}$,912 (1972).

209. J.A. Mangano and J.H. Jacob, Appl. Phys. Lett. $\underline{27}$(9),495 (1975).

210. J.J. Ewing and C.A. Brau, Appl. Phys. Lett. $\underline{27}$(6),350 (1975).

211. S.K. Searles and G.A. Hart, Appl. Phys. Lett. $\underline{27}$(4),243 (1975).

212. D.G. Sutton and G.A. Capelle, Aerospace Report ATR-76(7501)-S (1976).

213. F.B. Dunning, E.D. Stokes, and R.F. Stebbings, Opt. Comm. 6(1), 63 (1972).

214. F.B. Dunning, F.K. Tittel, and R.F. Stebbings, Opt. Comm. 7(3), 181 (1973).

215.a. R.W. Wallace, Opt. Comm. 4(4),316 (1971).

   b. J.M. Telle and C.L. Tang, Appl. Phys. Lett. 24(2),85 (1974).

   c. C. Gabel and M. Hercher, I.E.E.E. J. Quan. Elect. QE8(11),850 (1972).

216. J. Kuhl and H. Spitschan, Opt. Comm. 13(1),6 (1975).

217. Handbook of Lasers, Ed. R.J. Pressley (Chemical Rubber Co.: Cleveland,1971), pp.329-333.

218. A.V. Nowak, Ph.D. Thesis, Dept. of Chem. M.I.T., 1972.

219. S.D. Senturia and B.D. Wedlock, Electronic Circuits and Applications (M.I.T.:Cambridge,1972), Chapter 5.

220. Princeton Applied Research Corp., Lock-in Amplifier Model 120.

221. Lincoln Laboratory, M.I.T., Optics Report 1, 1971, Adv. Res. Prog. Agency, Dept. of Air Force, Elect. Sys. Div. Contract ESD-TR-2 (Sept. 1971), pp.35-46.

222. A.V. Nowak and J.I. Steinfeld, J. Chem. Phys. 57,5595 (1972).

223. Y. Beers, Introduction to the Theory of Error (Addison-Wesley: Reading,1957), Chapter 6.

224. L. Fox, An Introduction to Numerical Linear Algebra (Oxford:New York, 1965), Chapters 4 and 7.

225. P.P. Mader, A.S. Lucero, and E.P. Honorof, Amer. Soc. Mech. Eng. Paper No. 71-Av-17, presented at the Life Support and Environmental Control Conference, San Francisco, Ca. 12-14 July 1971.

226. J. Shewchun, et. al., Appl. Opt. 15(2),340 (1976).

227. L. Fox and D.F. Mayers, Computing Methods for Scientists and Engineers (Clarendon:Oxford,1968), p.92.

228. G.L. Squires, Practical Physics (McGraw-Hill:New York,1968), p.17.

229. A.D. Little, Inc. Model TDLS-II Tunable Diode Laser.

230. C.H. Gooch, Injection Electroluminescent Devices (Wiley:London, 1973), p.38.

231. Laser Analytics Inc. Diode Laser.

232. R. Elst and A. Oskam, J. Mol. Spectroscopy 40,84 (1971).

233. H.C. Allen, Jr. and P.C. Cross, Molecular Vib-Rotors (Wiley: New York,1963), p.149.

234. D. Kivelson, E.B. Wilson, and D.R. Lide, J. Chem. Phys. 32(1), 205 (1960).

235. C.J. Tsao and B. Curnutte, J. Quant. Spectrosc. Rad. Transfer 2,41 (1962).

236. P.C. Pandey, K.K. Kirty, and S.L. Srivastava, J. Phys. B4,786 (1971).

237. G.P. Srivastava, H.O. Gautann, and A. Kumar, J. Phys. B6,743 (1973).

238. P.C. Pandey and S.L. Srivastava, J. Phys. B5,997 (1972).

239. D.S. Frankel, Ph.D. Thesis, Dept. of Chemistry M.I.T.,1974.

Cumulative List of Publications

1. J.I. Steinfeld, "Tunable Lasers and their Application in Analytical Chemistry," C.R.C. Critical Reviews of Analytical Chemistry 5, 225 (1975).

2. B.D. Green and J.I. Steinfeld, "Laser Absorption Spectroscopy: A Method for Monitoring Complex Trace Gas Mixtures," Environmental Sci. and Tech. (in press).

3. B.D. Green and J.I. Steinfeld, "Accurate Absorption Coefficients for Fifteen Gases at CO_2 Laser Frequencies," Appl. Opt. 15, 1688 (1976).

4. B.D. Green and J.I. Steinfeld, "Monitoring Complex Trace Gas Mixtures by Laser Absorption Spectrometry," 6th Inter-Society Conference on Environmental Systems (San Diego, July 1976); ASME Publication 76-ENAs-8.

5. B.D. Green and J.I. Steinfeld, "Monitoring Complex Trace-Gas Mixtures by Long-Path Laser Absorption Spectrometry," 3rd European Electro-Optics Conference (Geneva, October 1976).

6. "Monitoring Spacecraft Atmosphere Contaminants by Laser Absorption Spectroscopy," Final Technical Report.

In Preparation

B.D. Green and J.I. Steinfeld, "High-Resolution Spectroscopic Analysis and Pressure Broadening in Infrared Absorption Bands of Vinyl Chloride."

Distribution

P. Quattrone   (3)
NASA Ames Research Center

NASA Scientific and Technical Information Facility   (2)
P. O. Box 33, College Park, Maryland 20740

T. Wydeven   (2)
NASA Ames Research Center

J. Hollahan   (1)
NASA Ames Research Center

R. Johnson   (1)
Room 236/218, NASA Ames Research Center

K. Biemann   (1)
Massachusetts Institute of Technology

J. M. Deutch   (1)
Massachusetts Institute of Technology